2012

Ionic Materials for Applications in Sensing and Optoelectronics

Sergio L. de Rooy
Louisiana State University and Agricultural and Mechanical College

IONIC MATERIALS FOR APPLICATIONS IN SENSING AND OPTOELECTRONICS

A Dissertation
Submitted to the Graduate Faculty of the
Louisiana State University and
Agricultural and Mechanical College
In partial fulfillment of the
Requirements for the degree of
Doctor of Philosophy

In
The Department of Chemistry

By
Sergio L. de Rooy
M.S., Gadjah Mada University, 2007
May, 2012

DEDICATION

To my Parents Andre Friedrich de Rooy and Herwati Mieke Soemodihardjo.
To my son Oliver de Rooy, my wife Marketa de Rooy, and my brothers Julio de Rooy and Christian de Rooy for their continuous love, encouragement and support throughout the years.

ACKNOWLEDGEMENTS

I am very grateful to the following people for their support in this dissertation work:

Prof. Isiah M. Warner for providing me with the opportunity to join his research group, for his encouragement, guidance, and constant support. Thank you for believing in me; your energy and enthusiasm for science have been a great source of inspiration.

Doctoral Committee Members: Profs. Samuel D. Gilman, Kermit K. Murray, Robert L. Cook, and Christopher D. White for their time and helpful suggestions regarding this dissertation.

Dr. Min Li, Dr. David Bwambok, Dr. Susmita Das and **Dr. Bilal El-Zahab** for introducing me to ionic liquids, chirality, fluorescence spectroscopy, and nanotechnology. Thank you for the helpful discussions and reviewing of my manuscripts.

Postdoctoral Researchers: Dr. Vivian Fernand, Dr. Farhana Hasan, and Dr. Noureen Siraj for helpful suggestions in research and proofreading my dissertation.

Warner Research Group: Thank you for your stimulating suggestions and fruitful discussions as well as your support and friendship throughout the years.

TABLE OF CONTENTS

LIST OF TABLES

Table **Page**

LIST OF FIGURES

Figure **Page**

LIST OF SCHEMES

Scheme **Page**

LIST OF ABBREVIATIONS

Abbreviation	Name
1D	one-dimensional
AAO	anodic aluminum oxide
AlaOMe	alanine methyl ester
$AlCl_3$	aluminum chloride
$BETI^-$	bis(pentafluoroethane)sulfonimide
BF_4^-	trifluoroborate
$bmimFeCl_4$	1-butyl-3-methylimidazolium chloride
BNA	1,1′-binaphthyl-2,2′-diamine
BNP	1,1′-binaphthyl-2,2′-diyl hydrogenphosphate
C_4mimCl	1-butyl-3-methylimidazolium chloride
$C_4mimFeCl_4$	1-butyl-3-methylimidazolium tetrachloroferrate
CCD	charge-coupled device
CD	circular dichroism
$CDCl_3$	deuterated chloroform
CE	capillary electrophoresis
CHTA	[(3-chloro-2-hydroxypropyl) trimethylammonium]
	[bis(trifluoromethylsulfonyl)imide]
CN^-	cyanide
DCM	dichloromethane
DMSO	dimethyl sulfoxide
DSC	differential scanning calorimetry

$Dy(ClO_4)_3.6H_2O$	dysprosium perchlorate hexahydrate
EEM	Excitation-Emission Matrix Spectra
Eph	ephedrine
ESI-MS	electrospray ionization mass spectrometry
FLIM	fluorescence lifetime imaging microscopy
FRET	Førster resonance energy transfer
FT-IR	fourier transform infrared spectroscopy
GC	gas chromatography
GUMBOS	group of uniform materials based on organic salts
HPLC	high performance liquid chromatography
HR-MS	high resolution magnetic spectrometry
IL	ionic liquid
IleOMe	isoleucine methyl ester
ISC	intersystem crossing
KSCN	potassium thiocyanate
LMCIL	luminescent magnetic chiral ionic liquid
LeuOMe	leucine methyl ester
MCIL	magnetic chiral ionic liquid
MCP	mean centered plots
MeEph	methylephedrine
MeOH	methanol
MIL	magnetic ionic liquid
Naproxen	2-(6-methoxy-2-naphthyl)propionic acid

NIR	near infrared
NMR	nuclear magnetic resonance
NorEph	norephedrine
NP	nanoparticles
OFET	organic field effect transistor
OLED	organic light emitting device
PCIL	protic chiral ionic liquid
PF_6^-	hexafluorophosphate
$PheC_2$	phenylalanine ethyl ester
PheOMe	phenylalanine methyl ester
PIC	pseudoisocyanine
PMT	photomultiplier tube
PROP	propranolol
QD	quantum dots
R6G	rhodamine 6G chloride
RTIL	room temperature ionic liquid
SEM	scanning electron microscopy
SQUID	superconducting quantum interference device
TC	thiacyanine
TEM	transmission electron microscope
$TEMPO\text{-}OSO_3^-$	2,2,6,6-tetramethyl-1-piperidinyloxyl-4-sulfate
Tf_2N^-	bis(trifluoromethylsulfonyl)imide
TFAE	trifluoro-1-(9-anthryl)ethanol

TGA	thermal gravimetric analysis
TPB	tetraphenyl borate
TSCPC	time-correlated single-photon counting
TSIL	task specific ionic liquid
UV	ultraviolet
ValOMe	valine methyl ester
vis	visible

ABSTRACT

Organic salts consist of bulky anions and/or cations whose properties can be tailored for specific purposes. Ionic liquids (ILs) are (semi)organic salts with melting points below 100 ºC. They typically exhibit neglible vapor pressures, high thermal stability, wide liquidus range, and tunable solubility. Moreover specific functions can be built into their respective ions. The first part of the dissertation involves discussions of chiral ionic liquids with additional protic, magnetic, and magneto-luminescent properties, respectively. In addition to their enantioselective sensing capabilities, the ILs may find use in chiral separations and catalysis.

The second part of the dissertation involves discussions of fluorescent one-dimensional (1D) nano and microstructures from a group of uniform materials based on organic salts (GUMBOS). These GUMBOS are essentially 'frozen' ILs with melting points that range from 25 ºC to 250 ºC. Similar to their liquid 'cousins', GUMBOS can be tailored for a variety of applications. Further tunability is obtained through size-confinement effects as a result of the nano (and micro) scale of these materials. The 1D nanomaterials were prepared according to templated and self-assembly methods. In one study a porous alumina membrane was used as a sacrificial template for growing nanotubes, nanowires and nanoarrays from rhodamine 6G tetraphenylborate GUMBOS, [R6G][TPB]. These materials may find possible use in sensing, lasing and waveguiding applications. In another study a series of 1D thiacarbocyanine (TC) GUMBOS nano and microsized structures were obtained by ionic self-assembly through a modified reprecipitation approach. Blended nanomaterials consisting of multiple fluorophores were also prepared, exhibiting Förster Resonance Energy Transfer (FRET). The TC nano and microscale structures offer promise as multicolor-imaging and bioimaging agents, and in (bio)sensing applications.

CHAPTER 1

INTRODUCTION

1.1 Ionic Liquids

Ionic liquids (ILs) are salts that melt at temperatures below the boiling point of water. They consist of bulky organic cations and semi-organic anions.[1] Room temperature ionic liquids (RTILs) are salts that are liquid under ambient conditions. The low melting points of these salts are the result of a 'frustrated packing' of their ions due to inability of the ions to crystallize in an ordered lattice.[2] Over the last two decades, ILs have become increasingly popular because of the inherent ability to tune their physical properties. Applications of ILs include synthesis, catalysis, separations, sensing, electrochemistry, as well as energy storage and conversion.[1, 3]

1.1.1 Brief History of Ionic Liquids

Although Walden is widely credited with reporting ethylammonium nitrate in 1914 as the first IL, earlier reports of ILs date back as far as the mid nineteenth century.[4] In 1934 the first IL was patented for enhanced dissolution of cellulose.[5] Unfortunately, this finding did not garner much public or academic interest at the time.[4b] Hurley and Wier reported a series of chloroaluminate ILs in 1948, which they used in electroplating.[6] Osteryoung and Wilkes subsequently rediscovered most of these ILs in the late 1970s and early 1980s when studying electrochemical reactions.[7] Throughout the 1980s, Seddon and Hussey developed uses of these ILs for organic synthesis and catalysis.[8] In 1992 Wilkes and Zaworotko reported a series of ILs which exhibited enhanced stability against hydrolysis compared to their chloroaluminate-based predecessors.[9] Their work also evidenced that a range of different cations and anions could be paired to obtain RTILs. As a result, a large number of ILs were developed while significant research efforts were made to study their physical and chemical properties. Meanwhile in the

1990s and early 2000s, the use of ILs moved beyond electrochemistry and catalysis into other research areas, including separation[10] and material science[11] as well as energy applications.[3d]

1.1.2. Synthesis of Ionic Liquids

Ionic Liquids are fluids made up entirely of ions.[12] Common cations employed in ILs are based on quaternary ammonium, imidazolium, pyridinium, or phosphonium. Typical anions in order of increasing hydrophobicity include halides (X^-), cyanide (CN^-), tetrafluoroborate (BF_4^-), hexafluorophosphate (PF_6^-), bis(trifluoromethylsulfonyl)imide (Tf_2N^-), and tetraphenylborate (TPB^-).[13] Various pathways including quaternization, anion-metathesis, acid-base neutralization, and reactions with Lewis acids have been used to synthesize ILs.

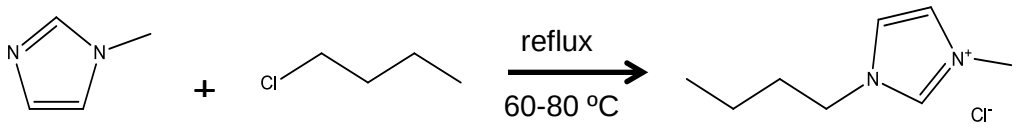

Figure 1.1. Synthesis of 1-butyl-3-methylimidazolium chloride.

Quaternization involves an S_N2 reaction between an alkyl halide and amine, phosphane, or thioether, typically performed at elevated temperature over the course of several hours up to a few days.[14] The required temperature and reaction time are determined by the reactivity of the alkyl halide. Reactivity of the halides increases down the periodic table, with iodide being the most reactive species, while increasing alkyl chain lengths result in a decrease in reactivity. As an example, the quaternization of 1-methylimidazole with butyl chloride is performed at 60-80 ºC under inert atmosphere (nitrogen or argon) for the duration of 48-72 hours. The reaction product, 1-butyl-3-methylimidazolium chloride (Figure 1.1) is a white or opaque crystalline solid, which is insoluble in the starting materials. The IL is typically purified through several washing steps with ethyl acetate and/or diethyl ether to remove unreacted starting materials.

Finally the product is dried under vacuum for several hours after which it is stored in a desiccator to minimize absorption of moisture.[15]

A metathesis or ion-exchange reaction is employed in the preparation of ILs when an organic anion is introduced.[16] This reaction is performed after completion of the aforementioned alkylation. Alternatively an anion-exchange reaction can be employed in preparing an IL where the precursor is already a quaternary amine (phosphane or thioether). An example of such an anion-exchange reaction is the preparation of 1-butyl-3-methylimidazolium hexafluorophosphate from 1-butyl-3-methylimidazolium chloride and sodium hexafluorophosphate (Figure 1.2). This reaction is typically performed in a biphasic mixture of water and dichloromethane (DCM) under ambient conditions and is completed in 12 to 24 hours. A slight molar excess of sodium hexafluorophosphate is required to push the reaction to completion. After the reaction has been completed, the aqueous phase is discarded and the IL containing organic phase is washed several times with distilled water to remove any remaining sodium chloride byproduct. Finally DCM is removed under reduced pressure, yielding the pure IL.[15]

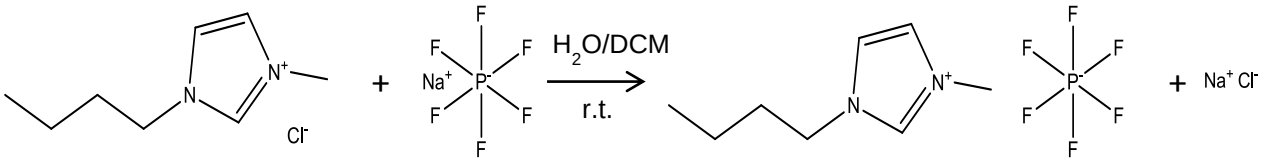

Figure 1.2. Synthesis of 1-butyl-3-methylimidazolium hexafluorophosphate.

Acid-base neutralization is another reaction type utilized in the synthesis of ILs. During this reaction, a neutral Brønsted base is reacted with an acid, resulting in proton transfer and the formation of a protic ionic liquid (PIL). For instance, the synthesis of ethylammonium nitrate reported by Walden, was formed by reacting ethylamine and nitric acid together (Figure 1.3).[4a] The neutralization reaction is performed in aqueous environment where the acid is slowly added

to the base (or *vice versa*) at 4 ºC. Water is subsequently removed through freeze-drying followed by lyophilization.

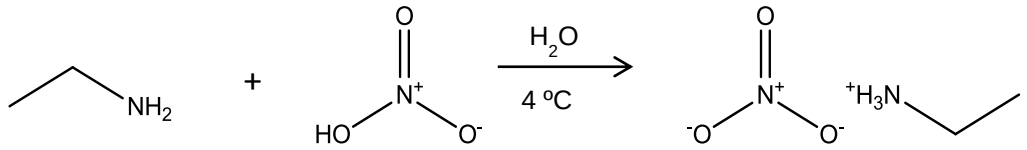

Figure 1.3. Synthesis of ethylammonium nitrate.

Alternatively, ILs can also be prepared by reaction of a Lewis acid with a Lewis base, i.e. a quaternary ammonium, phosphonium or sulfonium halide with a transition metal halide. Some of the earliest reported ILs were prepared by reacting an imidazolium chloride with aluminum chloride in equimolar amounts (Figure 1.4).[7b] The use of excess aluminum chloride with respect to 1-butyl-3-methylimidazolium chloride may result in the formation of higher order chloroaluminate ions (Figure 1.5).

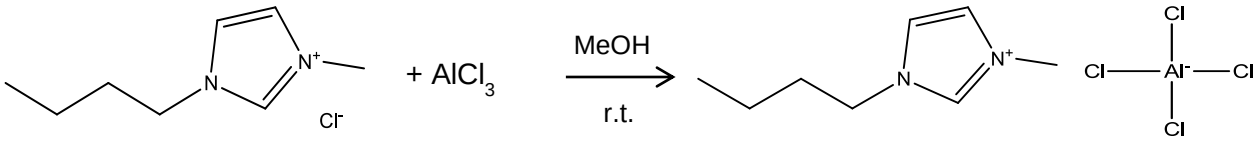

Figure 1.4. Synthesis of 1-butyl-3-methylimidazolium tetrachloroaluminate.

1.1.3. Physical and Chemical Properties of Ionic Liquids

The negligible vapor pressure, wide liquidus range, good thermal stability, and high ionic conductivity of ILs has earned them the reputation of green alternatives to their molecular counterparts.[17] Recently, however, these claims have been called into question as more (cyto)toxicity data on ILs has become available.[18] Nonetheless, ILs have been elevated from an academic curiosity to tailorable salts with serious industrial applicability. It is estimated that the number of possible ILs is close to 10^{18} (quintillion).[19]

These liquid salts owe their low vapor pressure to strong interionic interactions. The non-symmetrical ions with large charge delocalization prevent the closed packing commonly encountered in salt crystal lattices. The sub-optimal arrangement of ions occurs at significantly lower melting points for ILs than inorganic salts.[20] Thermal stability in ILs is largely dependent on the nature of the bond strength between carbon and heteroatom within the cation as well as hydrogen bonding with this heteroatom.[21] As ions have relatively high ion mobility in ILs, i.e. can freely move with respect to each other, these salts exhibit good conductivity in the liquid state.[22] Physical and chemical properties of ILs can be modified by altering the chemical structure of their constituent ions, i.e. the type of cation, the length and type of cation substituent(s), the type of anion, etc.[23]

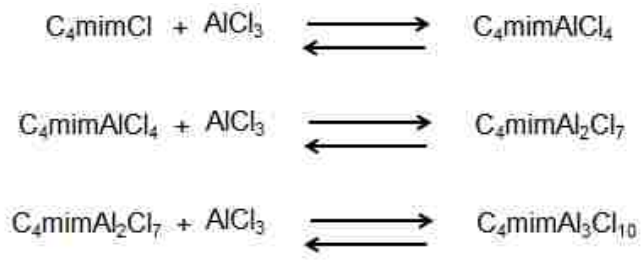

Figure 1.5. Formation of higher order chloroaluminate ILs with excess aluminum chloride.

Typical ILs are polar and thus miscible with polar solvents such as methanol, acetone, dichloromethane but immiscible with non-polar ones such as hexane, toluene, and diethylether. The type of cation or anion of ILs has a major impact on polarity and water solubility.[24] A common polarity probe utilized in determining the relative polarity of ILs, is Reichardt's betaine dye, which exhibits a polarity dependent solvatochromic shift of the lowest energy π-π^* absorption band.[25] Generally, ILs containing anions consisting of halides, tetrafluoroborate, and transition metal complexes are highly miscible with water, whereas those containing tetrafluorophosphate, bis(trifluoromethylsulfonylimide), and tetraphenylborate anions are not.[24]

The types of substituents that are attached to the cation also impact the polarity and solubility of ILs in water. Thus longer, nonpolar alkyl side chains render ILs less polar and reduce their solubility in water.

The majority of ILs have viscosities that are one or two orders of magnitudes higher than that of water, ranging from 10 mPas to 500 mPas.[26] They owe their high viscosities to an ability to undergo hydrogen bonding as well as van der Waals and electrostatic interactions.[27] In imidazolium-based ILs the viscosity increases with longer alkyl side chains due to enhanced van der Waals interactions. When the cation is kept constant, a decrease in viscosity is noted with increasing charge delocalization within anions.

As is the case with polarity and viscosity, melting points of ILs are also largely dependent on the structure of the respective ions. The symmetry, size, charge, and shape of cations and anions impact the melting behavior of ILs.[28] Longer alkyl side chains on IL cations increase van der Waals interactions, but reduce crystal packing (lattice energy). As a result, an increase in alkyl side chain initially leads to a decrease in melting point. However as alkyl side chains further increase in length, the van der Waals interactions become prevalent over lattice energies, leading to an increase in melting point. Larger anions with increased charge delocalization on the other hand lead to lower melting points.[28]

1.1.4. Task-Specific ILs

As mentioned earlier, the physical and chemical properties of ILs can be tuned through the pairing of ions with particular structures. Therefore, ILs can be designed by incorporating specific functional groups into the respective ions. To this end, Rogers and coworkers set out to develop ILs containing amine and thiol moieties to extract cadmium and mercury ions from aqueous environments. Hence, the concept of task specific ionic liquids (TSILs) was

conceived.[29] In addition to TSILs designed for the extraction of heavy metals, other TSILs with protic,[30] chiral,[31] magnetic,[32] and luminescent[33] properties have since been reported.

1.1.4.1. Protic Ionic Liquids

Protic ionic liquids (PILs) are a particular class of ILs synthesized through proton transfer from a Brønsted acid to a base. They are capable of hydrogen bonding and typically have non-negligible vapor pressure, i.e. some of them can be distilled.[34] As acid-base reactions are considered chemical equilibria, McFarlane has argued that the term PILs should only be reserved for those species that are at least 99% ionic in nature.[35] The acidic or basic properties of PILs have made them attractive as solvents and catalysts in organic synthesis.[36] In addition, PILs have found use in chromatography as mobile phase modifiers[37] and in stationary phases[38] due to their acidic/basic properties, solubility in water and relative ease of preparation. The ability to transfer protons has also made PILs the subject of study for ionic MALDI matrices, where they have been employed successfully with peptides, proteins and other biomolecules.[39] Additional applications of PILs are found in biocatalysis,[40] polymer fuel cells,[41] and lubricants.[42]

1.1.4.2. Chiral Ionic Liquids

1.1.4.2.1. The importance of Chirality

The term chirality is derived from the Greek ‘kheir’ which means hand and denotes a stereo-chemical asymmetry.[43] Enantiomers are molecules exhibiting chirality, i.e. they are non-superimposable mirror images of each another.[44] A mixture of enantiomers is termed a racemate. These molecules interact differently with their surroundings, especially with other chiral molecules. For example, in limonene one enantiomer is responsible for the odor of orange while the other enantiomer for the fragrance of lemon.[45] Likewise, in carvone one enantiomer has the scent of caraweed seed, whereas the other enantiomer smells like spearmint.[46] Since most

molecules that are responsible for biological systems are chiral molecules, chirality can have significant implications in the design of pharmaceutical drugs. The use of Thalidomide, a sedative-hypnotic drug that was marketed as a racemate in the 1960s, provides such an example. In Thalidomide one enantiomer successfully ameliorated morning-sickness in pregnant women. Unfortunately, the other enantiomer resulted in severe birth defects. Consequently the Food and Drug Administration (FDA) has put in place legislation that requires the pharmaceutical industry to produce stereochemically pure homochiral drugs.[47] As a result, of the top ten drugs sold in 2011, all contained a single enantiomer as active ingredient.[48] Due to these regulations, the need for developing analytical methods to distinguish between enantiomers and separate racemates, has grown immensely. To this end, several chiral selectors have been identified, including cyclodextrins,[49] polysaccharides,[50] molecular micelles,[51] macrocyclic antibiotics,[52] and more recently chiral ionic liquids.[53]

1.1.4.2.2. Chiral Ionic Liquids in Asymmetric Synthesis and Catalysis

Chiral Ionic Liquids (CILs) are another group of TSILs which are characterized by either a chiral cation or anion or in some cases both.[54] These ILs have played a major role in organic and analytical chemistry for the synthesis of chiral molecules[55] and detection or separation of racemates[56] respectively. Both of these pathways which allow for enantiopure compounds to be obtained are of major significance in the pharmaceutical industry.

In 1997, Howarth and coworkers reported *N*,*N*-bis[(2*S*)-2-methylbutyl]imidazolium bromide as the first CIL containing a chiral cation, for use as a Lewis catalyst in Diels-Alder reactions.[55] Two years later Seddon *et al.* reported 1-butyl-3-methylimidazolium lactate, a CIL with a chiral anion (Figure 1.6). Similar to *N*,*N*-bis[(2*S*)-2-methylbutyl]imidazolium bromide, this CIL was also successfully employed in asymmetric catalysis.[57] These results have led to the

development of a variety of CILs over the last decade. Their role in asymmetric catalysis encompasses chiral ligands, chiral solvents, and IL supported auxiliaries as well as chiral organocatalysts.[58] Numerous review articles on CILs have since been published.[31, 53, 58-59] In addition to their important role in organic synthesis and catalysis, CILs have immensely impacted analytical chemistry where they have been used in chiral sensing and separations.[56]

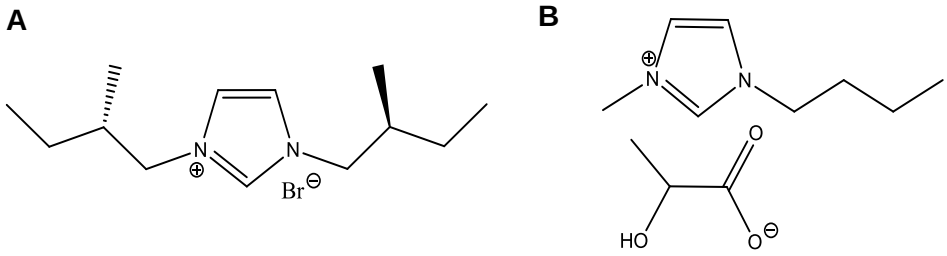

Figure 1.6. First ionic liquids with chiral cation (A) and chiral anion (B).

1.1.4.2.3. Chiral Ionic Liquids in Enantioselective Sensing

The first use of CILs in spectroscopic chiral recognition was reported by Wasserscheid *et al.* In 2002, the authors reported an ephedrinium-based CIL obtained from the chiral pool.[60] In order to perform chiral recognition studies, a racemic mixture of Mosher's salt was added to the enantiopure CIL as a chiral shift reagent. When ^{19}F-NMR measurements were subsequently performed, a splitting of the signal was observed for the CF_3-moiety of the Mosher's salt. These results indicated a difference in chiral interaction between the CIL and both enantiomers of the chiral shift reagent (Figure 1.7). Various other studies have since been conducted, utilizing Mosher's salt for investigation of the diastereomeric (chiral) interaction with CILs.[56a, 61]

Another application of CILs in chiral recognition appears in the form of fluorescence spectroscopy. Tran and coworkers measured the fluorescence of (*S*)-[(3-chloro-2-hydroxypropyl) trimethylammonium] [bis(trifluoromethylsulfonyl)imide] (CHTA), which played the role of solvent and chiral selector in the presence of different enantiomeric ratios of certain chiral,

fluorescent analytes (Figure 1.8).[62] The results were interpreted by means of a partial least squares method. Bwambok *et al.* synthesized a fluorescent, amino acid-derived CIL, which enabled the study of enantiomeric interaction with non-fluorescent chiral analytes, monitoring the change in fluorescence signal of the CIL.[56a]

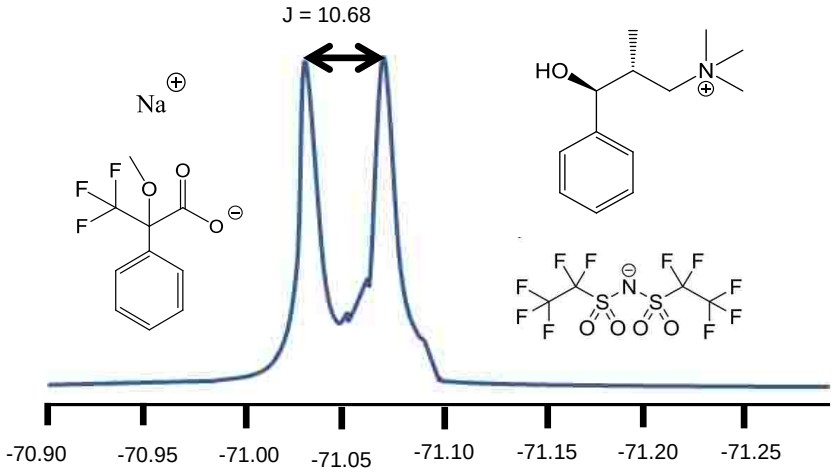

Figure 1.7. Enantiomeric interaction of racemic Mosher's salt with chiral ionic liquid (Adapted from reference 49).

Following the success with fluorescence spectroscopy, Tran *et al*. went on to investigate the use of Near Infrared (NIR) spectroscopy for the study of CILs in chiral discrimination. NIR spectroscopy is a non-destructive and potentially universal technique, based on absorption bands of characteristic molecular bonds such as O-H, N-H, C-H, and N-O present in organic and inorganic molecules. In the presence of different enantiomeric compositions of R and S atenolol (or other chiral drugs), diasteromeric interactions led to changes in the NIR spectra. After calibration (by measuring the signal of varying ratios of enantiomers) a sample with unknown enantiomeric concentrations of R and S can be analyzed with the aid of statistical methods.[63]

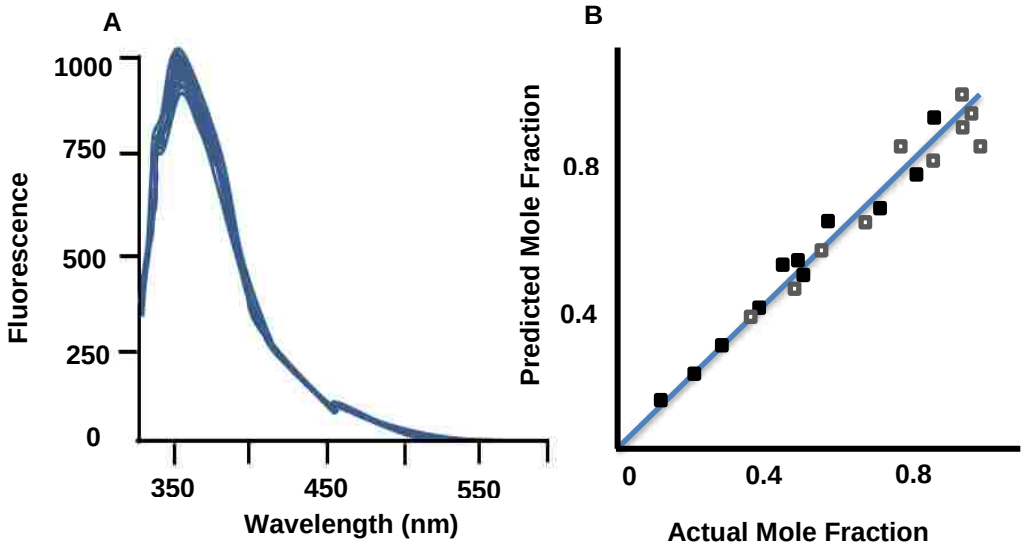

Figure 1.8. Fluorescence spectra of 34 solutions of warfarin at 10 μM, with different enantiomeric compositions in CIL (S-CHTA) (A) and plot of predicted versus actual mole fractions of (R)-warfarin and (S)-warfarin (B) (Adapted from reference 61).

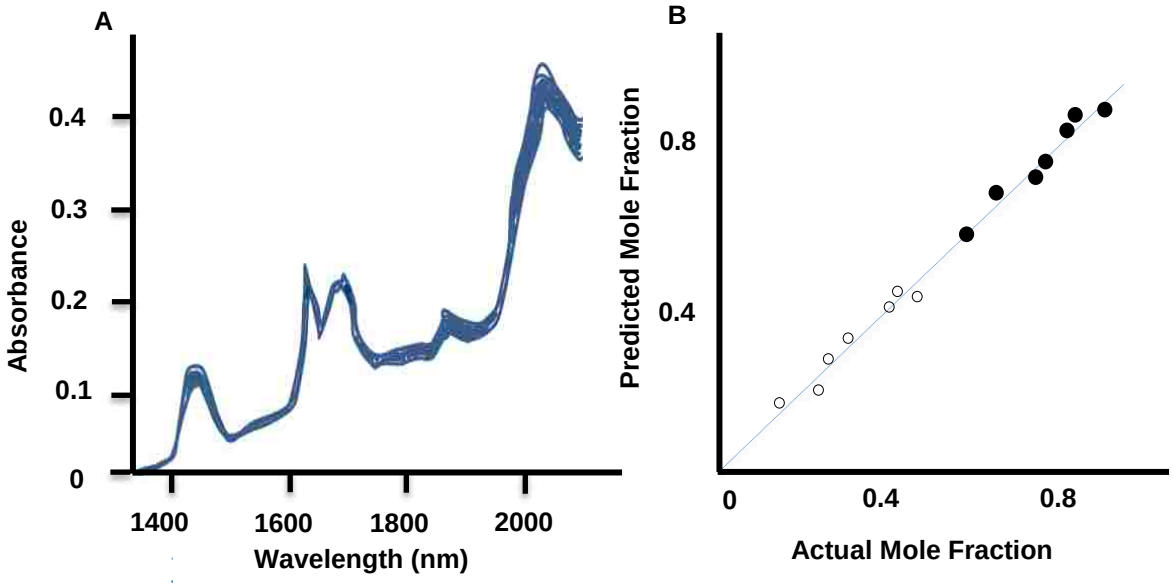

Figure 1.9. NIR spectra of 17 solutions of atenolol at 60 mM, with different enantiomeric compositions in CIL (S-CHTA) (A) and plot of predicted versus actual mole fractions of R-warfarin and S-atenolol (B) (Adapted from reference 62).

1.1.4.2.4. Chiral Ionic Liquids in Enantiomeric Separations

Chiral stationary phases comprising of chiral selectors dissolved in non-chiral ILs were first reported in 2001.[64] However, the first CIL stationary phase based on an ephedrinium-based CIL, was reported by Armstrong and coworkers in 2004.[65] This novel chiral stationary phase was successfully employed in the separation of various chiral alcohols, diols, sulfoxides, epoxides, and acetamides. Figure 1.9 depicts an enantiomeric separation of various chiral alcohols using this stationary phase. Unfortunately separation with this CIL exhibited a sharp decrease in separation efficiency after prolonged usage. These findings were believed to be the result of partial racemization of the CILs due to dehydration which occurred at temperatures above 140 ºC.

Yuan *et al*. reported (R)-N,N,N-Trimethyl-2-aminobutanolbis(trifluoromethanesulfon)-imidate as the first CIL to be used in high performance liquid chromatography (HPLC) and capillary electrophoresis (CE).[66] The CIL functioned as a mobile phase additive in the enantiomeric separation of various amines, alcohols, acids, and amino-acids.

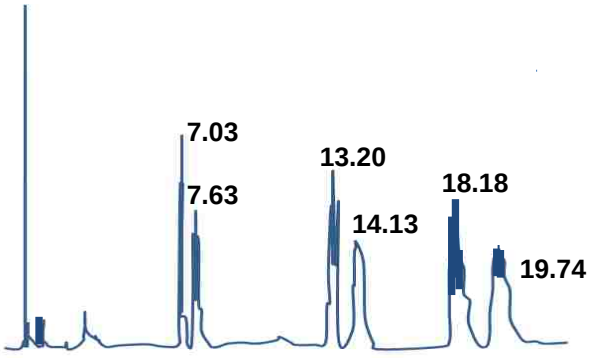

Figure 1.10. GC chromatogram of enantiomeric separation of (from left to right) sec-phenetyl alcohol, 1-phenyl-1-butanol, and trans-1,2-cyclohexanediol on fused-silica capillary coated with (1S,2R)-(+)-N, N-dimethylephedrinium-bis(trifluoromethanesulfon) imidate (Adapted from reference 63).

Rizvi and Shamsi have also reported two amino-acid derived surfactant-type CILs and their polymers for the enantiomeric separation of chiral acids in micellar electrokinetic

chromatography (MEKC).[67] Successful chiral separation was believed to be highly dependent on opposite charges between chiral selector and chiral analytes as well as three-point interaction. Francois *et al*. studied two choline-derived CILs for the enantiomeric separation of a series of pharmaceutical arylpropionic acids with CE.[68] Unfortunately, enantioselectivity was not reported when these CILs were used as additives, except when methylated β-cyclodextrins (β-CDs) were present as co-additives. Thus, the separation mechanism was believed to be due to synergistic effects between the β-CDs and CILs upon interacting with the chiral analytes. Similarly, Tran and Mejac have also reported enantiomeric separation in CE with (*S)*-[3-(chloro-2-hydroxypropyl)trimethylammonium] [bis(trifluoromethylsulfonyl)imide].[56b] Successful enantiomeric separation of a series of pharmaceutical amines and arylpropionic acids required the use of two additional chiral selectors besides the CIL.

1.1.4.3. Magnetic Ionic Liquids

Chloroaluminate RTILs discussed in section 1.1.1 received widespread interest because of their use as solvents in electroplating studies.[69] Other ILs based on different transition metal chloride complexes were similarly investigated for their electrochemical properties. Examples include titanium[70] and molybdenum-based[71] ILs, reported by Osteryoung *et al*. as well as niobium,[72] copper,[73] nickel, and iron-based[74] ILs reported by Hussey *et al*. More recently Hayashi and Hamaguchi described the discovery of the first magnetic ionic liquid (MIL) in the form of 1-butyl-3-methylimidazolium tetrachloroferrate ($[C_4mim][FeCl_4]$).[32] Measurements performed on a superconducting quantum interference device (SQUID) revealed a large magnetic susceptibility of 40.6 x 10^{-6} emu g^{-1} based on high–spin d_5 iron(III) in the form of the $[FeCl_4^-]$ anion. Figure 1.11 depicts the magnetic response of $[C_4mim][FeCl_4]$ to an external magnetic field.

Other MILs containing iron, dysprosium,[75] manganese,[76] cobalt,[76a, 77] and gadolinium[76a] metal anions paired with alkylimidazolium, tetraalkylammonium, and phosphonium cations have since been reported. A number of imidazolium-based MILs with the organic anion, 2,2,6,6-tetramethyl-1-piperidinyloxyl-4-sulfate (TEMPO-OSO_3) were additionally reported by Saito and coworkers.[78] These MILs exhibited low conductivities and fluidities.

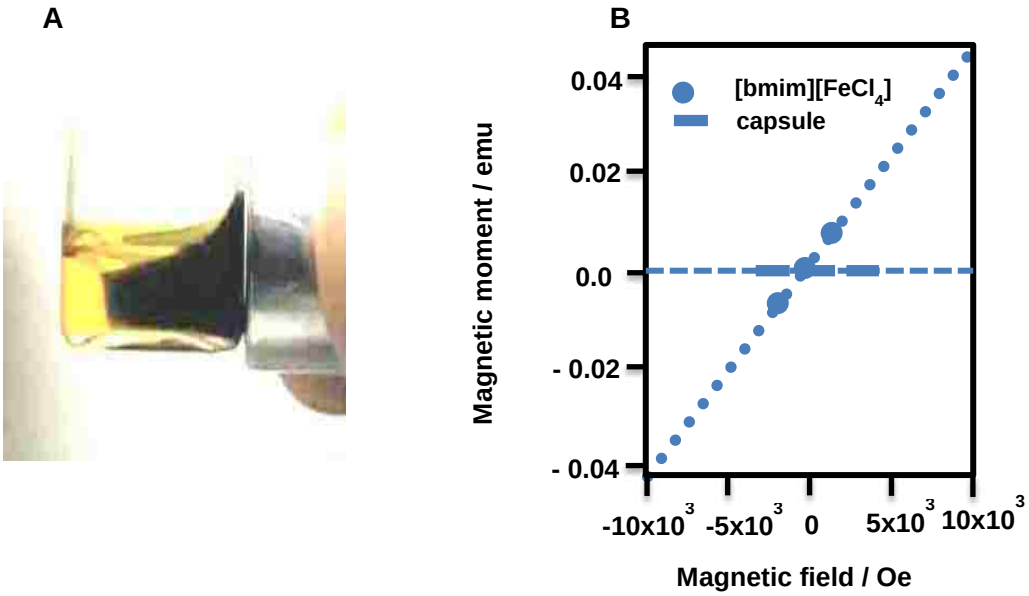

Figure 1.11. Magnetic response of MIL [C_4mim][$FeCl_4$] to external magnetic field (A) and relationship between magnetic moment and applied magnetic field of MIL as well as empty capsule (blank) (B) (Adapted from reference 32).

Due to their relatively high magnetic susceptibility and ease of synthesis, the tetrachloroferrate based MILs have received a significant amount of attention. For example, the thermomorphic behavior of [C_4mim][$FeCl_4$] and [C_{12}mim][$FeCl_4$] was thoroughly investigated. These MILs exhibited thermally induced demixing at weight fractions below 35%, allowing the MILs to be recovered upon heating between room temperature and 100ºC.[79] Polymerized versions of the MILs were prepared in the form of poly(1-vinyl-3-butylimidazolium chloride) and poly(diallyldimethylammonium chloride). These polymeric gels showed a strong response to

an external magnetic field and were employed as reusable catalyst in Friedel-Crafts alkylation.[80] Alternatively MILs were used as templates for the synthesis of polypyrrole nanostructures.[81] In the absence of a magnetic field, spherical polypyrrole nanoparticles were formed, whereas in the presence of an external magnetic field, nanorods and nanotubes were obtained. In another study, our group prepared nanoparticles from a MIL by using a reverse micelle, templating approach.[82] In using different concentrations of the MIL, it was possible to tune the sizes of the nanoparticles. Bica *et al.* developed a chiral camphor-derived imidazolium IL with [$FeCl_4^-$] as anion. This IL was used in diastereoselective Diels-Alder reaction between acrylic acid and cyclopentadiene [83] The chiral cation and metal-containing anion both aided in the catalytic reaction, however the magnetic properties of the IL were not investigated.

1.1.4.4. Luminescent ILs

The terminology of luminescent ILs has typically been reserved for those ILs with organometallic anions, exhibiting photo-physical properties. These ILs are characterized by electron transitions that involve unfilled d and f orbitals. Moreover, such ILs have long excited state fluorescence lifetimes.

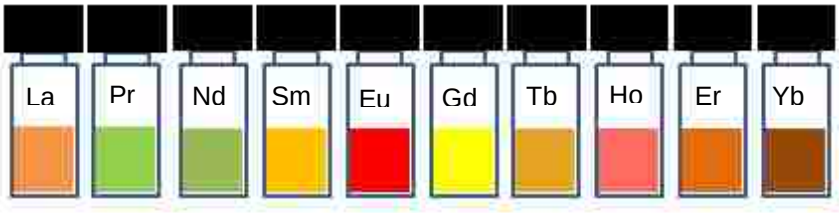

Figure 1.12. Ionic liquids of the type $[C_4mim]_4[Ln(NCS)_7(H_2O)]$ with Ln = La, Pr, Nd, Sm, Eu, Gd, Tb, Ho, Er, and Yb (Adapted from reference 83).

Binnemans and coworkers prepared a number of lanthanide based ILs with the general formula $[C_{14}mim]_{x-3}[Ln(NCS)_x(H_2O)_y]$ (x = 6-8; y = 0-2), where Ln = La, Pr, Nd, Sm, Eu, Gd, Tb, Ho, Er, or Yb.[84] These metal-containing ILs were transparent and exhibited strong luminescence. They

are believed to be promising candidates in catalytic and spectroscopic applications. Along the same line, Mudring and coworkers also reported a series of highly luminescent ILs with anions containing europium complexes of bis(trifluoromethanesulfonyl)imide (Tf_2N).[85]

1.1.4.4.1. Luminescent Magnetic ILs

Mudring and coworkers also reported a lanthanide containing IL based on Dysprosium with a $4f^9$ electron configuration. This particular IL is highly paramagnetic in addition to its strong luminescence, thus rendering an IL with dual functionality.[75]

1.1.4.4.2. Fluorescent Ionic Liquids

The terminology of fluorescent ILs is typically reserved for organic rather than organometallic ions, contrary to luminescent ILs. These ions have no unfilled d and f orbitals and excited state fluorescence lifetimes are much shorter. Studies performed by Paul *et al.* have shown that conventional imidazolium-based ILs are not completely transparent in the UV-region.[86] ILs such as $[C_2mim][X]$ and $[C_4mim][X]$ (X = Cl, BF_4, PF_6) show an excitation-dependent fluorescence which span a large part of the visible light region. However, the fluorescence exhibited by these ILs was relatively weak. Functional ILs with stronger fluorescence have been developed. Dong *et al*. prepared a series of 1-[*n*-(*N*-carbazole)alkyl]-3-methylimidazolium bromide [carbazoleC*n*mim]Br (*n* = 6, 10, and 12) ILs.[87] These carbazole-tailed ILs exhibited a strong fluorescence, independent of excitation wavelength. The authors suggested that these ILs may find use in optical and electrochemical applications due to the role of carbazole in photoconductivity and charge-transport.

Bwambok *et al.* reported an amino-acid derived IL with dual functionality, chirality and fluorescence embedded in the cation of L-phenylalanine ethyl ester bis(trifluoromethane)sulfonamide ($[L\text{-}PheC_2][Tf_2N]$).[56a] The IL exhibited multiple excitation and

emission peaks and was employed as fluorescence sensor for non-fluorescent chiral analytes and various sugars. Recently, there have been several reports of chemoresponsive fluorescent ILs. For example, Wei *et al.* reported a hydrophilic, symmetric imidazolium IL, $[(C_4)_2mim][Cl]$ that was used as probe for hemoglobin.[88] In addition, Loe-Mie *et al*. have developed a micro-total analysis system in which a fluorogenic TSIL with a 8-hydroxyquinoline benzoate unit was used in extraction and sensing of mercury cations.[89] Furthermore, Baker and coworkers have recently reported an IL in which a trihexyltetradecylphosphonium cation was paired with the photoacidic trianion 8-hydroxypyrene-1,3,6-trisulfonate (HPTS, pyranine) to yield a fluorescent IL that served as chemosensor for a series of amine vapors with different pKa values.[90]

1.1.5. Ionic Liquids and Nanomaterials

Nanomaterials are those materials with at least one dimension below 100 nm. These materials often exhibit size-dependent properties, different from those of the bulk materials.[91] Applications for nanomaterials have increased exponentially over the last two decades and include a plethora of areas including prostheses and implants,[92] electrochromic displays,[93] high energy density batteries,[94] 'smart' magnetic materials,[95] and sustainable energy.[96] Over the past few years there has been an increased interest in the use of ILs for the synthesis of nanomaterials. Ionic liquids are particularly interesting as solvents for nanoparticle synthesis due to their wide solvation range and neglible vapor pressure which allows for reactions at higher temperatures than typically possible with organic solvents, and more importantly the ability of ILs to undergo hydrogen bonding.[11b] The latter allows for 'molecular recognition' and 'self-organization', typically only encountered in protic solvents such as water. The first nanomaterials prepared in ILs were obtained through electrosynthesis and include transition-metal[11a] and semiconductor nanoparticles.[97] Other applications of ILs in the synthesis of nanomaterials include the use of ILs

as templates for the preparation of mesoporous silica,[98] coaxial electrospinning of carbon nanotubes and cellulose in ILs,[99] and transferable graphene sheets in polymeric ILs.[100] Polymeric ILs are obtained though polymerization of ILs with unsaturated alkyl side-chains and are typically solids at ambient temperature and pressure. Recently nanoparticles and inverse opals were also prepared from polymeric ILs.[101]

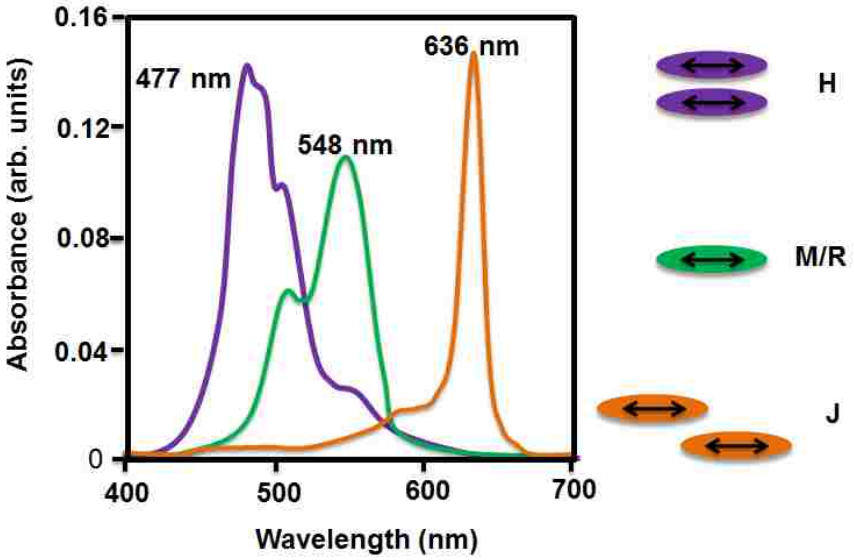

Figure 1.13. Dye aggregation observed in pseudo isocyanine (PIC) (Adapted from reference 110).

1.1.6. Molecular Dye Aggregates in Ionic Liquids and Nanomaterials

Almost 70 years ago, Scheibe and Jelly independently observed deviations from the Lambert-Beer law when pseudoisocyanine chloride (PIC) was dissolved in water at concentrations in the millimolar range.[102] These finding were correctly attributed by Scheibe to a supermolecular polymerization of dye molecules (aggregation), as the result of desolvation.[102a, b] Aggregates that are characterized by a narrow absorption band that has shifted to longer wavelengths compared to the monomer species (bathochromic shift) are referred to as J aggregates (J signifies Jelley). The J aggregates typically display a high quantum yield with a very small Stokes shift (near resonance) and arrange themselves in brickwork or head-to-tail

assemblies (Figure 1.14).[103] Aggregates that display an absorption band shifted to shorter wavelengths (hypsochromic) compared to the monomer species are referred to as H-aggregates (H signifies hypsochromic).[104] Figure 1.13 illustrates the absorbance spectrum of monomeric/random species as well as J and H aggregates in PIC dye. The H aggregates often exhibit large Stokes shifts and low fluorescence quantum yields and arrange themselves in a card-pack manner (Figure 1.14).[105] Applications of J aggregates include non-linear optics,[106] spectral sensitizers in photography[107] and dye-sensitized solar cells,[108] whereas those of H-aggregates include optical recording[109] and energy harvesting systems.[110]

The extent of dye aggregation is highly dependent on various factors, including concentration, solvent polarity, temperature, pH, and ionic strength and can be tuned accordingly.[111] Recently, Pandey and coworkers reported the controlled J and H-aggregation of cyanine dyes.[112] Highly basic solutions were added to cyanine dyes dissolved in water and ILs. It was found that the IL with a tetrafluoroborate anion ($[BF_4]^-$) yielded H-aggregates, whereas only J aggregates were observed in the case of other anions. These observations were attributed to hydrolytic properties of $[BF_4]^-$. Similarly, dye aggregation has also garnered significant interest in the development of nanomaterials. Organic dye molecules with their extensive conjugation are materials of interest because of their biological, chemical, magnetic, optical, and electronic properties.[113] There is currently a strong impetus to develop organic materials that aggregate into larger nanoscale structures such as nanorods, nanowires, nanobelts, and nanotubes as these one-dimensional (1D) nanostructures typically display size-dependent optical, electronic, and optoelectronic properties.[113-114] As a result 1D nanostructures have been developed from perylenes,[115] anthracenes,[116] porphyrins,[117] as well as their derivatives and serve as device components in sensors,[115] lasers,[114] field-effect transistors,[118] and light-emitting diodes.[119]

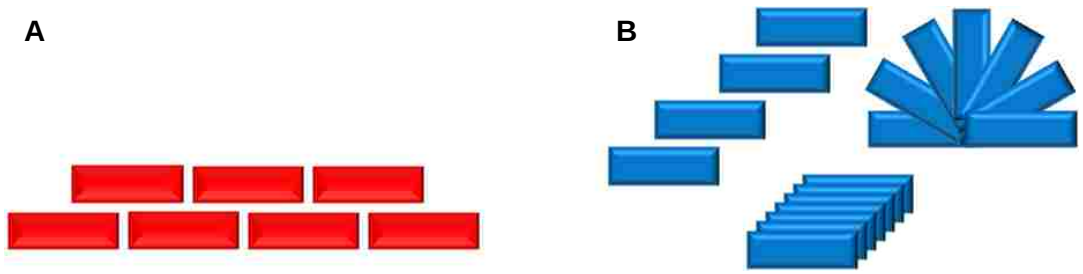

Figure 1.14. Molecular aggregation of organic dyes depicting (A) J-aggregates - brick-work arrangement and (B) H-aggregates - card-pack arrangement.

1.1.7. Förster Resonance Energy Transfer in Ionic Liquids and Nanomaterials

Förster resonance energy transfer (FRET) is the non-radiative transfer of energy through long-range dipole-dipole coupling between a donor fluorophore and acceptor chromophore in the excited electronic state.[120] This energy transfer is distance dependent and requires that the donor and acceptor are in close proximity to one another (1-10 nm). The donor fluorophore can be envisioned as an oscillating dipole which undergoes an energy exchange with the acceptor chromophore of similar resonance frequency. As the result of FRET, fluorescence of the donor is quenched, resulting in that of the acceptor being enhanced.[120] This non-radiative transfer of energy has found various applications in biological and material sciences. Figure 1.15 depicts FRET between two cyanine dyes (Cy3 and Cy5), where the area of overlap between the donor emission and the acceptor absorption is denoted as the spectral overlap region. The spectral overlap integral between a donor and acceptor pair can be calculated using the formula

$$J(\lambda) = \int_0^\infty \varepsilon(\lambda) f(\lambda) \lambda^4 d\lambda \qquad (1)$$

where $J(\lambda)$ is the overlap integral, ε is the extinction coefficient of the acceptor, f is the normalized emission spectrum of the donor, and λ is the wavelength. The energy transfer efficiency can similarly be calculated using the formula

$$E = 1 - \frac{F_{DA}}{F_D} \qquad (2)$$

where F_{DA} and F_D represent the integrated fluorescence intensity of the donor in the presence and absence of acceptor, respectively.[120]

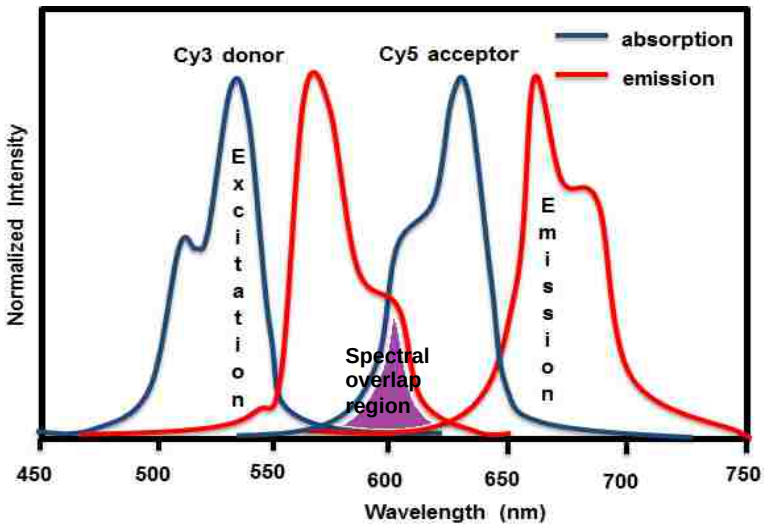

Figure 1.15. Föster Resonance Energy Transfer between Cy3 and Cy5 donor-acceptor pair.

To date there have been several studies of FRET in ionic liquid media. In one study energy transfer was investigated from coumarin 480 (C480) to rhodamine 6G (R6G) in an IL micro-emulsion, by use of pico and femtosecond emission spectroscopy.[121] It was found that various regions of the micro-emulsion could be probed by exciting the donor species at different wavelengths. The IL/surfactant/benzene micro-emulsions exhibited decay times of 1, 250, and 3900 ps. These decay times were the respective results of direct contact between donor and acceptor, donor in between surfactant and IL with acceptor within the IL pool, and finally donor located on outer periphery of the micro-emulsion and acceptor within the core of the IL. In

another study FRET was investigated between 1-butyl-3-methylimidazolium chloride ([C_4mim][Cl]) and R6G in the presence or absence of guar gum as a gelling agent.[122] Excitation was varied from 260 to 620 nm, resulting in sole emission from R6G. A similar excitation-wavelength-dependent fluorescence was observed in R6G-modified polymeric ionic liquid films.[123] In addition, a yeast cytochrome C labeled with R6G moiety was investigated as a model to probe the unfolding proteins in various IL environments.[124]

The use of FRET is especially desirable for biological applications, where interactions and conformational changes in bio-macromolecules occur at the nanoscale. To this end, the use of nanomaterials such metal nanoparticles (NPs) and quantum dots (QDs) have proved especially successful as FRET donors and acceptors. There are numerous studies in which gold (Au) NPs and quantum dots have been used in sensing platforms pertaining to bioanalysis. In one particular study, Au NPs and CdTe QDs were used as FRET donor-acceptor pair in the direct detection of glucose in serum.[125] This biosensor allowed for high selectivity in addition to a detection limit of 50 nM. In addition to NPs and QDs, 1D organic nanomaterials have recently been employed as FRET-based sensors. For example, tunable nanobelts were developed from 9,10-diphenylanthracene (DPA) doped with nile red (NR) at different ratios. The DPA-NR donor-acceptor pair exhibited tunable emission from blue to red and was utilized for sensing acidic and basic vapors.[126]

1.2. A Group of Uniform Materials Based on Organic Salts and Their Derived Nanomaterials

Although ILs are termed as organic salts with melting points below 100 ºC, the majority of applications have encompassed RTILs. Frozen ILs with melting points above room temperature have typically been regarded as unsuitable for the majority of applications. One exception can be found in the use of a frozen IL as medium for rewritable imaging.[127]

The Warner research group has developed novel nanoparticles derived from frozen ILs which combine the tunability of ILs with the ability of nanomaterials to exhibit size-dependent properties.[128] The term GUMBOS which is defined as a *Group of Uniform Materials Based on Organic Salts* was coined to also encompass organic salts with melting points higher than those of ILs. Thus, GUMBOS are essentially 'solid-state analogues' of RTILs with melting points ranging from 25 ºC to 250 ºC. These GUMBOS and nanomaterials derived from them, also denoted as nanoGUMBOS have since been prepared with magnetic,[82] near-infrared fluorescent,[129] as well as antimicrobial properties.[130]

1.2.1. Near Infrared (NIR) Fluorescent GUMBOS Nanoparticles

Similar to ILs described earlier, multiple GUMBOS can be prepared via anion-exchange reactions. In one study performed by our group, a cationic dye, 1,1',3,3,3',3'-Hexamethylindotricarbocyanine (HMT) iodide was exchanged with various anions, including bis(2-ethylhexyl)sulfosuccinate (AOT) sodium salt, tetrafluoroborate (BF_4) sodium salt, 3,5-bis(trifluoromethyl)phenyltrifluoroborate (TFPB) sodium salt, tetrakis[3,5-bis(1,1,1,3,3,3-hexafluoro-2-methoxy-2-propyl)-phenyl]borate (TFP4B) sodium salt, bis(trifluoromethane)sulfonamide (Tf_2N) lithium salt, and bis(pentafluoroethane)sulfonamide (Tf_2N) lithium salt. The HMT nanoGUMBOS were prepared by use of a template-free reprecipitation approach.[129b] The particle size and morphology were determined through dynamic light scattering (DLS) and transmission electron microscopy (TEM), respectively. The spectral properties of the GUMBOS and their nanomaterials were ascertained with absorbance and fluorescence spectroscopy. Absorbance spectra of ethanolic GUMBOS solutions displayed maxima at 742 nm similar to the parent compound [HMT][I]. In the case of nanoGUMBOS, absorbance measurements displayed additional shoulders or peaks that were red shifted and blue

shifted with respect to the monomer peak (742 nm). Deconvolution of the spectra indicated the overlap of essentially 3 different peaks. The monomer peak was found at ~735 nm and represents a random dye aggregation. The blue shifted peak which appeared at ~580 – 672 nm was assigned to an H-type of aggregation where the dye molecules stack in a parallel manner. The red shifted peak at ~753 – 783 nm was the result of a J-type of aggregation where the dyes are oriented in a staircase manner. Thus, the choice of anion dictates the type of dye aggregation and therefore the spectral properties of the nanoGUMBOS. Experimental results were confirmed with theoretical calculations though classical molecular dynamics simulations. In a related study [HMT][AOT] nanoGUMBOS were employed as contrast agents for biomedical imaging applications.[129a] The cellular uptake by monkey kidney fibroblast (Vero) cells was investigated and images obtained from (epi)fluorescence microscopy revealed that nanoGUMBOS were succesfully internalized.

1.3. Analytical Methods Used

1.3.1. Ultraviolet-Visible Spectroscopy

Ultraviolet-visible (UV-vis) spectroscopy is a molecular absorption technique that is used to study the absorption of light (photons) by molecules in the ultraviolet and visible region.[131] When absorption occurs, molecules are promoted from a ground state to an excited state. The resulting change in internal energy is associated with electronic transitions and can be recorded with a UV-vis spectrophotometer. In a UV-vis spectrometer the light is directed onto a monochromator that allows specific wavelengths to be selected and transmitted, thus illuminating the sample (transparent solution) which is placed in a cuvette. Light absorbed or transmitted by the sample is recorded though a detector (photomultiplier tube or diode array) and can be plotted against the wavelength to produce a spectrum. The Lambert-Beer law denoted as $A = \varepsilon bC$ relates the amount of light absorbed, termed absorbance (A) to the molar absorptivity (ε)

and concentration (*C*) of the analyte, and the path length (*b*) traversed by the light. In addition, UV-vis spectroscopy can serve as a quantitative method by plotting a calibration curve with known concentrations of the analyte.[131] A schematic of a UV-vis spectrometer is depicted in figure 1.16.

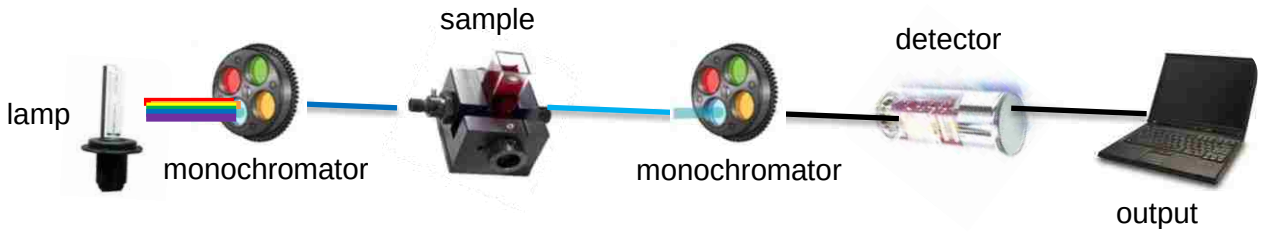

Figure 1.16. Schematic diagram of a UV-vis spectrometer.

1.3.2. Circular Dichroism Spectroscopy

Circular dichroism (CD) spectroscopy is a particular type of absorption spectroscopy that is used for studying chiral molecules, including amino acids and proteins. This technique is based on the ability of some chiral molecules to absorb left circularly polarized light to a different extent than right circularly polarized light. As a result two enantiomers of a chiral molecule display absorption bands with opposite sign.[132] A schematic of a CD instrument is shown in figure 1.17.

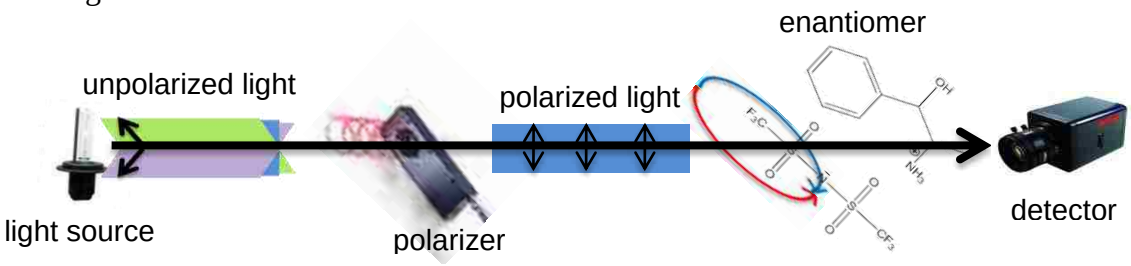

Figure 1.17. Schematic representation of a CD spectropolarimeter.

1.3.3. Fluorescence Spectroscopy

The process of fluorescence can be best illustrated with the Perrin-Jablonksi diagram (Figure 1.18).[120] Upon irradiation, molecules absorb light, resulting in promotion to an excited singlet electronic state (S_n). Since the timeframe is very fast (10^{-15} s) compared to other competing processes, the Franck-Condon principle states that displacement of the nuclei is negligible.[133] The excited molecules undergo internal conversion, which is a non-radiative transition between higher to lower singlet states. Once the lowest excited singlet state is reached, a radiative transition also known as fluorescence can occur as molecules return to the ground state. In addition to fluorescence, intersystem crossing, another non-radiative process can take place. This process entails a transition from a singlet to a triplet excited state. After internal conversion to the lowest triplet excited state, a radiative transition termed phosphorescence can occur. The excited state lifetime of phosphorescence lies between 10^{-6} and 1 s, compared to 10^{-10} to 10^{-7} s in the case of fluorescence.[120]

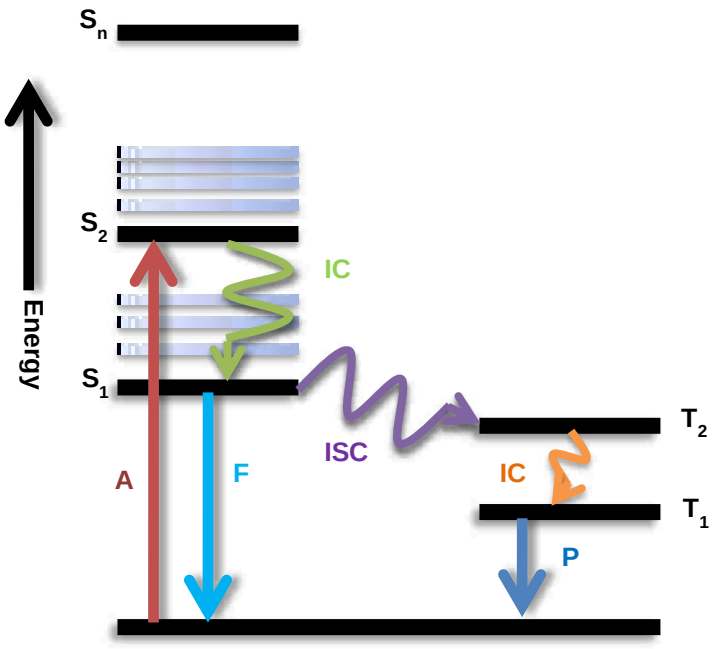

Figure 1.18. Perrin-Jablonski diagram.

A fluorimeter consists of a xenon light source, excitation and emission monochromators (or filters), a sample compartment, and photomultiplier tube (PMT), photodiode, or CCD detector (Figure 1.19). The first monochromator allows for light ranging from 200 nm to 900 nm to be selected for illumination of the sample. Emitted light collected at right angle to the incident light passes through the second monochromator to remove scattered rays before reaching the detector.[120, 133]

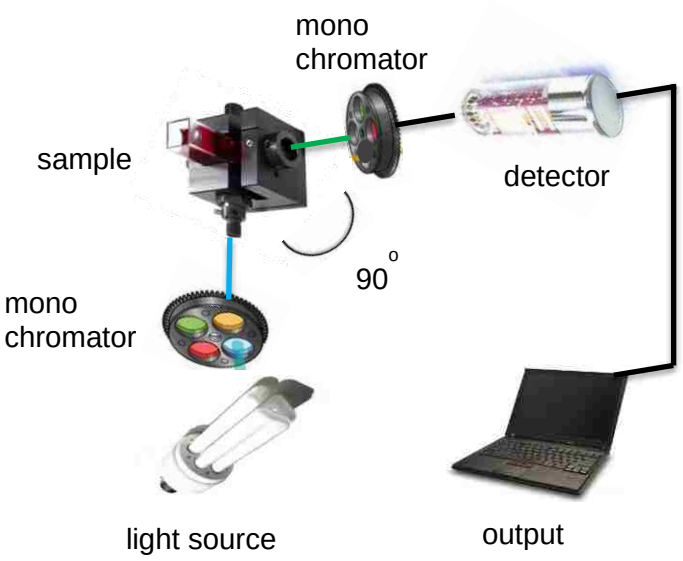

Figure 1.19. Schematic representation of a spectrofluorimeter.

1.3.4. Fluorescence Microscopy

Fluorescence microscopy is an optical microscopy method with an increasingly important role in the biomedical and materials sciences.[134] The sample under investigation can be either inherently fluorescent or doped with fluorescent markers. Irradiation of the fluorescent molecules results in absorption followed by emission of light at a longer wavelength i.e. fluorescence. A fluorescence microscope consists of a xenon-arc or mercury vapor lamp, excitation filter, dichroic mirror, and emission filter. The excitation filter ensures that the light incident on the

sample is monochromatic and of the right wavelength. The dichroic mirror is used to separate the excitation and emission paths and the emission filter prevents excitation light from reaching the detector (Figure 120).[135]

1.3.5. Scanning Electron Microscopy

Scanning electron microscopy (SEM) requires electrons to irradiate a sample while raster-scanning the surface. Electrons are far more energetic than visible light, therefore SEM allows for magnifications up to a thousand fold higher compared to optical microscopy.[136] The sample under investigation is coated with a thin conductive metal layer and placed on opposite side of an 'electron gun', which is typically a tungsten heating element. The electron beam is focused and directed through magnetic lenses which can bend the electrons in the desired direction. Once the electrons strike the surface of the sample, secondary electrons are emitted which are detected with a photomultiplier tube. Subsequently, these signals allow for an image of the sample to be built.[137] A schematic of an SEM is depicted in figure 1.21.

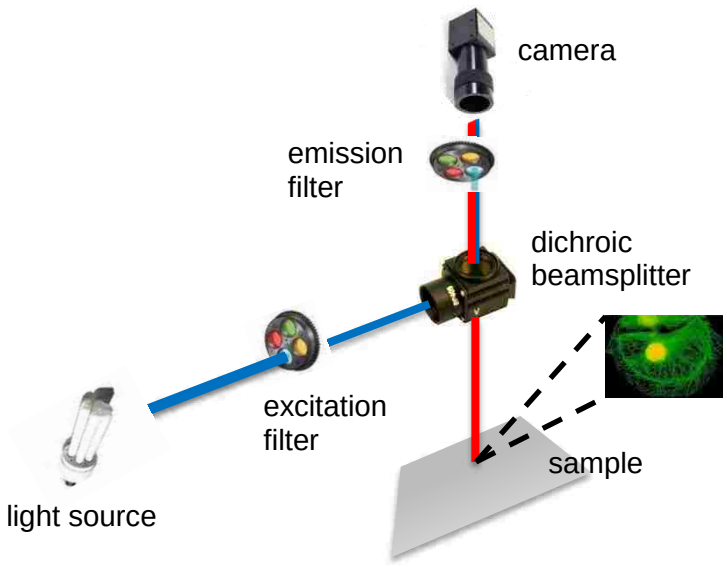

Figure 1.20. Schematic depiction of a fluorescence microscope.

1.3.6. Transmission Electron Microscopy

Similar to SEM, transmission electron microscopy (TEM) also requires electrons for irradiating the sample, where a series of magnetic lenses are used to focus the electron beam.[138] Contrary to SEM however, electrons penetrate through the sample which has been spotted on a carbon-coated copper grid, to reach a phosphorescent screen (detector), located on the opposite side of the electron beam. Where electrons impinge on the sample, fewer electrons traverse to reach the detector. The resulting electronic signals are used to create an image of the sample, similar to the negative of a polaroid photograph.[138-139] A schematic of a TEM is depicted in figure 1.22.

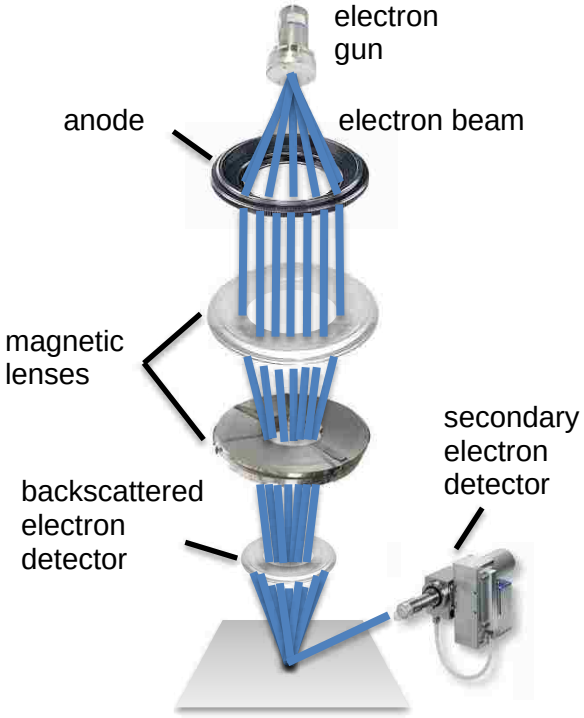

Figure 1.21. Schematic depiction of a scanning electron microscope.

1.3.7. Superconducting Quantum Interference Device

A superconducting quantum interference device (SQUID) is a sensitive magnetometer which consists of a semiconductor loop with one or more Josephson junctions, also known as weak links.[140] When an electrical current is passed across a Josephson junction, an interference signal is measured due to quantum tunneling of electron pairs. As a magnetic sample moves through the loop, an electrical current is induced, thus altering the interference signal measured across the Josephson links. The change in electrical current is proportional to the magnetic susceptibility of the sample.[141] Figure 1.23 shows a schematic representation of a SQUID.

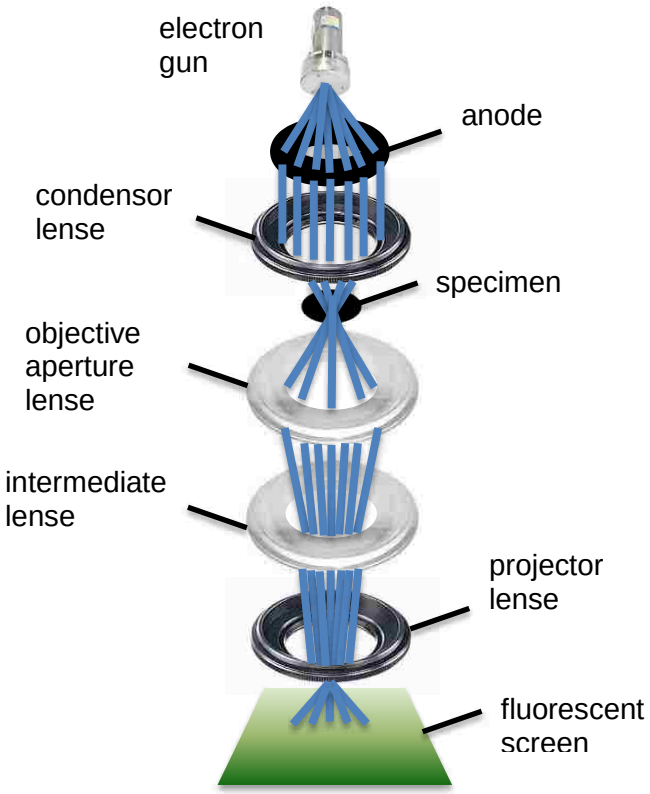

Figure 1.22. Schematic depiction of a transmission electron microscope.

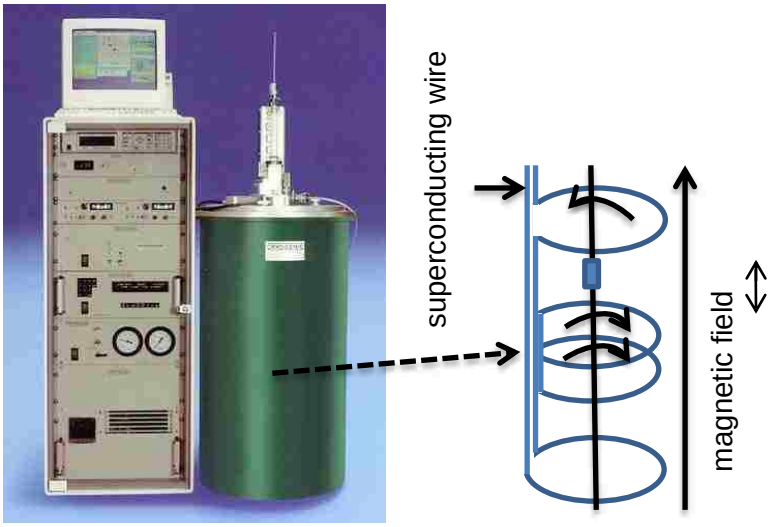

Figure 1.23. Schematic representation of a SQUID. (Adapted from reference 140)

1.4. Scope of the Dissertation

This dissertation is composed of two parts and describes the use of functional ionic materials for applications in sensing and optoelectronics. In the first part, bifunctional and trifunctional room temperature ionic liquids (RTILs) with enantioselective properties are discussed. The second part describes one-dimensional fluorescent nanomaterials derived from frozen ionic liquids also known as a Group of Uniform Materials Based on Organic Salts (GUMBOS) obtained through template and self-assembly methods.

In the second chapter, the synthesis and characterization of a series of ephedrinium-based protic chiral ILs (PCILs) derived from primary, secondary, and tertiary amines are discussed. The enantiomeric recognition capabilities of these PCILs were investigated with a series of chiral analytes. The aim of this study was to determine the effect of the degree of amine alkylation on the PCILs' physical properties and chiral recognition capability. In the third chapter, bifunctional magnetic chiral ILs (MCILs) comprised of chiral cations, and derived amino acids coupled with

magnetic anions, are discussed.[61b] The chiral recognition capability was studied with steady-state fluorescence spectroscopy and the magnetic susceptibility was also confirmed with SQUID. These MCILs offer enormous potential in asymmetric catalysis and chiral extraction. The fourth chapter discusses a series of trifunctional ILs with amino-acid derived chiral cations and dysprosium-based anions. These luminescent magnetic chiral ionic liquids (LMCILs) exhibited strong luminescence, paramagnetic susceptibility, and chiral recognition capability as confirmed by steady-state fluorescence and SQUID. Similar to the MCILs discussed in chapter 3, these ILs offer applications in chiral sensing and catalysis. In the fifth chapter, a series of 3 thiacarbocyanine-based frozen ILS or GUMBOS with increasing methyne chain lengths are discussed. The GUMBOS assembled into one-dimensional micro and nanostructures upon application of a reprecipitation approach from an ethanolic solution in water. The nanomaterials exhibited characteristic photophysical properties as evidenced by UV-vis absorption spectroscopy as well as fluorescence spectroscopy and fluorescence microscopy. Further studies resulted in the formation of binary and ternary nano/microscale structures when mixtures of two or three GUMBOS were employed during the reprecipitation. These binary and ternary nano/microstructures exhibited intraparticle Förster Resonance Energy Transfer (FRET), thus allowing these materials to be used in optoelectronics, bioimaging, and energy harvesting applications. The sixth chapter discusses fluorescent GUMBOS prepared through ion-pairing of a rhodamine 6G (R6G) cation with a bulky tetraphenylborate (TPB) anion. One-dimensional (1D) nanostructures, including nanowires, tubes, and nanoarrays were fabricated employing a template method. These 1D fluorescent nanostructures may find use in sensing and optoelectronics.

1.5. References

1. Welton, T., Room-temperature ionic liquids. Solvents for synthesis and catalysis. *Chemical Reviews* **1999,** *99* (8), 2071-2083.

2. Del Pópolo, M. G.; Voth, G. A., On the Structure and Dynamics of Ionic Liquids. *The Journal of Physical Chemistry B* **2004,** *108* (5), 1744-1752.

3. (a) Berthod, A.; Ruiz-Angel, M.; Carda-Broch, S., Ionic liquids in separation techniques. *Journal of Chromatography A* **2008,** *1184* (1-2), 6-18; (b) Siddharth, P., Analytical applications of room-temperature ionic liquids: A review of recent efforts. *Analytica Chimica Acta* **2006,** *556* (1), 38-45; (c) Buzzeo, M. C.; Evans, R. G.; Compton, R. G., Non-Haloaluminate Room-Temperature Ionic Liquids in Electrochemistry—A Review. *ChemPhysChem* **2004,** *5* (8), 1106-1120; (d) Wishart, J. F., Energy applications of ionic liquids. *Energy & Environmental Science* **2009,** *2* (9), 956-961.

4. (a) Walden, P., *Bull. Acad. Imper. Sci. (St Petersburg),* **1914** (1800), 405 - 422 ; (b) Wilkes, J. S., A short history of ionic liquids - from molten salts to neoteric solvents. *Green Chemistry* **2002,** *4* (2), 73-80.

5. Graenacher, C. Cellulose Solution. 1934.

6. Hurley, F. H.; Wier, J. T. P., The Electrodeposition of Aluminum from Nonaqueous Solutions at Room Temperature. *Journal of The Electrochemical Society* **1951,** *98* (5), 207-212.

7. (a) Chum, H. L.; Koch, V. R.; Miller, L. L.; Osteryoung, R. A., Electrochemical Scrutiny of Organometallic Iron Complexes and Hexamethylbenzen in a Room-Temperature Molten-Salt. *Journal of the American Chemical Society* **1975,** *97* (11), 3264-3265; (b) Wilkes, J. S.; Levisky, J. A.; Wilson, R. A.; Hussey, C. L., Dialkylimidazolium chloroaluminate melts: a new class of room-temperature ionic liquids for electrochemistry, spectroscopy and synthesis. *Inorganic Chemistry* **1982,** *21* (3), 1263-1264.

8. (a) Scheffler, T. B.; Hussey, C. L.; Seddon, K. R.; Kear, C. M.; Armitage, P. D., Molybdenum Chloro Complexes in Room-Temperature Chloroaluminate Ionic Liquids - Stabilization of $MoCl_6^{2-}$and $MoCl_6^{3-}$. *Inorganic Chemistry* **1983,** *22* (15), 2099-2100; (b) Scheffler, T. B.; Hussey, C. L., Electrochemical study of tungsten chloro complex chemistry in the basic aluminum chloride-1-methyl-3-ethylimidazolium chloride ionic liquid. *Inorganic Chemistry* **1984,** *23* (13), 1926-1932; (c) Sun, I. W.; Ward, E. H.; Hussey, C. L.; Seddon, K. R.; Turp, J. E., Electrochemistry and spectroelectrochemistry of the hexachloroiridate(III) and -(IV) complexes in the basic aluminum chloride-1-methyl-3-ethylimidazolium chloride room-temperature ionic liquid. *Inorganic Chemistry* **1987,** *26* (13), 2140-2143.

9. Wilkes, J. S.; Zaworotko, M. J., Air and water stable 1-ethyl-3-methylimidazolium based ionic liquids. *Journal of the Chemical Society, Chemical Communications* **1992,** (13), 965-967.

10. G. Huddleston, J.; D. Rogers, R., Room temperature ionic liquids as novel media for 'clean' liquid-liquid extraction. *Chemical Communications* **1998,** (16), 1765-1766.

11. (a) Dupont, J.; Fonseca, G. S.; Umpierre, A. P.; Fichtner, P. F. P.; Teixeira, S. R., Transition-metal nanoparticles in imidazolium ionic liquids: Recycable catalysts for biphasic hydrogenation reactions. *Journal of the American Chemical Society* **2002,** *124* (16), 4228-4229; (b) Antonietti, M.; Kuang, D. B.; Smarsly, B.; Yong, Z., Ionic liquids for the convenient synthesis of functional nanoparticles and other inorganic nanostructures. *Angewandte Chemie-International Edition* **2004,** *43* (38), 4988-4992.

12. Earle, M. J.; Seddon, K. R., Ionic liquids. Green solvents for the future. *Pure and Applied Chemistry* **2000,** *72* (7), 1391-1398.

13. Plechkova, N. V.; Seddon, K. R., Applications of ionic liquids in the chemical industry. *Chemical Society Reviews* **2008,** *37* (1), 123-150.

14. Smith, M. B. M., Jerry *Advanced Organic Chemistry: Reactions, Mechanisms, and Structure*. 5th edition ed.; Wiley-Interscience: New York, 2001.

15. Suarez, P. A. Z.; Dullius, J. E. L.; Einloft, S.; De Souza, R. F.; Dupont, J., The use of new ionic liquids in two-phase catalytic hydrogenation reaction by rhodium complexes. *Polyhedron* **1996,** *15* (7), 1217-1219.

16. Chauvin, Y., Olefin metathesis: The early days (Nobel lecture). *Angewandte Chemie-International Edition* **2006,** *45* (23), 3740-3747.

17. Rogers, R. D.; Seddon, K. R., Ionic liquids - Solvents of the future? *Science* **2003,** *302* (5646), 792-793.

18. Zhao, D.; Liao, Y.; Zhang, Z., Toxicity of Ionic Liquids. *CLEAN – Soil, Air, Water* **2007,** *35* (1), 42-48.

19. Seddon, K. R. The International George Papatheodorou Symposium, 1999; 1999; p 131.

20. Ngo, H. L.; LeCompte, K.; Hargens, L.; McEwen, A. B., Thermal properties of imidazolium ionic liquids. *Thermochimica Acta* **2000,** *357-358* (0), 97-102.

21. Wasserscheid, P.; Keim, W., Ionic liquids - New "solutions" for transition metal catalysis. *Angewandte Chemie-International Edition* **2000,** *39* (21), 3772-3789.

22. Fannin, A. A.; Floreani, D. A.; King, L. A.; Landers, J. S.; Piersma, B. J.; Stech, D. J.; Vaughn, R. L.; Wilkes, J. S.; Williams, J. L., Properties of 1,3-Dialkylimidazolium Chloride Aluminum-Chloride Ionic Liquids .2. Phase-Transitions, Densities, Electrical Conductivities, and Viscosities. *Journal of Physical Chemistry* **1984,** *88* (12), 2614-2621.

23. Hu, Y.-F.; Xu, C.-M., Effect of the structures of ionic liquids on their physical-chemical properties and the phase behavior of mixtures involving ionic liquids. *Chem. Rev.* **2005**.

24. Ranke, J.; Othman, A.; Fan, P.; Mueller, A., Explaining Ionic Liquid Water Solubility in Terms of Cation and Anion Hydrophobicity. *International Journal of Molecular Sciences* **2009,** *10* (3), 1271-1289.

25. Carmichael, A. J.; Seddon, K. R., Polarity study of some 1-alkyl-3-methylimidazolium ambient-temperature ionic liquids with the solvatochromic dye, Nile Red. *Journal of Physical Organic Chemistry* **2000,** *13* (10), 591-595.

26. Jacquemin, J.; Husson, P.; Padua, A. A. H.; Majer, V., Density and viscosity of several pure and water-saturated ionic liquids. *Green Chemistry* **2006,** *8* (2), 172-180.

27. Bonhote, P.; Dias, A. P.; Papageorgiou, N.; Kalyanasundaram, K.; Gratzel, M., Hydrophobic, highly conductive ambient-temperature molten salts. *Inorganic Chemistry* **1996,** *35* (5), 1168-1178.

28. Fredlake, C. P.; Crosthwaite, J. M.; Hert, D. G.; Aki, S. N. V. K.; Brennecke, J. F., Thermophysical Properties of Imidazolium-Based Ionic Liquids. *Journal of Chemical & Engineering Data* **2004,** *49* (4), 954-964.

29. Visser, A. E.; Swatloski, R. P.; Reichert, W. M.; Mayton, R.; Sheff, S.; Wierzbicki, A.; Davis, J. H.; Rogers, R. D., Task-specific ionic liquids for the extraction of metal ions from aqueous solutions. *Chemical Communications* **2001,** (01), 135-136.

30. Greaves, T. L.; Drummond, C. J., Protic Ionic Liquids: Properties and Applications. *Chemical Reviews* **2007,** *108* (1), 206-237.

31. Baudequin, C.; Baudoux, J.; Levillain, J.; Cahard, D.; Gaumont, A.-C.; Plaquevent, J.-C., Ionic liquids and chirality: opportunities and challenges. *Tetrahedron: Asymmetry* **2003,** *14* (20), 3081-3093.

32. Hayashi, S.; Hamaguchi, H. O., Discovery of a magnetic ionic liquid bmim FeCl4. *Chemistry Letters* **2004,** *33* (12), 1590-1591.

33. Binnemans, K., Lanthanides and actinides in ionic liquids. *Chemical Reviews* **2007,** *107* (6), 2592-2614.

34. (a) Earle, M. J.; Esperanca, J.; Gilea, M. A.; Lopes, J. N. C.; Rebelo, L. P. N.; Magee, J. W.; Seddon, K. R.; Widegren, J. A., The distillation and volatility of ionic liquids. *Nature* **2006,** *439* (7078), 831-834; (b) Rosamilia, A. E.; Strauss, C. R.; Scott, J. L., Distillable ionic liquids for a new multicomponent reaction. *Pure and Applied Chemistry* **2007,** *79* (11), 1869-1877.

35. MacFarlane, D. R.; Seddon, K. R., Ionic liquids - Progress on the fundamental issues. *Australian Journal of Chemistry* **2007,** *60* (1), 3-5.

36. (a) Hadded, M.; Biquard, M.; Letellier, P.; Schaal, R., Propriétés volumiques du nitrate d'éthylammonium fondu à 298 K et de ses mélanges avec l'eau. *Canadian Journal of Chemistry* **1985,** *63* (3), 565-570; (b) Zhu, A.; Jiang, T.; Wang, D.; Han, B.; Liu, L.; Huang, J.; Zhang, J.; Sun, D., Direct aldol reactions catalyzed by 1,1,3,3-tetramethylguanidine lactate without solvent. *Green Chemistry* **2005,** *7* (7), 514-517; (c) Zhao, G.; Jiang, T.; Gao, H.; Han, B.; Huang, J.; Sun, D., Mannich reaction using acidic ionic liquids as catalysts and solvents. *Green Chemistry* **2004,** *6* (2), 75-77; (d) Cole, A. C.; Jensen, J. L.; Ntai, I.; Tran, K. L. T.; Weaver, K. J.; Forbes, D. C.; Davis, J. H., Novel Brønsted Acidic Ionic Liquids and Their Use as Dual Solvent−Catalysts. *Journal of the American Chemical Society* **2002,** *124* (21), 5962-5963.

37. (a) Shetty, P. H.; Youngberg, P. J.; Kersten, B. R.; Poole, C. F., Solvent properties of liquid organic salts used as mobile phases in microcolumn reversed-phase liquid chromatography. *Journal of Chromatography A* **1987,** *411* (0), 61-79; (b) Poole, C. F.; Kersten, B. R.; Ho, S. S. J.; Coddens, M. E.; Furton, K. G., Organic salts, liquid at room temperature, as mobile phases in liquid chromatography. *Journal of Chromatography A* **1986,** *352* (0), 407-425; (c) Colin F, P., Chromatographic and spectroscopic methods for the determination of solvent properties of room temperature ionic liquids. *Journal of Chromatography A* **2004,** *1037* (1-2), 49-82.

38. (a) Kersten, B. R.; Poole, C. F., Influence of concurrent retention mechanisms on the determination of stationary phase selectivity in gas chromatography. *Journal of Chromatography A* **1987,** *399* (0), 1-31; (b) Arancibia, E. L.; Castells, R. C.; Nardillo, A. M., Thermodynamic study of the behaviour of two molten organic salts as stationary phases in gas chromatography. *Journal of Chromatography A* **1987,** *398* (0), 21-29.

39. (a) Armstrong, D. W.; Zhang, L.-K.; He, L.; Gross, M. L., Ionic Liquids as Matrixes for Matrix-Assisted Laser Desorption/Ionization Mass Spectrometry. *Analytical Chemistry* **2001,** *73* (15), 3679-3686; (b) Anderson, J. L.; Ding, J.; Welton, T.; Armstrong, D. W., Characterizing Ionic Liquids On the Basis of Multiple Solvation Interactions. *Journal of the American Chemical Society* **2002,** *124* (47), 14247-14254.

40. Madeira Lau, R.; Sorgedrager, M. J.; Carrea, G.; van Rantwijk, F.; Secundo, F.; Sheldon, R. A., Dissolution of Candida antarctica lipase B in ionic liquids: effects on structure and activity. *Green Chemistry* **2004,** *6* (9), 483-487.

41. (a) Susan, M. A. B. H.; Noda, A.; Mitsushima, S.; Watanabe, M., Bronsted acid-base ionic liquids and their use as new materials for anhydrous proton conductors. *Chemical Communications* **2003,** (8), 938-939; (b) Noda, A.; Susan, M. A. B. H.; Kudo, K.; Mitsushima, S.; Hayamizu, K.; Watanabe, M., Brønsted Acid−Base Ionic Liquids as Proton-Conducting Nonaqueous Electrolytes. *The Journal of Physical Chemistry B* **2003,** *107* (17), 4024-4033; (c) Susan, A. B. H.; Yoo, M. Y.; Nakamoto, H.; Watanabe, M., A novel Bronsted acid-base system as anhydrous proton conductors for fuel cell electrolytes. *Chemistry Letters* **2003,** *32* (9), 836-837.

42. Qu, J.; Truhan, J.; Dai, S.; Luo, H.; Blau, P., Ionic liquids with ammonium cations as lubricants or additives. *Tribology Letters* **2006,** *22* (3), 207-214.

43. Kelvin, W. T., *Baltimore lectures on molecular dynamics and the wave theory of light*. C.J. Clay and Sons: London, 1904.

44. Kreuzfeld, H. J.; Hateley, M. J., 125 years of enantiomers - Back to the roots - Jacobus Henricus van't Hoff 1852-1911. *Enantiomer* **1999,** *4* (6), 491-496.

45. Mosandl, A.; Hener, U.; Kreis, P.; Schmarr, H. G., Enantiomeric distribution of α-pinene, β-pinene and limonene in essential oils and extracts. Part 1. Rutaceae and gramineae. *Flavour and Fragrance Journal* **1990,** *5* (4), 193-199.

46. Friedman, L.; Miller, J. G., Odor Incongruity and Chirality. *Science* **1971,** *172* (3987), 1044-1046.

47. Strong, M., FDA policy and regulation of stereoisomers: Paradigm shift and the future of safer, more effective drugs. *Food and Drug Law Journal* **1999,** *54* (3), 463-487.

48. Hirschler, B. World's top-selling drugs in 2014 vs 2010. http://www.reuters.com/article/2010/04/13/roche-avastin-drugs-idUSLDE63C0BC20100413 (accessed December 17, 2011).

49. Bicchi, C.; D'Amato, A.; Rubiolo, P., Cyclodextrin derivatives as chiral selectors for direct gas chromatographic separation of enantiomers in the essential oil, aroma and flavour fields. *Journal of Chromatography A* **1999,** *843* (1–2), 99-121.

50. Franco, P.; Senso, A.; Oliveros, L.; Minguillón, C., Covalently bonded polysaccharide derivatives as chiral stationary phases in high-performance liquid chromatography. *Journal of Chromatography A* **2001,** *906* (1–2), 155-170.

51. Williams, A. A.; Fakayode, S. O.; Alptuerk, O.; Jones, C. M.; Lowry, M.; Strongin, R. M.; Warner, I. M., Determination of enantiomeric compositions of analytes using novel fluorescent chiral molecular micelles and steady state fluorescence measurements. *Journal of Fluorescence* **2008,** *18* (2), 285-296.

52. Armstrong, D. W.; Tang, Y.; Chen, S.; Zhou, Y.; Bagwill, C.; Chen, J.-R., Macrocyclic Antibiotics as a New Class of Chiral Selectors for Liquid Chromatography. *Analytical Chemistry* **1994,** *66* (9), 1473-1484.

53. Ding, J.; Armstrong, D. W., Chiral ionic liquids: Synthesis and applications. *Chirality* **2005,** *17* (5), 281-292.

54. Yu, S.; Lindeman, S.; Tran, C. D., Chiral Ionic Liquids: Synthesis, Properties, and Enantiomeric Recognition. *The Journal of Organic Chemistry* **2008,** *73* (7), 2576-2591.

55. Howarth, J.; Hanlon, K.; Fayne, D.; McCormac, P., Moisture stable dialkylimidazolium salts as heterogeneous and homogeneous Lewis acids in the Diels-Alder reaction. *Tetrahedron Letters* **1997,** *38* (17), 3097-3100.

56. (a) Bwambok, D. K.; Challa, S. K.; Lowry, M.; Warner, I. M., Amino Acid-Based Fluorescent Chiral Ionic Liquid for Enantiomeric Recognition. *Analytical Chemistry* **2010,** *82* (12), 5028-5037; (b) Tran, C. D.; Mejac, I., Chiral ionic liquids for enantioseparation of pharmaceutical products by capillary electrophoresis. *Journal of Chromatography A* **2008,** *1204* (2), 204-209.

57. Earle, M. J.; McCormac, P. B.; Seddon, K. R., Diels-Alder reactions in ionic liquids - A safe recyclable alternative to lithium perchlorate-diethyl ether mixtures. *Green Chemistry* **1999,** *1* (1), 23-25.

58. Bica, K.; Gaertner, P., Applications of chiral ionic liquids. *European Journal of Organic Chemistry* **2008,** (19), 3235-3250.

59. Patil, M. L.; Sasai, H., Recent developments on chiral ionic liquids: Design, synthesis, and applications. *Chemical Record* **2008,** *8* (2), 98-108.

60. Wasserscheid, P.; Bosmann, A.; Bolm, C., Synthesis and properties of ionic liquids derived from the 'chiral pool'. *Chemical Communications* **2002,** (3), 200-201.

61. (a) de Rooy, S. L.; Li, M.; Bwambok, D. K.; El-Zahab, B.; Challa, S.; Warner, I. M., Ephedrinium-Based Protic Chiral Ionic Liquids for Enantiomeric Recognition. *Chirality* **2011,** *23* (1), 54-62; (b) Li, M.; De Rooy, S. L.; Bwambok, D. K.; El-Zahab, B.; DiTusa, J. F.; Warner, I. M., Magnetic chiral ionic liquids derived from amino acids. *Chemical Communications* **2009,** (45), 6922-6924.

62. Tran, C. D.; Oliveira, D., Fluorescence determination of enantiomeric composition of pharmaceuticals via use of ionic liquid that serves as both solvent and chiral selector. *Analytical Biochemistry* **2006,** *356* (1), 51-58.

63. Tran, C. D.; Oliveira, D.; Yu, S. F., Chiral ionic liquid that functions as both solvent and chiral selector for the determination of enantiomeric compositions of pharmaceutical products. *Analytical Chemistry* **2006,** *78* (4), 1349-1356.

64. Berthod, A.; He, L.; Armstrong, D. W., Ionic liquids as stationary phase solvents for methylated cyclodextrins in gas chromatography. *Chromatographia* **2001,** *53* (1-2), 63-68.

65. Ding, J.; Welton, T.; Armstrong, D. W., Chiral ionic liquids as stationary phases in gas chromatography. *Analytical Chemistry* **2004,** *76* (22), 6819-6822.

66. Yuan, L. M.; Han, Y.; Zhou, Y.; Meng, X.; Li, Z. Y.; Zi, M.; Chang, Y. X., (R)-N,N,N-trimethyl-2-aminobutanol-bis(trifluoromethane-sulfon)imidate chiral ionic liquid used as chiral selector in HPCE, HPLC, and CGC. *Analytical Letters* **2006,** *39* (7), 1439-1449.

67. Rizvi, S. A. A.; Shamsi, S. A., Synthesis, Characterization, and Application of Chiral Ionic Liquids and Their Polymers in Micellar Electrokinetic Chromatography. *Analytical Chemistry* **2006,** *78* (19), 7061-7069.

68. François, Y.; Varenne, A.; Juillerat, E.; Villemin, D.; Gareil, P., Evaluation of chiral ionic liquids as additives to cyclodextrins for enantiomeric separations by capillary electrophoresis. *Journal of Chromatography A* **2007,** *1155* (2), 134-141.

69. Hurley, F. H.; Wier, T. P., Electrodeposition of Metals from Fused Quaternary Ammonium Salts. *Journal of the Electrochemical Society* **1951,** *98* (5), 203-206.

70. Carlin, R. T.; Osteryoung, R. A.; Wilkes, J. S.; Rovang, J., Studies of Titanium(IV) Chloride in a Strongly Lewis Acidic Molten Salt: Electrochemistry and Titanium NMR and Electronic Spectroscopy. *Inorganic Chemistry* **1990,** *29* (16), 3003-3009.

71. Carlin, R. T.; Osteryoung, R. A., Electrochemistry of Molybdenum Chloride Dimers in a. Basic Ambient Temperature Molten Salt. *Inorganic Chemistry* **1988,** *27* (8), 1482-1488.

72. Quigley, R.; Barnard, P. A.; Hussey, C. L.; Seddon, K. R., Electrochemical and Spectroscopic Characterization of $(Nb_6Cl_{12})^{z+}$ Chloride Clusters in the Aluminum Chloride-1-Methyl-3-ethylimidazolium Chloride Molten Salt. *Inorganic Chemistry* **1992,** *31* (7), 1255-1261.

73. Laher, T. M.; Hussey, C. L., Copper(I) and Copper(II) Chloro Complexes in the Basic Aluminum Chloride-1-Methyl-3-Ethylimidazolium Chloride Ionic Liquid. *Inorganic Chemistry* **1983,** *22* (22), 3247-3251.

74. Laher, T. M.; Hussey, C. L., Electrochemical Studies of Chloro Complex-Formation in Low-Temperature Chloroaluminate Melts .1. Iron(II), Iron(III), and Nickel(II). *Inorganic Chemistry* **1982,** *21* (11), 4079-4083.

75. Mallick, B.; Balke, B.; Felser, C.; Mudring, A.-V., Dysprosium room-temperature ionic liquids with strong luminescence and response to magnetic fields. *Angewandte Chemie-International Edition* **2008,** *47* (40), 7635-7638.

76. (a) Del Sesto, R. E.; McCleskey, T. M.; Burrell, A. K.; Baker, G. A.; Thompson, J. D.; Scott, B. L.; Wilkes, J. S.; Williams, P., Structure and magnetic behavior of transition metal based ionic liquids. *Chemical Communications* **2008,** (4), 447-449; (b) Pitula, S.; Mudring, A.-V., Synthesis, Structure, and Physico-optical Properties of Manganate(II)-Based Ionic Liquids. *Chemistry – A European Journal* **2010,** *16* (11), 3355-3365.

77. Del Sesto, R. E.; Corley, C.; Robertson, A.; Wilkes, J. S., Tetraalkylphosphonium-based ionic liquids. *Journal of Organometallic Chemistry* **2005,** *690* (10), 2536-2542.

78. Yoshida, Y.; Tanaka, H.; Saito, G., Organic Paramagnetic Ionic Liquids Based on Anion Containing 2,2,6,6-Tetramethyl-1-piperidinyloxyl Radical Moiety. *Chemistry Letters* **2007,** *36* (9), 1096-1097.

79. Xie, Z.-L.; Taubert, A., Thermomorphic Behavior of the Ionic Liquids [C4mim][FeCl4] and [C12mim][FeCl4]. *ChemPhysChem* **2011,** *12* (2), 364-368.

80. Dobbelin, M.; Jovanovski, V.; Llarena, I.; Claros Marfil, L. J.; Cabanero, G.; Rodriguez, J.; Mecerreyes, D., Synthesis of paramagnetic polymers using ionic liquid chemistry. *Polymer Chemistry* **2011,** *2* (6), 1275-1278.

81. Kim, J.-Y.; Kim, J.-T.; Song, E.-A.; Min, Y.-K.; Hamaguchi, H.-o., Polypyrrole Nanostructures Self-Assembled in Magnetic Ionic Liquid as a Template. *Macromolecules* **2008,** *41* (8), 2886-2889.

82. Tesfai, A.; El-Zahab, B.; Kelley, A. T.; Li, M.; Garno, J. C.; Baker, G. A.; Warner, I. M., Magnetic and Nonmagnetic Nanoparticles from a Group of Uniform Materials Based on Organic Salts. *Acs Nano* **2009,** *3* (10), 3244-3250.

83. Bica, K.; Gmeiner, G.; Reichel, C.; Lendl, B.; Gaertner, P., Microwave-Assisted Synthesis of Camphor-Derived Chiral Imidazolium Ionic Liquids and Their Application in Diastereoselective Diels-Alder Reaction. *Synthesis* **2007,** *2007* (EFirst), 1333,1338.

84. Nockemann, P.; Thijs, B.; Postelmans, N.; Van Hecke, K.; Van Meervelt, L.; Binnemans, K., Anionic Rare-Earth Thiocyanate Complexes as Building Blocks for Low-Melting Metal-Containing Ionic Liquids. *Journal of the American Chemical Society* **2006,** *128* (42), 13658-13659.

85. Tang, S.; Babai, A.; Mudring, A.-V., Europium-Based Ionic Liquids as Luminescent Soft Materials. *Angewandte Chemie International Edition* **2008,** *47* (40), 7631-7634.

86. Paul, A.; Mandal, P. K.; Samanta, A., On the Optical Properties of the Imidazolium Ionic Liquids. *The Journal of Physical Chemistry B* **2005,** *109* (18), 9148-9153.

87. Dong, B.; Gao, Y. a.; Su, Y.; Zheng, L.; Xu, J.; Inoue, T., Self-Aggregation Behavior of Fluorescent Carbazole-Tailed Imidazolium Ionic Liquids in Aqueous Solutions. *The Journal of Physical Chemistry B* **2009,** *114* (1), 340-348.

88. Chen, X.-W.; Liu, J.-W.; Wang, J.-H., A Highly Fluorescent Hydrophilic Ionic Liquid as a Potential Probe for the Sensing of Biomacromolecules. *The Journal of Physical Chemistry B* **2011,** *115* (6), 1524-1530.

89. Loe-Mie, F.; Marchand, G.; Berthier, J.; Sarrut, N.; Pucheault, M.; Blanchard-Desce, M.; Vinet, F.; Vaultier, M., Towards an Efficient Microsystem for the Real-Time Detection and Quantification of Mercury in Water Based on a Specifically Designed Fluorogenic Binary Task-Specific Ionic Liquid. *Angewandte Chemie International Edition* **2010,** *49* (2), 424-427.

90. Yung, K. Y.; Schadock-Hewitt, A. J.; Hunter, N. P.; Bright, F. V.; Baker, G. A., 'Liquid litmus': chemosensory pH-responsive photonic ionic liquids. *Chemical Communications* **2011,** *47* (16), 4775-4777.

91. (a) Burda, C.; Chen, X.; Narayanan, R.; El-Sayed, M. A., Chemistry and Properties of Nanocrystals of Different Shapes. *Chemical Reviews* **2005,** *105* (4), 1025-1102; (b) Rao,

C. N. R.; Cheetham, A. K., Science and technology of nanomaterials: current status and future prospects. *Journal of Materials Chemistry* **2001,** *11* (12), 2887-2894.

92. Liu, H.; Webster, T. J., Nanomedicine for implants: A review of studies and necessary experimental tools. *Biomaterials* **2007,** *28* (2), 354-369.

93. Cummins, D.; Boschloo, G.; Ryan, M.; Corr, D.; Rao, S. N.; Fitzmaurice, D., Ultrafast Electrochromic Windows Based on Redox-Chromophore Modified Nanostructured Semiconducting and Conducting Films. *The Journal of Physical Chemistry B* **2000,** *104* (48), 11449-11459.

94. Bruce, P. G.; Scrosati, B.; Tarascon, J.-M., Nanomaterials for Rechargeable Lithium Batteries. *Angewandte Chemie International Edition* **2008,** *47* (16), 2930-2946.

95. Gao, J.; Gu, H.; Xu, B., Multifunctional Magnetic Nanoparticles: Design, Synthesis, and Biomedical Applications. *Accounts of Chemical Research* **2009,** *42* (8), 1097-1107.

96. Serrano, E.; Rus, G.; García-Martínez, J., Nanotechnology for sustainable energy. *Renewable and Sustainable Energy Reviews* **2009,** *13* (9), 2373-2384.

97. Endres, F.; El Abedin, S. Z., Electrodeposition of stable and narrowly dispersed germanium nanoclusters from an ionic liquid. *Chemical Communications* **2002,** (8), 892-893.

98. Trewyn, B. G.; Whitman, C. M.; Lin, V. S. Y., Morphological control of room-temperature ionic liquid templated mesoporous silica nanoparticles for controlled release of antibacterial agents. *Nano Letters* **2004,** *4* (11), 2139-2143.

99. Miyauchi, M.; Miao, J.; Simmons, T. J.; Lee, J.-W.; Doherty, T. V.; Dordick, J. S.; Linhardt, R. J., Conductive Cable Fibers with Insulating Surface Prepared by Coaxial Electrospinning of Multiwalled Nanotubes and Cellulose. *Biomacromolecules* **2010,** *11* (9), 2440-2445.

100. Kim, T.; Lee, H.; Kim, J.; Suh, K. S., Synthesis of Phase Transferable Graphene Sheets Using Ionic Liquid Polymers. *Acs Nano* **2010,** *4* (3), 1612-1618.

101. (a) Yuan, J.; Antonietti, M., Poly(ionic liquid) Latexes Prepared by Dispersion Polymerization of Ionic Liquid Monomers. *Macromolecules* **2011,** *44* (4), 744-750; (b) Hu, X.; Huang, J.; Zhang, W.; Li, M.; Tao, C.; Li, G., Photonic Ionic Liquids Polymer for Naked-Eye Detection of Anions. *Advanced Materials* **2008,** *20* (21), 4074-+.

102. (a) Scheibe, G.; Rivas, A., A new method in quantitive emission spectral analysis adaptable also as a micro method. *Angewandte Chemie* **1936,** *49*, 0443-0446; (b) Scheibe, G., Auxiliary valency as the cause of variability in the absorption spectra in solutions. *Angewandte Chemie* **1937,** *50*, 0212-0219; (c) Jelley, E. E., Spectral absorption and fluorescence of dyes in the molecular state. *Nature* **1936,** *138*, 1009-1010.

103. (a) Wuerthner, F.; Kaiser, T. E.; Saha-Moeller, C. R., J-Aggregates: From Serendipitous Discovery to Supramolecular Engineering of Functional Dye Materials. *Angewandte Chemie-International Edition* **2011,** *50* (15), 3376-3410; (b) Fukutake, N.; Kobayashi, T., Size distribution of pseudoisocyanine (PIC) J-aggregates studied by near-field absorption spectroscopy. *Chemical Physics Letters* **2002,** *356* (3-4), 368-374.

104. (a) Czikklely, V.; Forsterling, H. D.; Kuhn, H., Extended dipole model for aggregates of dye molecules. *Chemical Physics Letters* **1970,** *6* (3), 207-210; (b) Nuesch, F.; Gratzel, M., H-Aggregation and Correlated Absorption and Emission of a Merocyanine Dye in Solution, at the Surface and in the Solid state. A Link Between Crystal Structure and Photophysical Properties. *Chemical Physics* **1995,** *193* (1-2), 1-17.

105. Wang, M. M.; Silva, G. L.; Armitage, B. A., DNA-templated formation of a helical cyanine dye J-aggregate. *Journal of the American Chemical Society* **2000,** *122* (41), 9977-9986.

106. (a) Girling, I. R.; Cade, N. A.; Kolinsky, P. V.; Jones, R. J.; Peterson, I. R.; Ahmad, M. M.; Neal, D. B.; Petty, M. C.; Roberts, G. G.; Feast, W. J., Second-harmonic generation in mixed hemicyanine: fatty-acid Langmuir-Blodgett monolayers. *J. Opt. Soc. Am. B* **1987,** *4* (6), 950-954; (b) Knoester, J., Collective Nonlinear-Optical Properties of Disordered J-Aggregates. *Advanced Materials* **1995,** *7* (5), 500-502.

107. Gilman, P. B., Review of Mechanisms of Supersensitization. *Photographic Science and Engineering* **1974,** *18* (4), 418-430.

108. (a) Sayama, K.; Tsukagoshi, S.; Mori, T.; Hara, K.; Ohga, Y.; Shinpou, A.; Abe, Y.; Suga, S.; Arakawa, H., Efficient sensitization of nanocrystalline TiO2 films with cyanine and merocyanine organic dyes. *Solar Energy Materials and Solar Cells* **2003,** *80* (1), 47-71; (b) Ehret, A.; Stuhl, L.; Spitler, M. T., Spectral sensitization of TiO2 nanocrystalline electrodes with aggregated cyanine dyes. *Journal of Physical Chemistry B* **2001,** *105* (41), 9960-9965.

109. Suzuki, M.-A.; Hashida, T.; Hibino, J.; Kishimoto, Y., Multiple Optical Memory using Photochromic Spiropyran Aggregates. *Molecular Crystals and Liquid Crystals Science and Technology. Section A. Molecular Crystals and Liquid Crystals* **1994,** *246* (1), 389-396.

110. (a) Kamat, P. V.; Fox, M. A., Photophysics and Photochemistry of Xanthene Dyes in Polymer-Solutions and Films. *Journal of Physical Chemistry* **1984,** *88* (11), 2297-2302; (b) Das, S.; Kamat, P. V., Can H-Aggregates Serve as Light-Harvesting Antennae? Triplet−Triplet Energy Transfer between Excited Aggregates and Monomer Thionine in Aersol-OT Solutions. *The Journal of Physical Chemistry B* **1998,** *103* (1), 209-215.

111. (a) Yao, H.; Isohashi, T.; Kimura, K., Electrolyte-induced mesoscopic aggregation of thiacarbocyanine dye in aqueous solution: Counterion size specificity. *Journal of Physical Chemistry B* **2007,** *111* (25), 7176-7183; (b) West, W.; Pearce, S., Dimeric State of Cyanine Dyes. *Journal of Physical Chemistry* **1965,** *69* (6), 1894-&; (c) Lamm, M. E.;

Neville, D. M., Dimer Spectrum of Acridine Orange Hydrochloride. *Journal of Physical Chemistry* **1965,** *69* (11), 3872-&; (d) Akins, D. L.; Macklin, J. W., Dependence of Raman-Scattering by Aggregated 2,2'-Cyanine on pH and Excitation Wavelength. *Journal of Physical Chemistry* **1989,** *93* (16), 5999-6007; (e) Valdesaguilera, O.; Neckers, D. C., Aggregation Phenomena in Xanthene Dyes. *Accounts of Chemical Research* **1989,** *22* (5), 171-177.

112. Kumar, V.; Baker, G. A.; Pandey, S., Ionic liquid-controlled J- versus H-aggregation of cyanine dyes. *Chemical Communications* **2011,** *47* (16).

113. Liu, H.; Xu, J.; Li, Y.; Li, Y., Aggregate Nanostructures of Organic Molecular Materials. *Accounts of Chemical Research* **2010,** *43* (12), 1496-1508.

114. (a) Zhao, Y. S.; Fu, H.; Peng, A.; Ma, Y.; Xiao, D.; Yao, J., Low-Dimensional Nanomaterials Based on Small Organic Molecules: Preparation and Optoelectronic Properties. *Advanced Materials* **2008,** *20* (15), 2859-2876; (b) Zhao, Y. S.; Fu, H.; Peng, A.; Ma, Y.; Liao, Q.; Yao, J., Construction and Optoelectronic Properties of Organic One-Dimensional Nanostructures. *Accounts of Chemical Research* **2010,** *43* (3), 409-418.

115. Zang, L.; Che, Y.; Moore, J. S., One-Dimensional Self-Assembly of Planar pi-Conjugated Molecules: Adaptable Building Blocks for Organic Nanodevices. *Accounts of Chemical Research* **2008,** *41* (12), 1596-1608.

116. (a) Xiao, J.; Yin, Z.; Yang, B.; Liu, Y.; Ji, L.; Guo, J.; Huang, L.; Liu, X.; Yan, Q.; Zhang, H.; Zhang, Q., Preparation, characterization, physical properties, and photoconducting behaviour of anthracene derivative nanowires. *Nanoscale* **2011,** *3* (11); (b) Wu, J. H.; Guan, Z.; Xu, T. Z.; Xu, Q.-H.; Xu, G. Q., Tetracene-Doped Anthracene Nanowire Arrays: Preparation and Doping Effects. *Langmuir* **2011,** *27* (10), 6374-6380.

117. (a) Lee, S. J.; Hupp, J. T.; Nguyen, S. T., Growth of Narrowly Dispersed Porphyrin Nanowires and Their Hierarchical Assembly into Macroscopic Columns. *Journal of the American Chemical Society* **2008,** *130* (30), 9632-9633; (b) Fathalla, M.; Neuberger, A.; Li, S.-C.; Schmehl, R.; Diebold, U.; Jayawickramarajah, J., Straightforward Self-Assembly of Porphyrin Nanowires in Water: Harnessing Adamantane/β-Cyclodextrin Interactions. *Journal of the American Chemical Society* **2010,** *132* (29), 9966-9967.

118. (a) Briseno, A. L.; Aizenberg, J.; Han, Y.-J.; Penkala, R. A.; Moon, H.; Lovinger, A. J.; Kloc, C.; Bao, Z., Patterned Growth of Large Oriented Organic Semiconductor Single Crystals on Self-Assembled Monolayer Templates. *Journal of the American Chemical Society* **2005,** *127* (35), 12164-12165; (b) Briseno, A. L.; Mannsfeld, S. C. B.; Jenekhe, S. A.; Bao, Z.; Xia, Y., Introducing organic nanowire transistors. *Materials Today* **2008,** *11* (4), 38-47.

119. (a) Kim, F. S.; Ren, G.; Jenekhe, S. A., One-Dimensional Nanostructures of π-Conjugated Molecular Systems: Assembly, Properties, and Applications from Photovoltaics, Sensors, and Nanophotonics to Nanoelectronics†. *Chemistry of Materials* **2010,** *23* (3), 682-732; (b) Zheng, J. Y.; Yan, Y.; Wang, X.; Zhao, Y. S.; Huang, J.; Yao,

J., Wire-on-Wire Growth of Fluorescent Organic Heterojunctions. *Journal of the American Chemical Society* **2012,** *134* (6), 2880-2883.

120. Lakowicz, J. R., *Principles of Fluorescence Spectroscopy* 2nd ed.; Kluwer: New York, 1999.

121. Adhikari, A.; Das, D. K.; Sasmal, D. K.; Bhattacharyya, K., Ultrafast FRET in a Room Temperature Ionic Liquid Microemulsion: A Femtosecond Excitation Wavelength Dependence Study. *The Journal of Physical Chemistry A* **2009,** *113* (16), 3737-3743.

122. Izawa, H.; Wakizono, S.; Kadokawa, J.-i., Fluorescence resonance-energy-transfer in systems of Rhodamine 6G with ionic liquid showing emissions by excitation at wide wavelength areas. *Chemical Communications* **2010,** *46* (34), 6359-6361.

123. Wakizono, S.; Yamamoto, K.; Kadokawa, J.-i., FRET function of polymeric ionic liquid film containing rhodamine moieties for exhibiting emissions by excitation at wide wavelength areas. *Journal of Photochemistry and Photobiology a-Chemistry* **2011,** *222* (1), 283-287.

124. Baker, S. N.; Zhao, H.; Pandey, S.; Heller, W. T.; Bright, F. V.; Baker, G. A., Fluorescence energy transfer efficiency in labeled yeast cytochrome c: a rapid screen for ion biocompatibility in aqueous ionic liquids. *Physical Chemistry Chemical Physics* **2011,** *13* (9), 3642-3644.

125. Tang, B.; Cao, L.; Xu, K.; Zhuo, L.; Ge, J.; Li, Q.; Yu, L., A New Nanobiosensor for Glucose with High Sensitivity and Selectivity in Serum Based on Fluorescence Resonance Energy Transfer (FRET) between CdTe Quantum Dots and Au Nanoparticles. *Chemistry – A European Journal* **2008,** *14* (12), 3637-3644.

126. Zheng, J. Y.; Zhang, C.; Zhao, Y. S.; Yao, J., Detection of chemical vapors with tunable emission of binary organic nanobelts. *Physical Chemistry Chemical Physics* **2010,** *12* (40).

127. Rutten, F. J. M.; Tadesse, H.; Licence, P., Rewritable imaging on the surface of frozen ionic liquids. *Angewandte Chemie-International Edition* **2007,** *46* (22), 4163-4165.

128. Tesfai, A.; El-Zahab, B.; Bwambok, D. K.; Baker, G. A.; Fakayode, S. O.; Lowry, M.; Warner, I. M., Controllable formation of ionic liquid micro- and nanoparticles via a melt-emulsion-quench approach. *Nano Letters* **2008,** *8* (3), 897-901.

129. (a) Bwambok, D. K.; El-Zahab, B.; Challa, S. K.; Li, M.; Chandler, L.; Baker, G. A.; Warner, I. M., Near-Infrared Fluorescent NanoGUMBOS for Biomedical Imaging. *ACS Nano* **2009,** *3* (12), 3854-3860; (b) Das, S.; Bwambok, D.; El-Zahab, B.; Monk, J.; de Rooy, S. L.; Challa, S.; Li, M.; Hung, F. R.; Baker, G. A.; Warner, I. M., Nontemplated Approach to Tuning the Spectral Properties of Cyanine-Based Fluorescent NanoGUMBOS. *Langmuir* **2010,** *26* (15), 12867-12876.

130. Cole, M. R.; Li, M.; El-Zahab, B.; Janes, M. E.; Hayes, D.; Warner, I. M., Design, Synthesis, and Biological Evaluation of β-Lactam Antibiotic-Based Imidazolium- and Pyridinium-Type Ionic Liquids. *Chemical Biology & Drug Design* **2011,** *78* (1), 33-41.

131. Skoog, D. A. W., Donald M.; Holler, F. James, *Fundamentals of Analytical Chemistry*. 7th edition ed.; Saunders College Publishing: New York, 1996.

132. Rodger, A. N., Bengt., *Circular and Linear Dichroism*. 1st edition ed.; Oxford University Press: New York, 1997.

133. B., V., *Molecular Fluorescence: Principles and Applications*. Wiley-VCH: New York, 2002.

134. (a) Periasamy, A.; Wodnicki, P.; Wang, X. F.; Kwon, S.; Gordon, G. W.; Herman, B., Time-resolved fluorescence lifetime imaging microscopy using a picosecond pulsed tunable dye laser system. *Review of Scientific Instruments* **1996,** *67* (10), 3722-3731; (b) Valeur, B., *Molecular Fluorescence: Principles and Applications*. Wiley-VCH: 2001.

135. D., R. F. W., *Fluorescence Microscopy*. Cambridge University Press, 1992.

136. Reimer, L., *Scanning electron microscopy: physics of image formation and microanalysis*. Springer: 1998.

137. J., G., *Scanning electron microscopy and x-ray microanalysis*. 3rd ed.; Springer: 2003.

138. De Graef, M., *Introduction to conventional transmission electron microscopy*. Cambridge University Press: Cambridge, 2003.

139. Williams, D. B. C., C. B., *Transmission electron microscopy: Imaging*. Springer: 1996.

140. (a) Good, J. Cryogenic Limited. http://www.cryogenic.co.uk/products/measurement/s600x.asp (accessed March 14, 2012); (b) Weinstock, H., *SQUID sensors: fundamentals, fabrication, and applications*. Kluwer Academic Publishers: Dordrecht, 1996.

141. Clarke, J. B., A. I., *The SQUID handbook: Applications of SQUIDS and SQUID Systems*. Wiley-VCH: Weinhein, 2006; Vol. Volume 1.

CHAPTER 2

EPHEDRINIUM-BASED PROTIC CHIRAL IONIC LIQUIDS FOR ENANTIOMERIC RECOGNITION

2.1. Introduction

Over the last decade, an increased interest in the study of ionic liquids (ILs) has been observed from data in the literature.[1] Their unique physicochemical have allowed for the applications in a variety of different areas which include separations,[2] catalysis,[3] electrochemistry,[4] and spectroscopy.[5]

Chiral ionic liquids (CILs) have been used in gas chromatography as stationary phases,[6] as catalysts in organic synthesis,[7] and also as chiral selectors and solvents in fluorescence spectroscopy.[6-8] Protic ionic liquids (PILs) have proven successful for heterogeneous catalysis and for the synthesis of polymeric materials that are good proton conductors in fuel cells.[9] However, relatively few studies have been performed where physicochemical properties of structurally related PILs were investigated. In one study, the ionic conductivity and thermal properties of 21 ionic liquids, prepared through the reaction of various amines with tetrafluoro boric acid, were investigated. The measured properties appeared to be dependent on both cation and anion structure.[10] In another study, the physico-chemical properties of a series of alkylammonium-based PILs with different organic and inorganic anions were studied.[11] In the same study, the authors suggested that PILs could possibly be synthesized through rational design aimed at specific applications.

Ephedrine is an alkaloid that serves as a decongestant, stimulant, and appetite suppressant.[12] It belongs to a group of precursors which has been used for synthesizing CILs from the chiral pool. Wasserscheid and coworkers reported an aprotic *N*,*N*-dimethylephedrinium

IL employing a three step synthesis, which included a Leuckart–Wallach reaction with (-)-(1R, 2S)-ephedrine, followed by alkylation with dimethylsulfate and ion exchange with lithium bis(trifluoromethylsulfonyl)imide ([Li][Tf_2N]).[13] A green, solvent-less method was subsequently developed for the synthesis of similar CILs. For example, (1R, 2S)-N-methylephedrine was alkylated with bromoalkanes under microwave irradiation followed by ion-exchange.[14] This method yielded aprotic ephedrinium CILs with different alkyl chain lengths and anions. Several *N*,*N*-dimethylephedrinium-based ionic liquids were used for the enantiomeric gas chromatographic separation of a series of chiral compounds such as chiral alcohols (including diols), chiral sulfoxides, some chiral epoxides, and acetylated amines.[6b] In addition, the aprotic ephedrinium CIL was also employed for asymmetric glycine alkylation in the presence of optically active orthopalladated phenanthrylamine as a phase transfer catalyst.[13, 15]

In the current study protic chiral ionic liquids (PCILs) derived from structurally related alkaloids such as norephedrine (NorEph), ephedrine (Eph), and methylephedrine (MeEph) were synthesized through facile acid-base neutralization with fluorinated imide acids. This neutralization leads to the formation of a series of primary, secondary, and tertiary amine-based PCILs, respectively (Figure 2.1). Thus, the PCILs described are all protic in contrast to the aprotic ephedrinium CILs reported elsewhere.[13] Herein, we report the effects of the degree of alkylation (varying hydrogen bonding and van der Waals bonding capability, as well as steric hindrance) on the physicochemical properties and chiral recognition abilities of these ephedrinium based PCILs.

2.2. Materials and Methods

2.2.1. Chemicals and Materials

L-(−)-Norephedrine, D-(+)-norephedrine, (-)-ephedrine, (+)-ephedrine, (−)-*N*-methylephedrine, (+)-*N*-methylephedrine, racemic Mosher's acid and bis(trifluoromethanesulfonyl)imide were purchased from Sigma-Aldrich (Milwaukee, WI). Enantiomerically pure chiral analytes of propranolol, 1-(9-anthryl)-2,2,2-trifluoroethanol, 1,1′-binaphthyl-2,2′-diamine, 1,1′-binaphthyl-2,2′-diyl hydrogen phosphate, glucose, and serine were also purchased from Sigma-Aldrich (Milwaukee, WI). Bis(pentafluoroethane)sulfonimide was purchased from SynQuest Laboratories, Inc. (Alachua, FL). All solvents used including acetonitrile and dichloromethane were of HPLC grade (J.T. Baker, Philipsburg, NJ). Deuterated solvents such as chloroform-d_1, D_2O and dimethyl sulfoxide-d_6 were obtained from Sigma-Aldrich (Milwaukee, WI). All reagents were used without further purification. Triply deionized ultra-pure water (18.2 MΩ) obtained using an Elga model PURELAB Ultra™ water filtration system was used in the study.

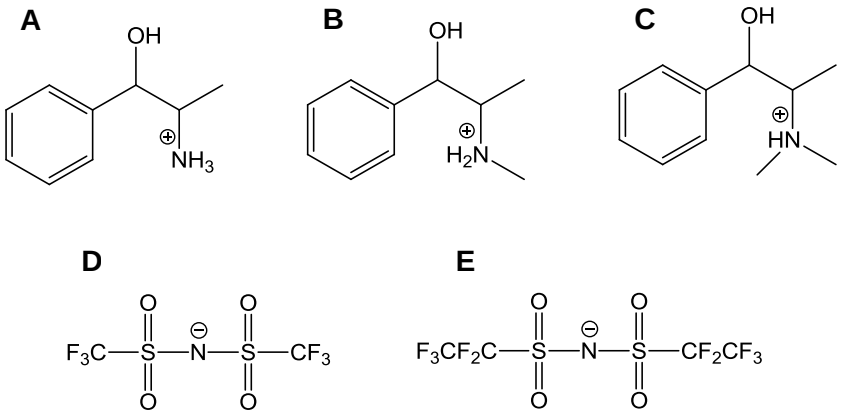

Figure 2.1. Structures of PCIL cations (A) [NorHeph$^+$], (B) [HEph$^+$], (C) [MeHEph$^+$] and anions (D) [Tf_2N^-] and (E) [BETI$^-$].

2.2.2. General Instrumental Methods

^{1}H-NMR (400 MHz) and ^{13}C-NMR (100 MHz) spectra were acquired by use of a Bruker AV-400 spectrometer. The ^{1}H-NMR and ^{13}C-NMR chemical shifts are given in parts per million (δ) with respect to TMS as an internal standard. ^{19}F NMR (236 MHz) spectra were acquired on a Bruker DPX 250 NMR spectrometer. Solvents used for preparing the samples were DMSO-d_6 for ^{1}H-NMR and ^{13}C-NMR and $CDCl_3$ for ^{19}F-NMR. Elemental analyses were conducted by Atlantic Microlab (Atlanta, GA). Samples were also analyzed with mass spectrometry on a Hitachi MS-8000 3DQ LC-ion trap mass spectrometer with electrospray and APCI ionization methods in both the positive and negative ion mode. The moisture contents of synthesized PCILs were measured with a Mettler Toledo DL32 Karl Fischer Coulometric titrator. Circular dichroism (CD) measurements were obtained by analyzing 1 mM methanolic solutions at room temperature in 4 mm quartz cuvettes on a Jasco-710 spectropolarimeter. Thermal stability was determined with a TGA Q50 thermogravimetric analyzer (TA Instrument Inc.) by heating 10 mg of sample under nitrogen at a rate of 15 °Cmin^{-1} from 25 to 550 °C. Similarly, thermal transistions were investigated with a DSC Q 100 differential calorimeter (TA Instrument Inc., USA) by cooling a 5-10 mg sample of PCIL to -80 °C and subsequently heating it at a rate of 5 °Cmin^{-1} to 150 °C.

Fluorescence analyses were performed in the steady-state mode on a Spex Fluorolog-3 spectrofluorimeter (model FL3-22TAU3; Jobin Yvon Edison, NJ) equipped with a 450 Watt Xe lamp and R928 PMT emission detector. Excitation and emission wavelengths with 3 nm bandpasses were selected as well as an integration time of 0.1 s per point. Fluorescence data was corrected by taking the quotient of the analyte signal and the reference signal.

2.2.3. Representative Procedure: Synthesis of [MeHEph][Tf_2N]

A known amount of (1S-2R)-methylephedrine; MeEph (0.50 g, 3.31 mmol) was dissolved in water and reacted with equimolar bis(trifluoromethanesulfonyl)imide by slow addition and stirring to obtain [MeHEph][Tf_2N] (Scheme 2.1). The neutralization reaction was performed in an ice bath for 6 hours. The mixture was subsequently stirred at room temperature for 12 hours. After water was removed *in vacuo* by freeze-drying, a viscous colorless liquid was obtained. The resulting PCIL was further purified by washing with small amounts of triple distilled water and subsequently freeze-dried by lyophilization. [MeHEph][Tf_2N], colorless liquid, 90.3 %, ^{1}H-NMR (250 MHz, DMSO-d_6) δ (ppm): 7.40 (s, 3H), 7.30 (s, 2H), 76.2 (s, 3H), 5.22 (d, 1H), 3.47 (m, 1H), 2.81 (s, 1H), 1.0 (d, J = 6.8 Hz, 3H). ^{13}C-NMR δ (ppm): 142.0, 128.7 127.9, 126.2, 121.6, 118.4, 115.2, 114.2, 69.0, 66.0, 41.2, 7.4. Anal Calcd for $C_{13}H_{18}F_6N_2O_5S_2$: C, 33.88; H, 3.90; N, 6.08. Found: C, 34.09; H, 3.81; N, 6.09.

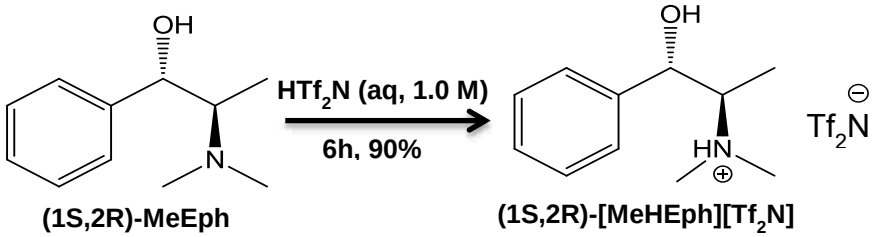

Scheme 2.1. Synthesis of [MeHEph][Tf_2N].

2.3. Results and Discussion

2.3.1. Synthesis and Characterization of Ephedrine-Based PCILs

The synthesized PCILs were characterized by use of ^{1}H and ^{13}C NMR, elemental analysis, and electrospray ionization mass spectrometry (ESI-MS). The results from ^{1}H and ^{13}C NMR were in agreement with the chemical structures of the PCILs and were further confirmed with elemental analysis. The respective ^{1}H and ^{13}C NMR spectra were also compared with

those of the precursors from which the PCILs were derived. As expected, the spectra were similar, since the chemical structures of the product PCILs only differed from the corresponding chiral precursors in their anions. Fluorine (^{19}F) NMR was used to confirm the success of neutralization (introduction of fluorinated anions). Mass spectrometry was conducted in the positive and negative ion mode. For [NorHEph][Tf_2N], [HEph][Tf_2N] and [MeHEph][Tf_2N] PCILs in the positive ion mode a strong peak is observed for each of the respective parent ions with m/z = 152.10, 166.12 and 180.13 confirming their presence. In the negative ion mode the presence of [Tf_2N^-] and [$BETI^-$] for [NorHEph][Tf_2N] and [NorHEph][BETI] was confirmed by strong peaks observed at m/z = 279.18 and 379.19.

In order to determine whether configurational integrity was maintained throughout the synthesis, circular dichroism (CD) was used to compare the bands of the starting materials and the PCIL products. The CD spectra of both enantiomers of MeEph and ionic liquids derived therefrom, [MeHEph][Tf_2N], are shown in Figure 2.2. The relative peak intensities of both enantiomers of MeEph and [MeHEph][Tf_2N] remained constant throughout the synthesis, suggesting that chirality was maintained.

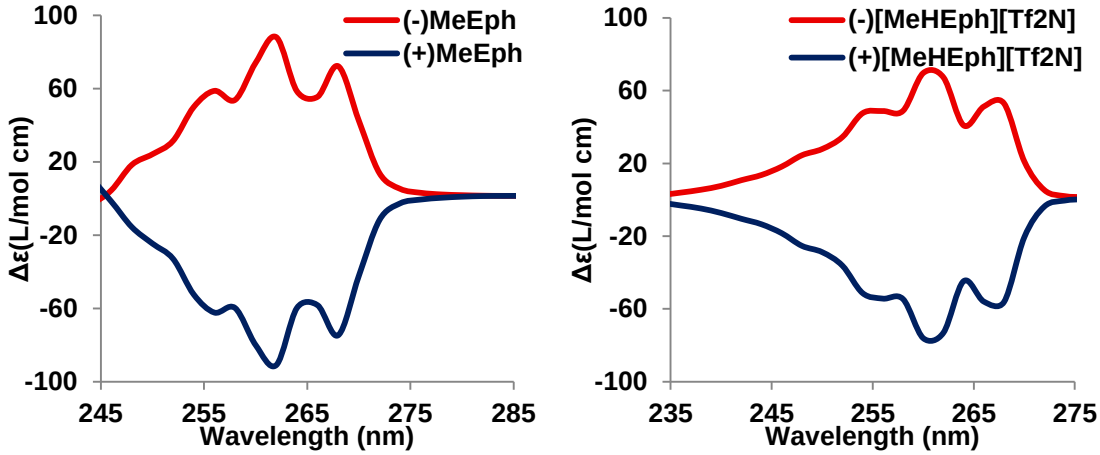

Figure 2.2. Circular dichroism of enantiomers (+ and -) of (A) 10 mM MeEph (starting material) and (B) 10 mM [MeHEph][Tf_2N] (PCIL) in methanol.

After purification, which was followed by freeze-drying overnight and subsequent purging with argon gas, the water content of the PCILs was determined using coulometric Karl-Fischer titration. The water content of the PCILs varied between 50 and 150 ppm (Table 2.1). All other PCILs were characterized in the same manner as [MeHEph][Tf_2N]. The PCILs were viscous liquids at room temperature.

2.3.2. Thermal Properties of PCILs

The thermal stabilities of the PCILs were studied by use of thermal gravimetric analysis (TGA). Samples were heated under nitrogen atmosphere at a rate of 15 °Cmin^{-1}, from room temperature up to 600 °C. Thermal decomposition of the PCILs started between 230 °C and 250 °C with onset temperatures around 400 °C (Table 2.2). PILs with ammonium, imidazolium, or other heterocyclic cations generally exhibit good thermal stabilities and low melting points when coupled with [Tf_2N^-] anions.[16] The ephedrinium-based PCILs with [Tf_2N^-] anions exhibited higher thermal stability than those with [$BETI^-$] anions (Table 2.2). These results were consistent with earlier reports for ammonium-based PILs where similar trends were observed.[17]

Table 2.1. Moisture content of PCILs measured by Karl-Fischer titration.

PCIL	H_2O content (ppm)	Mass (mg)
[NorHEph][Tf_2N]	93.0	7.2
[NorHEph][BETI]	99.8	10.0
[HEph][Tf_2N]	150.1	14.1
[HEph][BETI]	53.2	5.3
[MeHEph][Tf_2N]	55.9	8.6
[MeHEph][BETI]	47.5	11.8

The thermal properties of the PCILs where investigated by use of DSC. The PCILs were cooled from room temperature to -80 °C, followed by heating to 150 °C at a rate of 5 °C min^{-1} under nitrogen. Crystallization and melting transitions were not observed for the PCILs under these conditions. A glass transition (T_g) between -60 and -20 °C was observed for the PCILs

increasing in the order [NorHEph][Tf_2N], [HEph][Tf_2N], and [MeHEph][Tf_2N]. The [$BETI^-$]-containing PCILs displayed higher T_g values than the [Tf_2N^-]-containing PCILs, due to the higher polarizability of these anions. Similar results have been reported in the literature for previous studies. [18]

Table 2.2. Thermal properties of ephedrine-based PCILs.

CIL	T_g (°C)[a]	T_{start} (°C)[b]	T_{onset} (°C)[c]
[NorHEph][Tf_2N]	-53.9	216.4	414.8
[NorHEph][BETI]	-27.1	222.0	382.5
[HEph][Tf_2N]	-48.6	248.0	417.5
[HEph][BETI]	-31.2	249.2	383.5
[MeHEph][Tf_2N]	-41.3	242.6	436.3
[MeHEph][BETI]	-33.1	231.3	391.3

[a]Glass transition temperature. [b]The beginning decomposition temperature. [c]The temperature at which the sample loses weight at the fastest speed.

2.3.3. Enantiomeric Recognition Studies of PCILs towards Racemic Mosher's salt using ^{19}F-NMR

Enantiomeric recognition capabilities of the PCILs were investigated by employing a previously described method in which CILs derived from aminobutanol, valine, and methylephedrine were dissolved in a deuterated solvent with racemic Mosher acid sodium salt.[13] The chemical shift differences and peak splittings of the two diastereomeric associates were measured by use of ^{19}F-NMR, where the extent of peak splitting of CF_3 in Mosher's salt was related to the strength of diastereomeric interactions. Potassium Mosher's salt was obtained by neutralization of Mosher's acid solution with equimolar amounts of potassium hydroxide and subsequent freeze-drying and lyophilization. The feedstock solution for the ^{19}F-NMR tests was prepared by dissolving 121.3 mg racemic Mosher's salt (0.45 mmol) and 119.5 mg of crown ether (18C6, 0.45 mmol) in 15 mL $CDCl_3$ as previously reported.[19] The 18C6 was added to increase solubility of potassium Mosher's salt in chloroform-d_1 by forming a complex between

potassium and crown ether.[20] For ^{19}F-NMR analysis, a 5 fold molar excess of respective PCIL with regard to potassium Mosher's salt was dissolved in 0.5 mL of the feedstock solution.

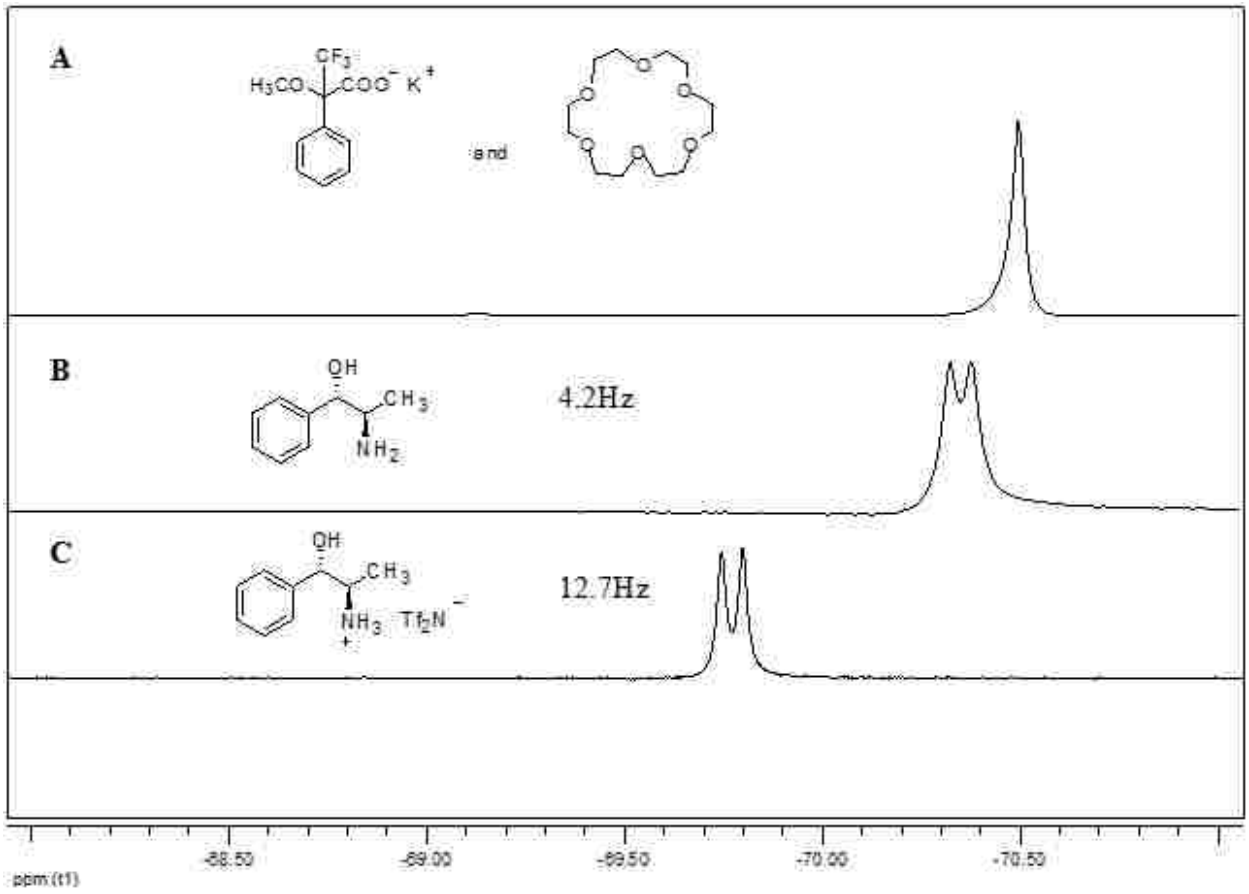

Figure 2.3. ^{19}F-NMR ($CDCl_3$) spectra of potassium Mosher's salt (A) without chiral selector, and with (B) (1S,2R)-NorEph, and (C) (1S,2R)-[NorHEph][Tf2N] chiral selector. Note that all the potassium Mosher's salt solutions contain 18C6.

The chiral recognition ability of the precursor NorEph was compared with that of the PCIL [NorHEph][Tf_2N]. In the absence of either NorEph or [NorHEph][Tf_2N], a single peak of -70.50 Hz chemical shift was observed for the Potassium Mosher's salt racemate. In the presence of NorEph or the [NorHEph][Tf_2N], peak splittings were observed, which are related to the strength of the diastereomeric interactions between potassium Mosher's salt racemate and the chiral compounds. The significantly greater peak splitting of potassium Mosher's salt with PCIL [NorHEph][Tf_2N] versus non-charged precursor NorEph as chiral selector suggests that a higher

chiral recognition ability was obtained by forming PCILs from the neutral NorEph (Figure 2.3). These results suggest the presence of a positive charge as an important factor for chiral discrimination by ion-pair interaction. The acidicity of [NorHEph][Tf_2N] relative to the basicity of NorEph may also contribute to improved chiral recognition of the PCIL. Shamsi and co-workers have reported that electrostatic interactions between the acidic analyte and cationic ionic liquid micelle played a profound role in enantioseparation.[21] In another study, Wasserscheid *et al.* have reported an asymmetric synthesis that solely relied on the strength of ion pairing in a CIL to induce high chirality in an asymmetric hydrogenation reaction.[22] This work demonstrates the importance of ion-pair interactions in chiral induction or chirality transfer. The chiral recognition abilities of the [Tf_2N^-]-containing PCILs including [$NorHEph^+$], [$HEph^+$] and [$MeHEph^+$] were also compared, i.e. the effect of (the degree of) amine alkylation on chiral recognition (Mosher's salt peak splitting) was investigated (Figure 2.4). The recorded values for these PCILs in the presence of Mosher's salt were 12.7 Hz, 5.7 Hz and 4.3 Hz, respectively (Figure 2.4). In addition to a larger peak splitting, the ^{19}F-NMR change in chemical shift for [NorHEph][Tf_2N] was also highest. Thus, it appears that as the extent of hydrogen bonding decreases and steric hindrance increases (i,e, going from the primary to the tertiary ephedrinium-based PCIL), chiral recognition ability of PCILs towards Mosher's salt decreased. Analysis of peak splitting for the [$BETI^-$]-containing PCILs displayed almost identical results. A control experiment was performed to determine the role of the [Tf_2N^-] anion in chiral recognition. The chiral recognition abilities of [NorHEph][Cl], [HEph][Cl], and [MeHEph][Cl] were determined. Interestingly, it was observed that chiral recognition ability of PCILs with [Tf_2N^-] anions was much higher than that of ionic compounds with Cl^- as anions. Chiral recognition studies performed by Wilhelm *et al.* indicate that the counteranions used in CILs play an important role

in chiral discrimination. A tenfold increase in peak splitting was observed when ^{19}F-NMR was carried out on Mosher's salt in the presence of enantiopure CIL with [Tf_2N^-] as counterion compared to [BF_4^-] as the counterion.

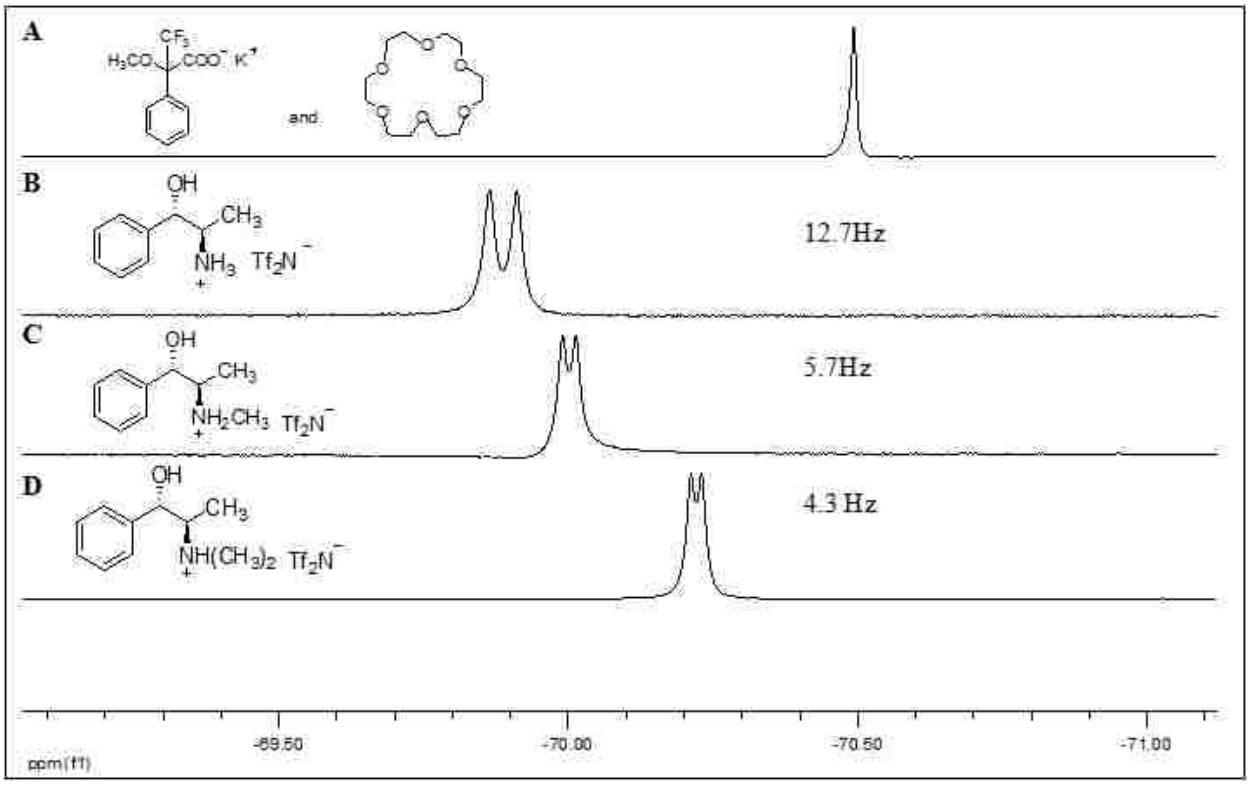

Figure 2.4. ^{19}F NMR ($CDCl_3$) spectra of potassium Mosher's salt (A), potassium Mosher's salt with (1S,2R)-[NorHEph][Tf_2N] as chiral selector (B), potassium Mosher's salt with (1S,2R)-[HEph][Tf_2N] as chiral selector (C), potassium Mosher's salt with (1S,2R)-[MeHEph].

2.3.4. Enantiomeric Recognition of Chiral Analytes by PCILs through the use of Steady-State Fluorescence Spectroscopy

After confirming enantioselectivity of the PCILs for Mosher's salt by use of ^{19}F-NMR, further investigations were performed employing fluorescence spectroscopy. Recently, a fluorescence spectroscopic method was reported for investigating chiral recognition between a CIL and both enantiomeric forms of various fluorescent drug analytes.[23] The two enantiomeric forms of chiral drug analytes exhibited different fluorescence intensities with the CIL as a result of the formation of specific diastereomeric complexes. As a result this method enabled the

determination of a particular enantiomer in a given sample. More recently amino acid based CILs were also synthesized in our laboratory and investigated for enantiomeric recognition.[8b, 24,25]

2.3.5. Intrinsic Fluorescence of PCILs

The ephedrinium PCILs display maximum absorbance at 257 nm, as illustrated for [MeHEph][Tf_2N] (Figure 2.5). In order to determine the optimum intrinsic fluorescence, an excitation emission matrix (EEM) scan was used for neat [MeHEph][Tf_2N]. A sharp fluorescence peak was recorded around 292 nm (Figure 2.5). The measurements were performed with a reduced volume cuvet (0.4 mL) with front-face illumination to minimize inner-filter effects. Due to the relatively high viscosity of [NorHEph][Tf_2N] and [HEph][Tf_2N], fluorescence measurements of the neat PCILs were limited to [MeHEph][Tf_2N]. In order to compare the PCILs as chiral selectors, 30 mM aqueous solutions were prepared for each. Solubility of the PCILs in water decreased in the order of [NorHEph][Tf_2N], [HEph][Tf_2N] and [MeHEph][Tf_2N], as a result of hydrogen bonding.

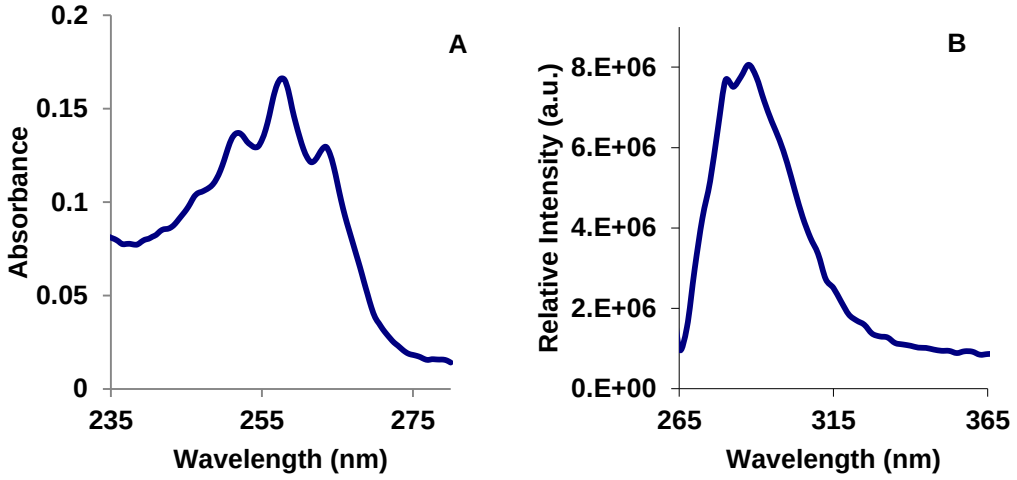

Figure 2.5. (A) UV-VIS spectrum of 10 mM [MeHEph][Tf_2N] in methanol. (B) Fluorescence of neat [MeHEph][Tf_2N] excited at 260 nm with front-face illumination.

2.3.6. Enantiomeric Recognition by use of Fluorescence Spectroscopy

Fluorescence spectroscopy was employed to determine the chiral recognition capability of the PCILs for fluorescent and non-fluorescent analytes in aqueous solutions. A series of analytes of pharmaceutical and biological significance were investigated for this purpose. The fluorescent analytes included propranolol (PROP), 1,1′-binaphthyl-2,2′-diamine (BNA), trifluoro-1-(9-anthryl)ethanol (TFAE) and 1,1′-binaphthyl-2,2′-diyl hydrogenphosphate (BNP) whereas the non-fluorescent analytes included serine and glucose (Figure 2.6).

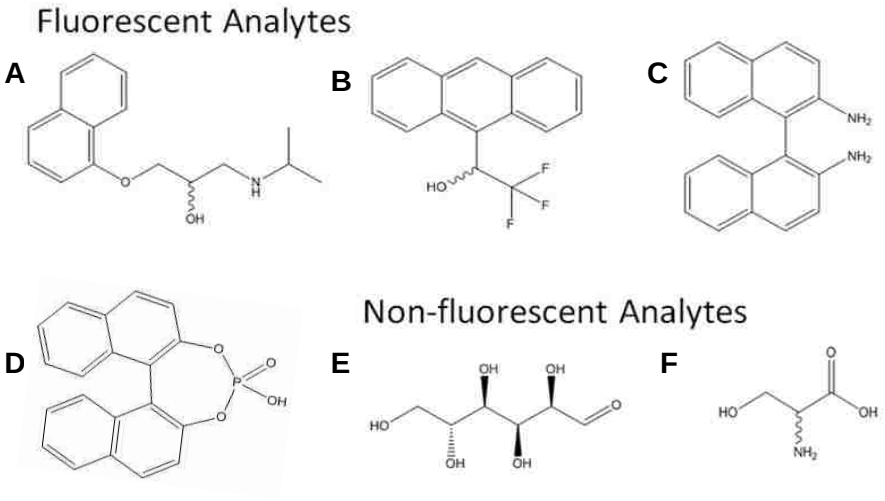

Figure 2.6. Fluorescent analytes (A) Propranolol, (B) 1-(9-Anthryl)-2,2,2-trifluoroethanol, (C) 1,1′-Binaphthyl-2,2′-diamine, (D) 1,1(-Binaphthyl-2,2)-diyl hydrogen phosphate, and non-fluorescent analytes (E) Glucose, (F) Serine.

Enantiomers for each analyte were prepared at 10 μM concentrations in 30 mM of aqueous PCIL solutions containing [Tf_2N^-] anions. In order to determine the wavelength-dependent fluorescence for the PCILs and the fluorescent chiral analytes, an excitation emission matrix (EEM) scan was run with excitation wavelengths ranging from 250 nm to 400 nm. The enantioselectivities of the PCILs were judged based on differences in the fluorescence bands with respect to shape and intensity, upon binding to different enantiomeric forms of the analyte. Based on the results obtained, it could be determined which PCIL exhibited the highest

enantioselectivity for a particular analyte. Since the PCILs and the chiral analytes were both fluorescent, the fluorescence signal intensity was monitored for the PCIL between 270 nm and 320 nm and for the analyte peaks between 320 nm and 520 nm. In order to amplify the differences in signal intensities, i.e. to clearly distinguish between fluorescence signals of both enantiomers, mean centered plots (MCPs) were employed. The difference was calculated between the average and individual fluorescence spectra for each enantiomer. As a result, a negative MCP spectrum was obtained for the lower intensity peak and a positive MCP spectrum for the higher intensity peak. Thus, MCP plots serve to aid in differentiating between individual enantiomers in the presence of PCILs (Figure 2.8).

In the absence of PCILs, the difference in fluorescence intensity between both enantiomers of the chiral analyte was negligible (below 1%) in the control tests. The fluorescence of TFAE enantiomers was measured in the presence of [Nor][HephTf_2N], [HEph][Tf_2N] and [MeHEph][Tf_2N] in aqueous solution. The difference in fluorescence intensity was most pronounced for [NorHeph][Tf_2N] (Figure 2.7). A similar trend was observed for propranolol. In the case of BNP the difference in fluorescence intensity was however more pronounced for [MeHEph][Tf_2N] (Figure 2.7). Thus, [NorHeph][Tf_2N] appeared to be a better chiral selector for TFAE and propranolol, whereas [MeHeph][Tf_2N] exhibited better chiral recognition for BNP and BNA. The fluorescence and MCP spectra for TFAE in [NorHeph][Tf_2N] and BNP in [MeHeph][Tf_2N] are shown in Figure 2.8. In addition to fluorescent analytes, non-fluorescent analytes were also investigated. Although the PCILs were intrinsically fluorescent, their chiral recognition abilities as seen by their fluorescence intensities were not significantly different from one another.

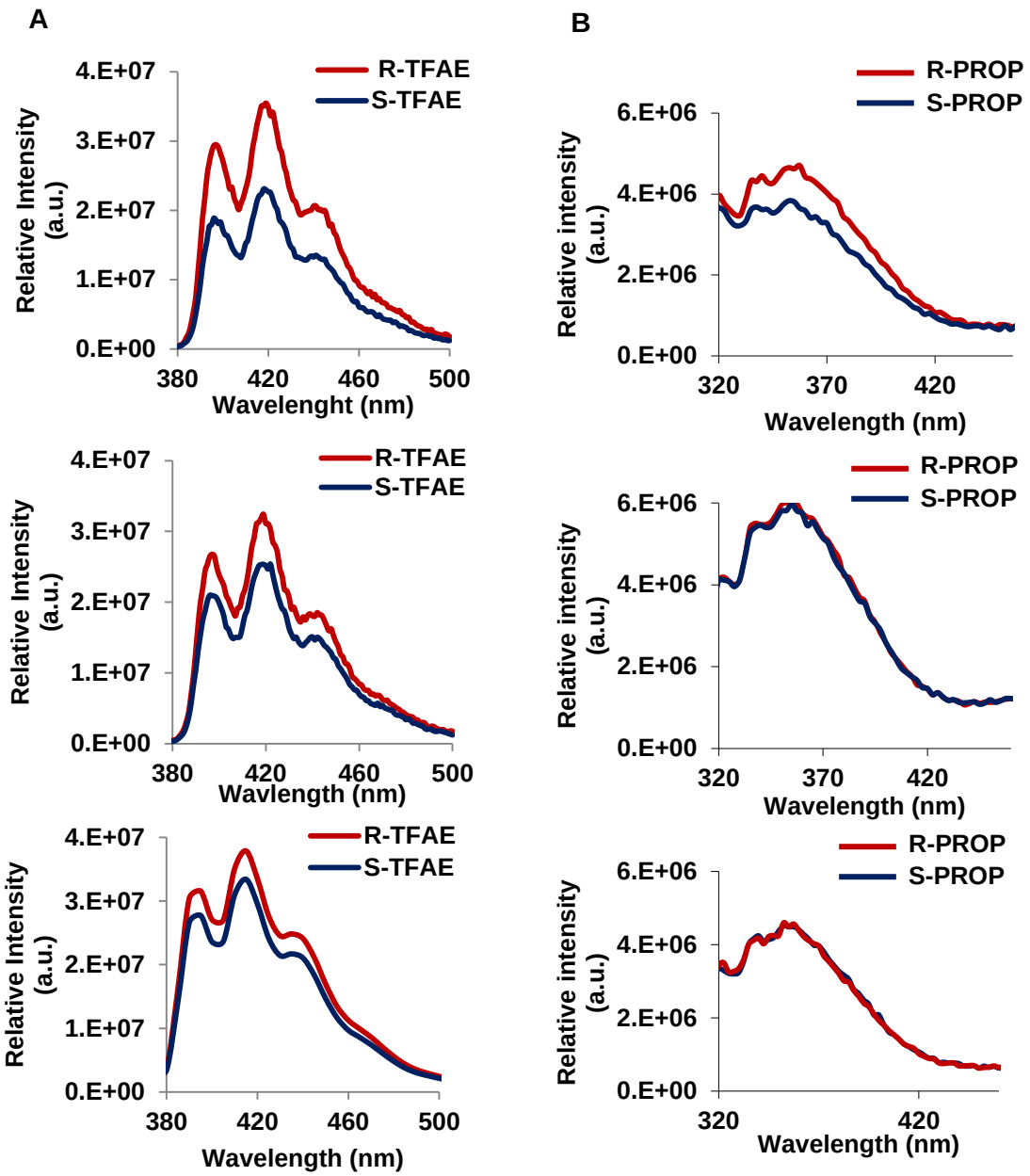

Figure 2.7. Fluorescence of 10 µM TFAE (A) and PROP (B) in aqueous solution with 30 mM [NorHEph][Tf2N], [HEph][Tf_2N], and [MeHEph][Tf_2N].

The results obtained suggest that the chiral interactions between the PCILs and chiral analytes in solution are strongly affected by hydrogen bonding and hydrophobic interactions between PCILs and analytes, similar to chiral molecular micelles. Alternatively, π- π interactions may also play an important role in chiral recognition between the PCILs and fluorescent analytes. The more polar analytes such as TFAE and propranolol may have interacted more favorably with [NorHEph][Tf_2N] as a result of hydrogen bond-donating groups in the PCIL and

hydrogen-bond acceptors in the analytes. Contrary, the less polar BNP interacted more favorably with [MeHEph][Tf_2N], since both compounds had lower hydrogen bonding capabilities.

It thus appears that the degree of amine alkylation in the PCIL could have a significant effect on the enantioselective recognition ability for different chiral compounds as seen by the observed change in fluorescence intensity.[26] The exact mechanism of chiral recognition is still unclear and further studies are conducted to determine the mechanism of chiral recognition by PCILs for analytes of varying hydrophobicity. In general, the results indicated that the PCILs reported here are suitable chiral fluorescent selectors, capable of discerning between different enantiomers of fluorescent analytes.

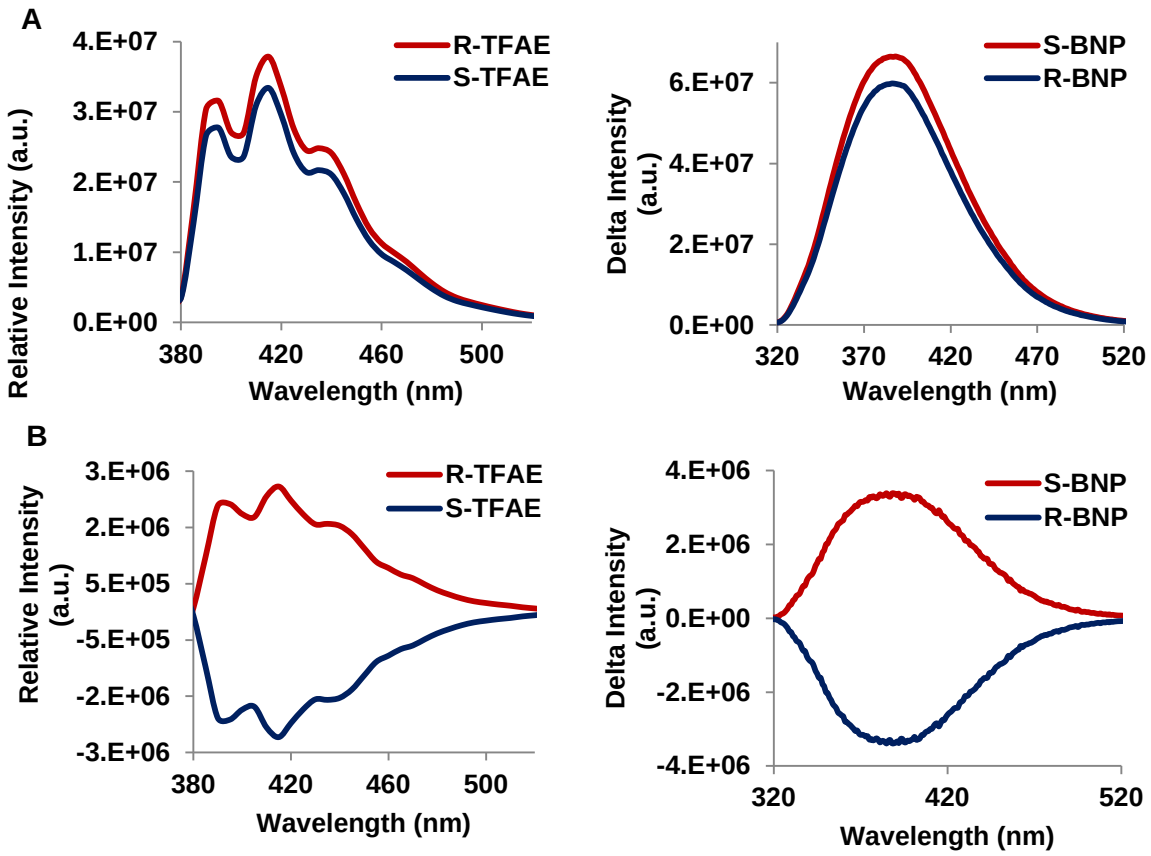

Figure 2.8. (A) Fluorescence and MCP spectra of 10 µM TFAE in aqueous solution with 30 mM [NorHEph][Tf_2N] (B) Fluorescence and MCP spectra of 10 µM BNP in aqueous solution with 30 mM [MeHEph][Tf_2N].

2.4. Conclusions

Ephedrinium-based protic chiral ionic liquids (PCILs) were synthesized using norephedrine, ephedrine and methylephedrine through a single-step acid-base neutralization reaction. Configurational integrity was maintained throughout the synthesis and the PCILs exhibited good thermal stability and chiral selectivity. Using ^{19}F-NMR, splitting of the Mosher's salt fluorine peak was most pronounced for [NorHEph][Tf_2N], implying that this particular PCIL exhibited the strongest chiral interaction with Mosher's salt. From fluorescence studies it was further observed that [NorHEph][Tf_2N] exhibited superior chiral recognition ability to TFAE compared with the other [Tf_2N^-] containing PCILs. In the case of BNP chiral recognition was optimal for [MeHEph][Tf_2N]. The PCILs also exhibited intrinsic fluorescence, which could allow for the study of chiral recognition capability of non-fluorescent analytes by monitoring a change in fluorescence intensity of the PCILs. Unfortunately a significant change in fluorescence intensity of the PCILs was not recorded in the presence of non-fluorescent chiral analytes. The ephedrinium-based PCILs reported here offer a range of potential applications as chiral selectors and solvents in fluorescence spectroscopy and potentially as stationary phases in chromatography, mobile phase modifiers in capillary electrophoresis. In addition they may find use in studying protein interactions and as catalysts in organic synthesis.

2.5. References

1. (a) Koel, M., Ionic liquids in chemical analysis. *Critical Reviews in Analytical Chemistry* **2005,** *35* (3), 177-192; (b) Endres, F.; El Abedin, S. Z., Air and water stable ionic liquids in physical chemistry. *Physical Chemistry Chemical Physics* **2006,** *8* (18), 2101-2116.

2. Poole, C. F., Chromatographic and spectroscopic methods for the determination of solvent properties of room temperature ionic liquids. *Journal of Chromatography A* **2004,** *1037* (1-2), 49-82.

3. Welton, T., Room-temperature ionic liquids. Solvents for synthesis and catalysis. *Chemical Reviews* **1999,** *99* (8), 2071-2083.

4. Buzzeo, M. C.; Evans, R. G.; Compton, R. G., Non-haloaluminate room-temperature ionic liquids in electrochemistry - A review. *Chemphyschem* **2004,** *5* (8), 1106-1120.

5. Tran, C. D., Ionic liquids for and by analytical Spectroscopy. *Analytical Letters* **2007,** *40* (13), 2447-2464.

6. (a) Jessop, P. G.; Stanley, R. R.; Brown, R. A.; Eckert, C. A.; Liotta, C. L.; Ngo, T. T.; Pollet, P., Neoteric solvents for asymmetric hydrogenation: supercritical fluids, ionic liquids, and expanded ionic liquids. *Green Chemistry* **2003,** *5* (2), 123-128; (b) Ding, J.; Welton, T.; Armstrong, D. W., Chiral ionic liquids as stationary phases in gas chromatography. *Analytical Chemistry* **2004,** *76* (22), 6819-6822.

7. Gruttadauria, M.; Riela, S.; Lo Meo, P.; D'Anna, F.; Noto, R., Supported ionic liquid asymmetric catalysis. A new method for chiral catalysts recycling. The case of proline-catalyzed aldol reaction. *Tetrahedron Letters* **2004,** *45* (32), 6113-6116.

8. (a) Tran, C. D.; Oliveira, D.; Yu, S. F., Chiral ionic liquid that functions as both solvent and chiral selector for the determination of enantiomeric compositions of pharmaceutical products. *Analytical Chemistry* **2006,** *78* (4), 1349-1356; (b) Bwambok, D. K.; Marwani, H. M.; Fernand, V. E.; Fakayode, S. O.; Lowry, M.; Negulescu, I.; Strongin, R. M.; Warner, I. M., Synthesis and characterization of novel chiral ionic liquids and investigation of their enantiomeric recognition properties. *Chirality* **2008,** *20* (2), 151-158.

9. (a) Aslanov, L. A.; Valetskii, P. M.; Zakharov, V. N.; Kabachii, Y. A.; Kochev, S. Y.; Romanovskii, B. V.; Yatsenko, A. V., Heterogeneous catalysis in ionic liquids: The heck reaction of bromobenzene with styrene over palladium supported on mesoporous carbon. *Petroleum Chemistry* **2008,** *48* (5), 360-365; (b) Tiyapiboonchaiya, C.; Pringle, J. M.; MacFarlane, D. R.; Forsyth, M.; Sun, J. Z., Polyelectrolyte-in-ionic-liquid electrolytes. *Macromolecular Chemistry and Physics* **2003,** *204* (17), 2147-2154; (c) Ohno, H.; Yoshizawa, M., Electrochemistry using ionic liquid 3. Evolution of ionic liquid as an electrolyte. *Electrochemistry* **2002,** *70* (2), 136-140; (d) Belieres, J. P.; Gervasio, D.; Angell, C. A., Binary inorganic salt mixtures as high conductivity liquid electrolytes for > 100 degrees C fuel cells. *Chemical Communications* **2006,** (46), 4799-4801.

10. Hirao, M.; Sugimoto, H.; Ohno, H., Preparation of novel room-temperature molten salts by neutralization of amines. *Journal of the Electrochemical Society* **2000,** *147* (11), 4168-4172.

11. Greaves, T. L.; Weerawardena, A.; Krodkiewska, I.; Drummond, C. J., Protic ionic liquids: physicochemical properties and behavior as amphiphile self-assembly solvents. *J Phys Chem B* **2008,** *112* (3), 896-905.

12. (a) Greenway, F. L., The safety and efficacy of pharmaceutical and herbal caffeine and ephedrine use as a weight loss agent. *Obes Rev* **2001,** *2* (3), 199-211; (b) Astrup, A.; Buemann, B.; Christensen, N. J.; Toubro, S.; Thorbek, G.; Victor, O. J.; Quaade, F., The effect of ephedrine/caffeine mixture on energy expenditure and body composition in

obese women. *Metabolism* **1992,** *41* (7), 686-8; (c) Roth, R. P.; Cantekin, E. I.; Bluestone, C. D.; Welch, R. M.; Cho, Y. W., Nasal decongestant activity of pseudoephedrine. *Ann Otol Rhinol Laryngol* **1977,** *86* (2 pt. 1), 235-42.

13. Wasserscheid, P.; Bosmann, A.; Bolm, C., Synthesis and properties of ionic liquids derived from the 'chiral pool'. *Chemical Communications* **2002,** (3), 200-201.

14. Thanh, G. V.; Pegot, B.; Loupy, A., Solvent-free microwave-assisted preparation of chiral ionic liquids from (-)-N-methylephedrine. *European Journal of Organic Chemistry* **2004,** (5), 1112-1116.

15. Mukherjee, D. K.; Ghosh, N., Enantio selective phase transfer alkylation using orthopalladated complex in chiral ionic liquid. *Catalysis Communications* **2008,** *9* (1), 40-44.

16. (a) Crosthwaite, J. M.; Muldoon, M. J.; Dixon, J. K.; Anderson, J. L.; Brennecke, J. F., Phase transition and decomposition temperatures, heat capacities and viscosities of pyridinium ionic liquids. *Journal of Chemical Thermodynamics* **2005,** *37* (6), 559-568; (b) Ohno, H.; Yoshizawa, M., Ion conductive characteristics of ionic liquids prepared by neutralization of alkylimidazoles. *Solid State Ionics* **2002,** *154*, 303-309.

17. Luo, H. M.; Huang, J. F.; Dai, S., Studies on thermal properties of selected aprotic and protic ionic liquids. *Separation Science and Technology* **2008,** *43* (9-10), 2473-2488.

18. Yoshizawa, M.; Ogihara, W.; Ohno, H., Design of new ionic liquids by neutralization of imidazole derivatives with imide-type acids. *Electrochemical and Solid State Letters* **2001,** *4* (6), E25-E27.

19. Li, M.; Gardella, J.; Bwambok, D. K.; El-Zahab, B.; de Rooy, S.; Cole, M.; Lowry, M.; Warner, I. M., Combinatorial Approach to Enantiomeric Discrimination: Synthesis and 19F NMR Screening of a Chiral Ionic Liquid-Modified Silane Library. *Journal of Combinatorial Chemistry* **2009,** *11* (6), 1105-1114.

20. Clavier, H.; Boulanger, L.; Audic, N.; Toupet, L.; Mauduit, M.; Guillemin, J. C., Design and synthesis of imidazolinium salts derived from (L)-valine. Investigation of their potential in chiral molecular recognition. *Chemical Communications* **2004,** (10), 1224-1225.

21. Rizvi, S. A. A.; Shamsi, S. A., Synthesis, characterization, and application of chiral ionic liquids and their polymers in micellar electrokinetic chromatography. *Analytical Chemistry* **2006,** *78* (19), 7061-7069.

22. Schulz, P. S.; Muller, N.; Bosmann, A.; Wasserscheid, P., Effective chirality transfer in ionic liquids through ion-pairing effects. *Angewandte Chemie-International Edition* **2007,** *46* (8), 1293-1295.

23. Tran, C. D.; Oliveira, D., Fluorescence determination of enantiomeric composition of pharmaceuticals via use of ionic liquid that serves as both solvent and chiral selector. *Analytical Biochemistry* **2006,** *356* (1), 51-58.

24. Bwambok, D. K.; Challa, S. K.; Lowry, M.; Warner, I. M., Amino Acid-Based Fluorescent Chiral Ionic Liquid for Enantiomeric Recognition. *Analytical Chemistry*.

25. Li, M.; De Rooy, S. L.; Bwambok, D. K.; El-Zahab, B.; DiTusa, J. F.; Warner, I. M., Magnetic chiral ionic liquids derived from amino acids. *Chemical Communications* **2009,** (45), 6922-6924.

26. (a) Williams, A. A.; Fakayode, S. O.; Alpturk, O.; Jones, C. M.; Lowry, M.; Strongin, R. M.; Warner, I. M., Determination of enantiomeric compositions of analytes using novel fluorescent chiral molecular micelles and steady state fluorescence measurements. *Journal of Fluorescence* **2008,** *18* (2), 285-296; (b) Willlams, A. A.; Fakayode, S. O.; Lowry, M.; Warner, I. M., A Versatile Chiral Selector for Determination of Enantiomeric Composition of Fluorescent and Nonfluorescent Chiral Molecules Using Steady-State Fluorescence Spectroscopy. *Chirality* **2009,** *21* (2), 305-315.

CHAPTER 3

MAGNETIC CHIRAL IONIC LIQUIDS DERIVED FROM AMINO ACIDS

3.1. Introduction

Ionic Liquids (ILs) can be designed for specific applications through the judicious choice of their constituent ions. The synthesis of chiral ionic liquids (CILs), including their applications such as asymmetric catalysis and synthesis,[1] chiral separation,[2] and enantioselective discrimination (Chapter 2), have been widely reported. Another interesting and growing area in IL research is the preparation of metal-containing ILs.[3] These novel functional ILs are regarded as promising new materials which can favorably combine the advantages of ILs with catalytic,[3c] spectroscopic,[3d] or magnetic[3e] properties that originate from the incorporated metal ion. A new class of magnetic ionic liquids (MILs) was discovered recently.[4] The MILs are mostly based on high-spin d^5 iron(III) in the form of tetrachloro- or tetrabromoferrate(III) with various counter cations. Owing to the high single-ion magnetic moments, these MILs exhibit a strong response to magnetic fields. Herein, we report the first examples of magnetic chiral ionic liquids (MCILs) that contain chiral and magnetic properties simultaneously. Both magneticity and chirality are investigated. They are new single-component chiral and magnetic materials that are free from phase separation compared with traditional ferrofluids that are based on suspension of colloidal or nanoparticles of magnetic materials in a carrier fluid.[5]

3.2. Materials and Methods

3.2.1. Chemicals and Materials

Amino acid methyl ester hydrochlorides including L-alanine methyl ester hydrochloride, L-valine methyl ester hydrochloride, L-leucine methyl ester hydrochloride, L-isoleucine methyl ester hydrochloride, and L-phenylalanine methyl ester hydrochloride were obtained from Sigma-

Aldrich (Milwaukee, WI, USA). Iron(III) chloride hexahydrate, (R)- and (S)-2,2,2-trifluoro-1-(9-anthryl)ethanol (TFAE), (R)- and (S)-1,1'-binaphthyl-2,2'-diamine (BNA), (R)- and (S)-2-(6-methoxy-2-naphthyl)propionic acid (naproxen) were also obtained from Sigma-Aldrich and used without further purification. Ethanol, methanol, acetonitrile, chloroform, and carbon tetrachloride were of anhydrous grade (Sigma-Aldrich, Milwaukee, WI), and all other organic solvents such as acetone, hexane, and water are of HPLC grade (J. T. Baker, Phillipsburg, NJ).

3.2.2. General Instrumental Methods

^{1}H NMR (400 MHz) and ^{13}C NMR (100 MHz) spectra were acquired by use of a Bruker Avance 400 NMR spectrometer. The ^{1}H and ^{13}C chemical shifts are given in parts per million (δ) with TMS as an internal standard. Due to the paramagnetic properties of the MCILs, very dilute sample solutions in deuterated DMSO were tested for ^{1}H and ^{13}C NMR characterization. ^{13}C NMR spectra were acquired after overnight scan. FT-IR was measured using a Bruker Tensor 27 FT-IR spectrometer. Samples were analyzed in pure form by use of a DuraSamp IR apparatus. All spectra were obtained using 32 scans for both sample and background, with a resolution of 4 cm^{-1}. Elemental analyses were contracted to Atlantic Microlab (Atlanta, GA). A Jasco-710 spectropolarimeter was used to obtain the CD spectra of MCILs. To characterize the MCILs, their visible absorption spectra were measured using a Shimadzu UV-3101PC UV–Vis–near-IR scanning spectrometer (Shimadzu, Columbia, MD). Absorption was collected using a 1.0 cm^{2} quartz cuvette at room temperature and the blank was subtracted from each spectrum.

The magnetic susceptibility and magnetization of the MCILs were measured using approximately 80 to 100 mg of the sample in a Quantum Design superconducting quantum interference device (SQUID) magnetometer (San Diego, CA, USA) for temperatures between 5 and 300 K and fields between -50 000 and 50 000 Oe.

A TA Q50 thermal gravimetric analyzer (TA Instruments, New Castle, DE) was used to analyze the thermal stability of MCILs and their decomposition behaviours. MCIL samples (about 3-4 mg) were scanned from room temperature to 600 °C under nitrogen flow (50 ml/min) with a heating rate of 10 °C/min. Values for the onset degradation temperature and peak temperature were determined from the derivative TGA curves. Glass transition behaviors of MCILs were investigated using a Q100 differential scanning calorimeter (TA Instruments, New Castle, DE). MCIL samples (about 5 mg) were placed in sealed aluminium crucibles and run under a nitrogen flow (50 ml/min). The samples were cooled and heated using the following sequence: cooled to -80 °C, equilibrated at -80 °C, and isothermal for 3 min at -80 °C; then heated to 150 °C with a rate of 5 °C/min, isothermal for 3 min at 150 °C; then cooled to -80 °C with a rate of 5 °C/min, isothermal for 3 min at -80 °C; finally heated to 150 °C with a rate of 5 °C/min.

Steady-state fluorescence measurements were recorded at room temperature by use of a Spex Fluorolog-3 spectrofluorimeter (model FL3-22TAU3; Jobin Yvon, Edison, NJ) equipped with a 450-W xenon lamp and R928P photomultiplier tube (PMT) emission detector. Fluorescence emission spectra were collected in a 4-mm quartz fluorescence cuvette with slit widths set for entrance exit bandwidths of 4 nm on both excitation and emission monochromators for BNA, 2 nm for TFAE, and 1.5 nm for naproxen, respectively. Fluorescence for BNA, TFAE, and naproxen were respectively monitored at excitation wavelengths of 365, 365, and 280 nm. In addition, all fluorescence spectra were blank subtracted before data analysis.

3.2.3. Synthesis of Amino Acid Derived Magnetic Chiral Ionic Liquids (MCILs)

Generally, MCILs were synthesized by a reaction between L-amino acid methyl ester hydrochloride and iron(III) chloride hexahydrate in anhydrous methanol at room temperature for 12 h (Scheme 3.1). The evaporation of methanol and water afforded the MCIL products.

3.3. Results and Discussion

3.3.1. Synthesis and Characterization of MCILs

A typical synthesis procedure for L-[PheOMe][$FeCl_4$] is as follows. To a solution of L-phenylalanine methyl ester hydrochloride (1.00 g, 4.6 mmol) in anhydrous methanol (10 mL) was added iron(III) chloride hexahydrate (1.26 g, 4.6 mmol) in anhydrous methanol (10 mL) at room temperature. The yellow mixture solution was stirred at room temperature for 12h after which the methanol was removed by rotary evaporation. The viscous brownish liquid obtained after removal of methanol was washed with a small amount of water. Upon decantation of the upper water phase, residual water was removed by freeze-drying on a lyophilizer overnight. The final product of L-[PheOMe][$FeCl_4$] is a brownish viscous liquid.

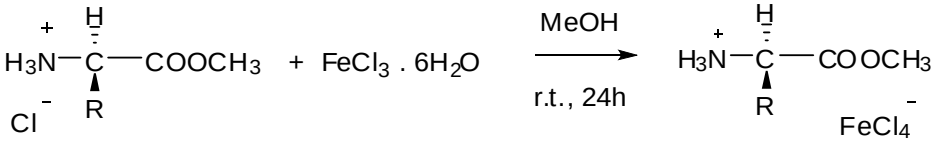

Scheme 3.1. Synthesis of magnetic chiral ionic liquids (MCILs).

The identity and purity of the five MCILs were determined by ^{1}H, ^{13}C NMR, FT-IR, and C, H, N elemental analysis.

- **L-[AlaOMe][$FeCl_4$]**, brownish viscous liquid, yield 88%, ^{1}H NMR (400 MHz, DMSO-d_6), δ (ppm): 8.47 (broad, 3H), 4.06 (m, 1H), 3.74 (s, 3H), 1.41 (d, 3H). ^{13}C NMR (100 MHz, DMSO-d_6), δ (ppm): 170.6, 53.6, 48.3, 16.3. IR (neat), ν (cm^{-1}): 3197, 2945, 1747,

1571, 1433, 1263, 1174, 1176. Anal. Calcd for $C_4H_{10}Cl_4FeNO_2$, C, 15.92; H, 3.34; N, 4.64. Found: C, 15.27; H, 3.98; N, 5.09.

- **L-[ValOMe][FeCl$_4$]**, brownish viscous liquid, yield 90%, ^{1}H NMR (400 MHz, DMSO-d_6), δ (ppm): 8.45 (broad, 3H), 3.75 (m, 1H), 3.66 (s, 3H), 3.26 (m, 1H), 0.87 (d, 6H). ^{13}C NMR (100 MHz, DMSO-d_6), δ (ppm): 169.7, 57.7, 53.5, 31.4, 16.9. IR (neat), ν (cm^{-1}): 3184, 2955, 1721, 1586, 1477, 1440, 1253, 1242. Anal. Calcd for $C_6H_{14}Cl_4FeNO_2$, C, 21.85; H, 4.28; N, 4.25. Found: C, 20.97; H, 5.23; N, 4.01.
- **L-[LeuOMe][FeCl$_4$]**, brownish viscous liquid, yield 91%, ^{1}H NMR (400 MHz, DMSO-d_6), δ (ppm): 8.46 (broad, 3H), 3.73 (m, 1H), 3.57 (s, 3H), 3.17 (m, 2H), 1.48 (m, 1H), 0.77 (d, 6H). ^{13}C NMR (100 MHz, DMSO-d_6), δ (ppm): 168.7, 59.7, 39.4, 32.9, 29.7, 17.3. IR (neat), ν (cm^{-1}): 3175, 2956, 2866, 1724, 1575, 1471, 1438, 1367, 1249. Anal. Calcd for $C_7H_{16}Cl_4FeNO_2$, C, 24.45; H, 4.69; N, 4.07. Found: C, 24.50; H, 5.08; N, 4.03.
- **L-[IleOMe][FeCl$_4$]**, brownish viscous liquid, yield 87%, ^{1}H NMR (400 MHz, DMSO-d_6), δ (ppm): 8.69 (broad, 3H), 3.67 (m, 1H), 3.72 (s, 3H), 3.34 (m, 1H), 1.23 (m, 2H), 0.86 (t, 6H). ^{13}C NMR (100 MHz, DMSO-d_6), δ (ppm): 169.5, 56.4, 53.0, 36.3, 25.6, 14.7, 11.9. IR (neat), ν (cm^{-1}): 3175, 2956, 2866, 1724, 1575, 1471, 1438, 1367, 1249. Anal. Calcd for $C_7H_{16}Cl_4FeNO_2$, C, 24.45; H, 4.69; N, 4.07. Found: C, 24.16; H, 5.37; N, 3.98.
- **L-[PheOMe][FeCl$_4$]**, brownish viscous liquid, yield 92%, ^{1}H NMR (400 MHz, DMSO-d_6), δ (ppm): 8.46 (broad, 3H), 7.32 (d, 2H), 7.27 (d, 1H), 7.20 (m, 2H), 4.27 (m, 1H), 3.65 (s, 3H), 3.14 (d, 2H). ^{13}C NMR (100 MHz, DMSO-d_6), δ (ppm): 170.2, 129.8, 129.1, 127.8, 53.7, 53.1, 31.2. IR (neat), ν (cm^{-1}): 3183, 2937, 1724, 1573, 1438, 1257, 1246.

Anal. Calcd for $C_{10}H_{14}Cl_4FeNO_2$, C, 31.78; H, 3.73; N, 3.71. Found: C, 30.68; H, 4.14; N, 3.61.

The visible absorption spectra of the five MCILs were measured using a UV-vis spectrometer to spectroscopically characterize the MCILs (Figure 3.1). All the MCILs exhibited similar absorption curves with three major peaks at 532, 618, and 685. These peaks are well known as characteristic peaks of tetrachloroferrate(III).[6] The near identical absorption behavior and peak wavelengths were also observed for conventional MILs such as 1-butyl-3-methyl-imidazolium tetrachloroferrate(III).[4a, b]

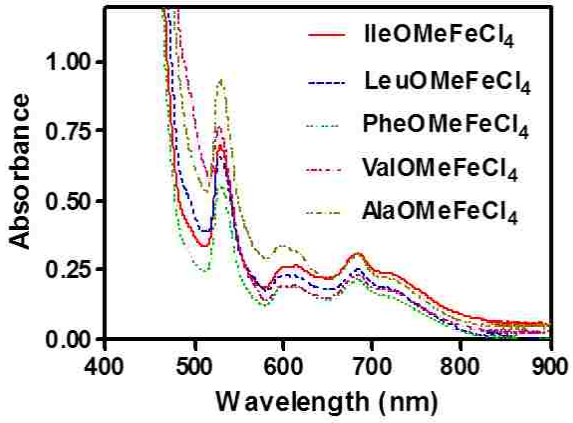

Figure 3.1. Visible absorption spectra of MCILs in acetonitrile.

3.3.2. Thermal Properties of MCILs

The thermal properties of the MCILs, including thermal stabilities and phase transition behaviors were investigated by use of thermal gravimetric analysis (TGA) and differential scanning calorimetry (DSC), respectively (Table 3.1). According to the TGA curves, these MCILs are thermally stable up to about 190 ºC in a nitrogen atmosphere. A two-stage decomposition process was observed for all the MCILs. The first one is rapid and the loss in mass is about 40-50% in nitrogen. The rapid degradation may suggest a

dissociative nature of the decomposition proceeding without participation of oxygen.[7] On the other hand, oxidation of the residual carbon may predominate in the second stage. This two-step thermal decomposition behavior was discerned previously for tetrabutylammonium tetrachloroferrate(III).[7] According to the DSC thermograms, all MCILs exhibited low glass transition temperatures between -30 and -50 ºC, however no significant melting points were identified (Table 3.1.). These results clearly evidence the presence of a phase transition upon decreasing temperature, which takes the MCILs from a readily stable liquid to the glass form. It is worth noting that regular molecular solvents generally do not exhibit the glass transition behavior. Therefore, the polymer-like behavior and high degree of order observed for the MCILs might lead to a significant transfer or induction of chirality from the MCILs to reactants or products. As a general trend, the glass transition temperature increased with the increase in molecular weight of MCILs. It was found that the glass transition temperature steadily increased as the alkyl chain elongates from butyl to octyl of the imidazolium cations in alkylimidazolium tetrachloroferrate(III) MILs.[3e]

Table 3.1. Thermal properties of MCILs determined by TGA and DSC.

MCILs	T_g (^{0}C) [a]	T_{start} (ºC) [b]	T_{onset} (ºC) [c]	T_{onset2} (ºC) [d]
L-[AlaOMe][$FeCl_4$]	-47.6	197.3	231.1	304.3
L-[ValOMe][$FeCl_4$]	-44.8	215.7	235.5	325.5
L-[LeuOMe][$FeCl_4$]	-39.2	196.1	220.4	311.7
L-[IleOMe][$FeCl_4$]	-41.1	216.5	236.9	327.4
L-[PheOMe][$FeCl_4$]	-30.5	195.3	217.5	296.5

[a] Glass transition temperature. [b] The beginning decomposition temperature. [c] The temperature at which sample loses weight at fastest speed. [d] The second beginning decomposition temperature.

3.3.3. Magnetic Properties of MCILs

All the MCILs contain tetrachloroferrate(III) anions with d^5 configuration, and exhibit paramagnetic behavior at room temperature. The magnetic susceptibility of the MCILs was

measured using a Quantum Design superconducting quantum interference device (SQUID) magnetometer. The magnetization at 300 K was measured in the magnetic field range of -50 000 to 50 000 Oe. The results show an expected linear dependence on the applied magnetic field according to Curie's law (Figure 3.2). From the slopes of the fitted lines, the respective molar magnetic susceptibilities of L-[AlaOMe][$FeCl_4$], L-[ValOMe][$FeCl_4$], L-[IleOMe][$FeCl_4$], and L-[PheOMe][$FeCl_4$] were obtained as χ_M = 0.0134, 0.0129, 0.0127, and 0.0135 emu mol^{-1} (Table 3.2), which fit well to the expected value for Fe(III).[3e] The effective magnetic moments (μ_{eff}) of the MCILs are determined as values between 5.52 and 5.66 μ_B in accordance with the S = 5/2 high-spin electronic state of iron(III) (spin-only value of 5.92 μ_B). The MCILs displayed very weak antiferromagnetic interactions as seen from the Curie-Weiss temperatures (Table 3.2), confirming a lack of cluster formation within solution.

Table 3.2. Summary of magnetic properties of MCILs.

MCILs	Mw [a]	χ_M [b] (emu/mol)	χT [c] (emu K/mol)	μ_{eff} [d] (B.M.)	θ [e] (T)
L-[AlaO][$MeFeCl_4$]	299.78	0.0134	3.90	5.585	-2.4
L-[ValOMe][$FeCl_4$]	327.83	0.0129	3.86	5.556	-3.3
L-[IleOMe][$FeCl_4$]	341.86	0.0127	3.81	5.520	-3.1
L-[PheOMe][$FeCl_4$]	375.88	0.0135	4.01	5.663	-2.9

[a] Molecular weight. [b] Molar magnetic susceptibility. [c] Measured at 300K and H=1000G. [d] Effective magnetic moment. [e] Curie-Weiss temperature.

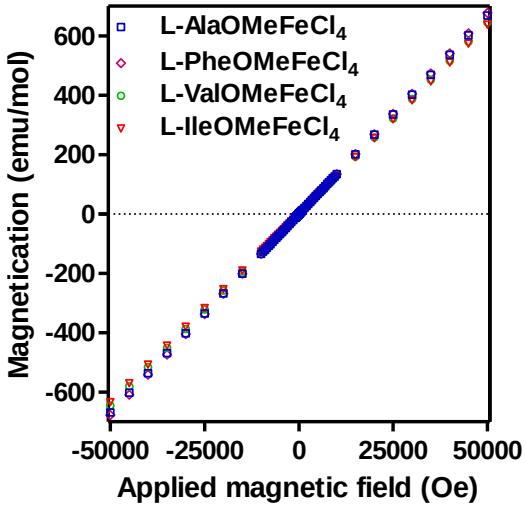

Figure 3.2. Field dependence of the magnetization of MCILs at 300 K.

3.3.4. Chiral Properties of MCILs

The enantiomeric purity of the MCILs was confirmed by circular dichroism (CD) measurements. Figure 3.3 shows CD spectra of L- and D-PheOMeFeCl$_4$, measured in methanol solutions. L-[PheOMe][FeCl$_4$] exhibits a positive CD band at 218 nm, with a maximum of 24 mdegrees. The fact that D-[PheOMe][FeCl$_4$] has a similar but negative CD band of equal magnitude at the same wavelength, further confirms the optical purity of both L- and D-[PheOMe][FeCl$_4$].[2h]

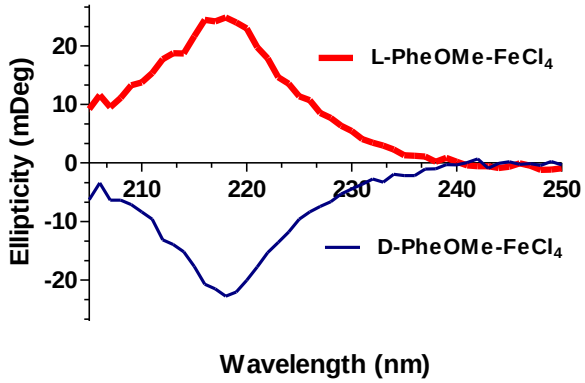

Figure 3.3. Circular dichroism spectra of L- and D-PheOMeFeCl$_4$ in methanol.

3.3.5. Enantiomeric Recognition of Chiral Analytes by MCILs through the use of Steady State Fluorescence Spectroscopy

Steady state fluorescence spectroscopy was further used to investigate the chiral recognition of fluorescent analytes in ethanol solutions using L-[AlaOMe][$FeCl_4$] as chiral selector (Figure 3.4). With (R)- and (S)-2,2,2-trifluoro-1-(9-anthryl)ethanol (TFAE) as analytes, the emission intensity difference between (R)- and (S)-TFAE confirmed the chiral discrimination ability of L-[AlaOMe][$FeCl_4$] (Figure 3.4).[2d, 8] Similarly, with L-[AlaOMe][$FeCl_4$] as chiral selector, the chiral discrimination of 1,1'-binaphthyl-2,2'-diamine (BNA) and 2-(6-methoxy-2-naphthyl)propionic acid (naproxen) were also investigated.

3.3.5. Enantiomeric Recognition of Chiral Analytes by MCILs through the use of Steady State Fluorescence Spectroscopy

Steady state fluorescence spectroscopy was further used to investigate the chiral recognition of fluorescent analytes in ethanol solutions using L-[AlaOMe][$FeCl_4$] as chiral selector (Figure 3.4).

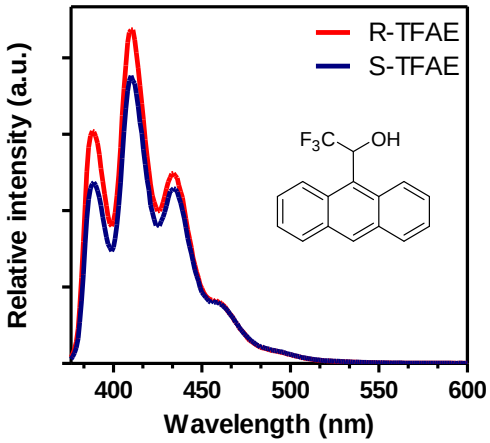

Figure 3.4. Fluorescence emission spectral plots of (R)- and (S)-TFAE enantiomers in the presence of L-AlaOMeFeCl4. The emission spectra of TFAE were collected at an excitation wavelength of 365 nm at room temperature.

With (R)- and (S)-2,2,2-trifluoro-1-(9-anthryl)ethanol (TFAE) as analytes, the emission intensity difference between (R)- and (S)-TFAE confirmed the chiral discrimination ability of L-[AlaOMe][$FeCl_4$] (Figure 3.4).[2d, 8] Similarly, with L-[AlaOMe][$FeCl_4$] as chiral selector, the chiral discrimination of 1,1'-binaphthyl-2,2'-diamine (BNA) and 2-(6-methoxy-2-naphthyl)propionic acid (naproxen) were also investigated.

3.4. Conclusion

In conclusion, novel magnetic chiral ionic liquids (MCILs) have been synthesized using a straightforward synthesis procedure. To the best of our knowledge, these are the first examples of room temperature ionic liquids that contain both chiral and magnetic properties. Their paramagnetic properties were confirmed by use of SQUID tests. In addition, their enantiomeric discrimination toward chiral analytes was verified by use of steady-state fluorescence spectroscopy. These novel chiral magnetic fluid materials with dual functionalities are expected to have great potential in a number of applications such as asymmetric catalysis and synthesis. Their strong response to a magnetic field and extremely low vapor pressure could be particularly beneficial by providing an easier way to recover and recycle the MCILs used as asymmetric catalysts. In addition, their magnetic property could also provide a means to manipulate the phase separation behavior in the liquid-liquid biphasic extraction. This may find interesting applications in the chiral extraction and enrichment of chiral compounds by use of magnetic field.

3.5. References

1. (a) Patil, M. L.; Sasai, H., Recent developments on chiral ionic liquids: Design, synthesis, and applications. *Chemical Record* **2008,** *8* (2), 98-108; (b) Baudequin, C.; Baudoux, J.; Levillain, J.; Cahard, D.; Gaumont, A. C.; Plaquevent, J. C., Ionic liquids and chirality: opportunities and challenges. *Tetrahedron-Asymmetry* **2003,** *14* (20), 3081-3093; (c) Headley, A. D.; Ni, B., Chiral imidazolium ionic liquids: Their synthesis and influence

on the outcome of organic reactions. *Aldrichimica Acta* **2007,** *40* (4), 107-117; (d) Chen, D.; Schmitkamp, M.; Francio, G.; Klankermayer, J.; Leitner, W., Enantioselective hydrogenation with racemic and enantiopure binap in the presence of a chiral ionic liquid. *Angewandte Chemie-International Edition* **2008,** *47* (38), 7339-7341; (e) Schulz, P. S.; Müller, N.; Bösmann, A.; Wasserscheid, P., Effective Chirality Transfer in Ionic Liquids through Ion-Pairing Effects. *Angewandte Chemie International Edition* **2007,** *46* (8), 1293-1295; (f) Luo, S.; Mi, X.; Zhang, L.; Liu, S.; Xu, H.; Cheng, J.-P., Functionalized Chiral Ionic Liquids as Highly Efficient Asymmetric Organocatalysts for Michael Addition to Nitroolefins. *Angewandte Chemie International Edition* **2006,** *45* (19), 3093-3097; (g) Schmitkamp, M.; Chen, D.; Leitner, W.; Klankermayer, J.; Francio, G., Enantioselective catalysis with tropos ligands in chiral ionic liquids. *Chemical Communications* **2007,** (39); (h) Bica, K.; Gmeiner, G.; Reichel, C.; Lendl, B.; Gaertner, P., Microwave-assisted synthesis of camphor-derived chiral imidazolium ionic liquids and their application in diastereoselective Diels-Alder reaction. *Synthesis-Stuttgart* **2007,** (9), 1333-1338.

2. (a) Wasserscheid, P.; Bosmann, A.; Bolm, C., Synthesis and properties of ionic liquids derived from the 'chiral pool'. *Chemical Communications* **2002,** (3), 200-201; (b) Levillain, J.; Dubant, G.; Abrunhosa, I.; Gulea, M.; Gaumont, A. C., Synthesis and properties of thiazoline based ionic liquids derived from the chiral pool. *Chemical Communications* **2003,** (23), 2914-2915; (c) Clavier, H.; Boulanger, L.; Audic, N.; Toupet, L.; Mauduit, M.; Guillemin, J. C., Design and synthesis of imidazolinium salts derived from (L)-valine. Investigation of their potential in chiral molecular recognition. *Chemical Communications* **2004,** (10), 1224-1225; (d) Bwambok, D. K.; Marwani, H. M.; Fernand, V. E.; Fakayode, S. O.; Lowry, M.; Negulescu, I.; Strongin, R. M.; Warner, I. M., Synthesis and characterization of novel chiral ionic liquids and investigation of their enantiomeric recognition properties. *Chirality* **2008,** *20* (2), 151-158; (e) Ding, J.; Welton, T.; Armstrong, D. W., Chiral ionic liquids as stationary phases in gas chromatography. *Analytical Chemistry* **2004,** *76* (22), 6819-6822; (f) Tran, C. D.; Mejac, I., Chiral ionic liquids for enantioseparation of pharmaceutical products by capillary electrophoresis. *Journal of Chromatography A* **2008,** *1204* (2), 204-209; (g) Rizvi, S. A. A.; Shamsi, S. A., Synthesis, characterization, and application of chiral ionic liquids and their polymers in micellar electrokinetic chromatography. *Analytical Chemistry* **2006,** *78* (19), 7061-7069; (h) Tran, C. D.; Oliveira, D., Fluorescence determination of enantiomeric composition of pharmaceuticals via use of ionic liquid that serves as both solvent and chiral selector. *Analytical Biochemistry* **2006,** *356* (1), 51-58.

3. (a) Nockemann, P.; Thijs, B.; Postelmans, N.; Van Hecke, K.; Van Meervelt, L.; Binnemans, K., Anionic rare-earth thiocyanate complexes as building blocks for low-melting metal-containing ionic liquids. *Journal of the American Chemical Society* **2006,** *128* (42), 13658-13659; (b) Mudring, A.-V.; Babai, A.; Arenz, S.; Giernoth, R., The "Noncoordinating" Anion Tf2N− Coordinates to Yb2+: A Structurally Characterized Tf2N− Complex from the Ionic Liquid [mppyr][Tf2N]. *Angewandte Chemie International Edition* **2005,** *44* (34), 5485-5488; (c) Bica, K.; Gaertner, P., Metal-Containing Ionic Liquids as Efficient Catalysts for Hydroxymethylation in Water. *European Journal of Organic Chemistry* **2008,** *2008* (20), 3453-3456; (d) Tang, S.;

Babai, A.; Mudring, A. V., Europium-based ionic liquids as luminescent soft materials. *Angewandte Chemie-International Edition* **2008,** *47* (40), 7631-7634; (e) Yoshida, Y.; Saito, G. Z., Influence of structural variations in 1-alkyl-3-methylimidazolium cation and tetrahalogenoferrate(III) anion on the physical properties of the paramagnetic ionic liquids. *Journal of Materials Chemistry* **2006,** *16* (13), 1254-1262; (f) Zhong, C.; Sasaki, T.; Jimbo-Kobayashi, A.; Fujiwara, E.; Kobayashi, A.; Tada, M.; Iwasawa, Y., Syntheses, Structures, and Properties of a Series of Metal Ion-Containing Dialkylimidazolium Ionic Liquids. *Bulletin of the Chemical Society of Japan* **2007,** *80* (12), 2365-2374.

4. (a) Hayashi, S.; Hamaguchi, H.-o., Discovery of a Magnetic Ionic Liquid [bmim]FeCl4. *Chemistry Letters* **2004,** *33* (12), 1590-1591; (b) Hayashi, S.; Saha, S.; Hamaguchi, H. O., A new class of magnetic fluids: bmim FeCl4 and nbmim FeCl4 ionic liquids. *Ieee Transactions on Magnetics* **2006,** *42* (1), 12-14; (c) Lee, S.; Ha, S.; You, C.-Y.; Koo, Y.-M., Recovery of magnetic ionic liquid [bmim]FeCl₄ using electromagnet. *Korean Journal of Chemical Engineering* **2007,** *24* (3), 436-437; (d) Lee, S. H.; Ha, S. H.; Ha, S.-S.; Jin, H.-B.; You, C.-Y.; Koo, Y.-M., Magnetic behavior of mixture of magnetic ionic liquid bmim FeCl(4) and water 10.1063/1.2710462. *Journal of Applied Physics* **2007,** *101* (9); (e) Sitze, M. S.; Schreiter, E. R.; Patterson, E. V.; Freeman, R. G., Ionic liquids based on FeCl3 and FeCl2. Raman scattering and ab initio calculations. *Inorganic Chemistry* **2001,** *40* (10), 2298-2304; (f) Zhang, Q. G.; Yang, J. Z.; Lu, X. M.; Gui, J. S.; Huang, Z., Studies on an ionic liquid based on FeCl3 and its properties. *Fluid Phase Equilibria* **2004,** *226*, 207-211.

5. (a) Berkovski, B. B., V., *Magnetic Fluids and Applications Handbook*. Begel House Inc.: New York, 1996; (b) Rosensweig, R. E., *Ferrohydrodynamics*. Cambridge University Press: Cambridge, 1985.

6. Friedman, H. L., The Visible and Ultraviolet Absorption Spectrum of the Tetrachloroferrate (III) Ion in Various Media. *Journal of the American Chemical Society* **1952,** *74* (1), 5-10.

7. Wyrzykowski, D.; Maniecki, T.; Pattek-Janczyk, A.; Stanek, J.; Warnke, Z., Thermal analysis and spectroscopic characteristics of tetrabutylammonium tetrachloroferrate(III). *Thermochimica Acta* **2005,** *435* (1), 92-98.

8. Monti, D.; Cantonetti, V.; Venanzi, M.; Ceccacci, F.; Bombelli, C.; Mancini, G., Interaction of a chirally functionalised porphyrin derivative with chiral micellar aggregates. *Chemical Communications* **2004,** (8), 972-973.

CHAPTER 4

MULTIFUNCTIONAL IONIC LIQUIDS WITH LUMINESCENT, MAGNETIC AND CHIRAL PROPERTIES

4.1. Introduction

Ionic Liquids (ILs) have increasingly been employed in a variety of research areas including synthesis, catalysis, materials science, and (bio)analytics. Consequently, a variety of functional ILs with magnetic,[1] luminescent,[2] photochromic,[3] electrochromic,[4] and chiral[5] properties have since been reported. The prospect of ILs incorporating more than one functionality opens new venues for their application. Recently, dysprosium-based ILs which exhibited dual functionality with intense luminescence and magnetic susceptibility were developed by Mudring *et al*.[6] More recently other bifunctional ILs with dual properties have been reported. For example, Branco *et al.* reported a series of electrochromic and magnetic ionic liquids containing iron, cobalt, and chrome-based EDTA coordination complexes.[4]

In previous studies (Chapter 3) we have combined amino-acid derived cations with tetrachloroferrate anions to obtain dual-functional magnetic, chiral ionic liquids (MCILs).[15] Likewise, an intrinsically fluorescent amino-acid derived chiral IL was also developed for chiral recognition studies of non-fluorescent chiral analytes.[7] Protic chiral ionic liquids were similarly reported and their chiral interactions with various analytes were investigated (Chapter 2). [8] Chiral ILs from natural products such as alkaloids and amino acids have found widespread application in enantiomeric catalysis and synthesis as well as chiral separations and sensing.[5] Herein we report, to the best of our knowledge, the first multifunctional luminescent, magnetic, and chiral ionic liquids (LMCILs). These LMCILs may find use in chiro-optical, magneto-optical and magneto-chiral applications.

4.2. Materials and Methods

4.2.1. Chemicals and Materials

Amino acid methyl ester hydrochlorides including L-alanine methyl ester hydrochloride, L-leucine methyl ester hydrochloride, L-valine methyl ester hydrochloride, and D-valine methyl ester hydrochloride were purchased from Sigma-Aldrich (Milwaukee, WI, USA). Potassium thiocyanate, dysprosium (III) oxide, perchloric acid (70%), (R)- and S(-)-1,1'-binaphthyl-2,2'-diyl hydrogenphosphate (BNP), 2,2,2-*trifluoro*-1-(9-anthryl)ethanol (TFAE), and propranolol (PROP), as well as ethanol, methanol, acetonitrile, and chloroform, were also obtained from Sigma-Aldrich and used as received. Acetone and hexane were acquired from J. T. Baker (Phillipsburg, NJ, USA).

4.2.2. General Instrumental Methods

^{1}H NMR (400 MHz) and ^{13}C NMR (100 MHz) spectra were acquired by use of a Bruker Avance 400 NMR spectrometer. The ^{1}H and ^{13}C chemical shifts are given in parts per million (δ) with TMS as an internal standard. All samples were dissolved in deuterated DMSO for NMR analysis.

FT-IR measurements were performed on a Bruker Tensor 27 FT-IR spectrometer. Samples were analyzed in pure form by use of a DuraSamp IR apparatus. All spectra were obtained using 32 scans for both sample and background, with a resolution of 4 cm^{-1}. Elemental analyses were contracted to Atlantic Microlab (Atlanta, GA).

A Jasco-710 spectropolarimeter was used to obtain the CD spectra of LMCILs. To characterize the LMCILs, their visible absorption spectra were measured using a Shimadzu UV-3101PC UV–Vis–near-IR scanning spectrometer (Shimadzu, Columbia, MD). Absorption was

collected using a 1.0 cm^2 quartz cuvette at room temperature and the blank was subtracted from each spectrum.

The magnetic susceptibility and magnetization of the LMCILs were measured using approximately 80 to 100 mg of the sample in a Quantum Design superconducting quantum interference device (SQUID) magnetometer (San Diego, CA, USA) for temperatures between 5 and 300 K and fields between -50 000 and 50 000 Oe.

A 2950 TGA HR V6.1A thermal gravimetric analyzer (TA Instruments, New Castle, DE, USA) was used to analyze the thermal stability of LMCILs and their decomposition behavior. Samples (about 3-4 mg) were scanned from room temperature to 500 ºC under nitrogen flow (50 mL/min) with a heating rate of 10 ºC/min. Values for the onset degradation temperature and peak temperature were determined from the derivative TGA curves.

Glass transition behavior of LMCILs was investigated using a TA SDT2960 (TA Instruments, New Castle, DE, USA). MCIL samples (about 5 mg) were put in sealed aluminum crucibles and run under a nitrogen flow (50 ml/min). Heating - cooling was performed using the following sequence: the sample was cooled to -60 °C, equilibrated at -60 °C, and maintained isothermally for 3 min at -60 °C; then heated to 150 °C with a rate of 10 °C/min, maintained isothermally for 3 min at 150 ºC; and finally cooled back to -60 °C.

4.2.3. Synthesis of Amino Acid Derived Luminescent Magnetic Chiral Ionic Liquids

A facile two-step synthesis procedure (Scheme 4.1) was used to prepare the luminescent magnetic chiral ionic liquids (LMCILs). In the first step, the three intermediate compounds, L-[AlaOMe][SCN], L-[ValOMe][SCN]), and L-[LeuOMe][SCN], were synthesized by reacting the respective aminoacid methyl ester hydrochlorides (1 equiv.) with KSCN (2 equiv.) in acetonitrile at room temperature for 2 days through anion-exchange reactions. $Dy(ClO_4)_3.6H_2O$ was obtained

by dissolving Dy_2O_3 in 70% $HClO_4$ aqueous solution followed by subsequent removal of water by lyophilization. In the second step, the three LMCILs, L-$[AlaOMe]_5[Dy(SCN)_8]$, L-$[ValOMe]_5[Dy(SCN)_8]$, and L-$[LeuOMe]_5[Dy(SCN)_8]$, were synthesized according to a previously reported procedure with slight modifications.[14] A typical synthesis procedure is as follows. A mixture of L-[ValOMe][SCN] (5 equiv.), KSCN (3 equiv.), and $Dy(ClO_4)_3.6H_2O$ (1 equiv.) was stirred in anhydrous ethanol at room temperature overnight. The white suspension of $KClO_4$ byproduct was removed by filtration and ethanol was evaporated by use of rotary evaporation. The residue was redissolved in anhydrous dichloromethane and the solution was allowed to stand overnight in a refrigerator. After filtration dichloromethane was evaporated under vacuum to afford the LMCILs which were further dried under vacuum for 48 h.

Caution: **Although we did not experience any problems in this work, special care should always be taken when perchlorates are handled due to a potential hazard of explosion.**

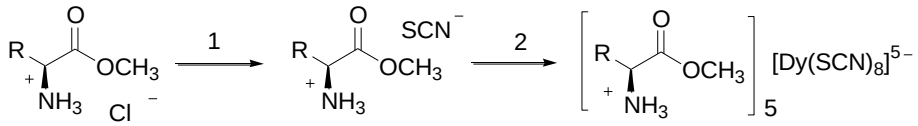

1. KSCN, acetonitrile, 48h, r.t.
2. KSCN, $Dy(ClO_4).6H_2O$, anhydrous EtOH, overnight, r.t.

Scheme 4.1. Synthesis of ILs with luminescent, magnetic, and chiral properties.

4.3. Results and Discussion

4.3.1. Synthesis and Characterization of LMCILs

The identity and purity of the three LMCILs were determined by ^1H, ^{13}C NMR, FT-IR, and C, H, N elemental analysis.

- **L-$[AlaOMe]_5[Dy(SCN)_8]$,** orange viscous liquid, yield 83%, ^1H NMR (400 MHz, DMSO-d6), δ (ppm): 8.24 (broad, 3H), 4.06 (m, 1H), 3.76 (s, 3H), 1.39 (d, 3H). ^{13}C

NMR (100 MHz, DMSO-d6), δ (ppm): 170.6, 130.4, 53.1, 48.5, 16.0. IR (neat), ν (cm^{-1}): 2953, 2053, 1730, 1588, 1458, 1246, 1198, 1107. Anal. Calcd for $[C_4H_{10}NO_2]_5[Dy(SCN)_8]$, C, 29.30; H, 4.39; N, 15.86. Found: C, 29.87; H, 3.98; N, 15.09.

- **L-[ValOMe]$_5$[Dy(SCN)$_8$],** orange viscous liquid, yield 84%, ^{1}H NMR (400 MHz, DMSO-d6), δ (ppm): 8.26 (broad, 3H), 3.89 (m, 1H), 3.66 (s, 3H), 3.26 (m, 1H), 0.91 (d, 6H). ^{13}C NMR (100 MHz, DMSO-d6), δ (ppm): 169.7, 57.7, 53.5, 31.4, 16.9. IR (neat), ν (cm^{-1}): 2965, 2053, 1733, 1588, 1487, 1438, 1285, 1236. Anal. Calcd for $[C_6H_{14}NO_2]_5[Dy(SCN)_8]$, C, 35.44; H, 5.48; N, 14.14. Found: C, 34.95; H, 5.16; N, 14.25.
- **L-[LeuOMe]$_5$[Dy(SCN)$_8$],** orange viscous liquid, yield 86%, ^{1}H NMR (400 MHz, DMSO-d6), δ (ppm): 8.29 (broad, 3H), 3.74 (m, 1H), 3.57 (s, 3H), 3.17 (m, 2H), 1.56 (m, 1H), 0.87 (d, 6H). ^{13}C NMR (100 MHz, DMSO-d6), δ (ppm): 170.9, 130.2, 53.5, 51.1, 24.2, 19.0. IR (neat), ν (cm^{-1}): 2960, 2869, 2055, 1732, 1588, 1492, 1441, 1370, 1225. Anal. Calcd for $[C_7H_{16}NO_2]_5[Dy(SCN)_8]$, C, 38.03; H, 5.64; N, 13.41. Found: C, 37.68; H, 5.08; N, 13.26.

Table 4.1. Thermal properties of LMCILs determined by TGA and DSC.

LMCILs	T_g (^{0}C) [a]	T_{start} (^{0}C) [b]	T_{onset} (^{0}C) [c]	T_{onset2} (^{0}C) [d]
L-$[AlaOMe]_5[Dy(SCN)_8]$	-30.9	147.2	231.1	291.7
L-$[ValOMe]_5[Dy(SCN)_8]$	-20.9	160.4	235.5	284.2
L-$[LeuOMe]_5[Dy(SCN)_8]$	-24.5	150.9	220.4	282.6

[a] Glass transition temperature. [b] The beginning decomposition temperature. [c] The temperature at which sample loses weight at fastest speed. [d] The second beginning decomposition temperature.

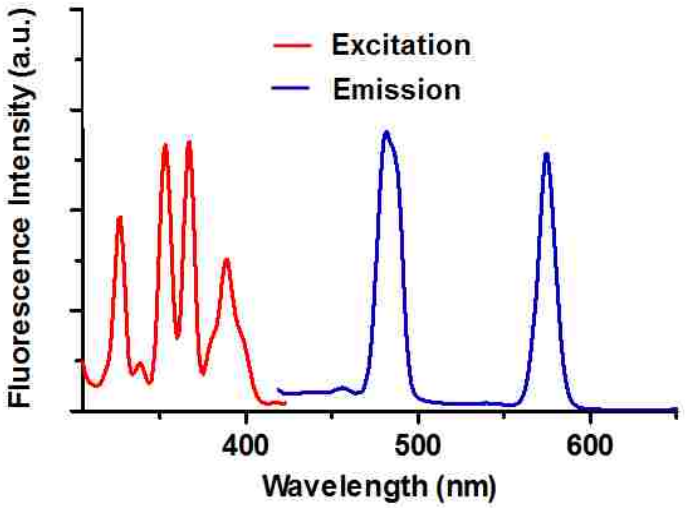

Figure 4.1. Excitation and emission spectra of L-$[ValOMe]_5[Dy(SCN)_8]$ in $CHCl_3$ (1 mM).

4.3.2. Thermal Properties of LMCILs

The thermal properties of these LMCILs, including thermal stabilities and phase transition behaviors, were investigated by use of thermal gravimetric analysis (TGA) and differential scanning calorimetry (DSC), respectively. Results obtained from TGA measurements (Table 4.1) indicate that the LMCILs remained thermally stable up to 150 ºC under nitrogen atmosphere. Their decomposition subsequently occurred in two steps. A rapid decomposition was observed during the first step, resulting in up to 40% loss of weight. During the second step, decomposition occurred at a lower rate, resulting in an additional 30% loss of weight. Similar results were obtained in previous studies with MCILs where decomposition was associated with pyrolysis in the first step and oxidation in the second step (Chapter 3).[9] Observations from DSC analyses revealed that the LMCILs did not display melting behavior. However, glass transitions were observed between -30 and -20 ºC for all LMCILs (Table 4.1). The formation of ionic glasses upon cooling is indicative of a semi-ordered structure within these chiral ILs, suggesting possible applications of these compounds for chiral induction/transfer in enantioselective synthesis.[10]

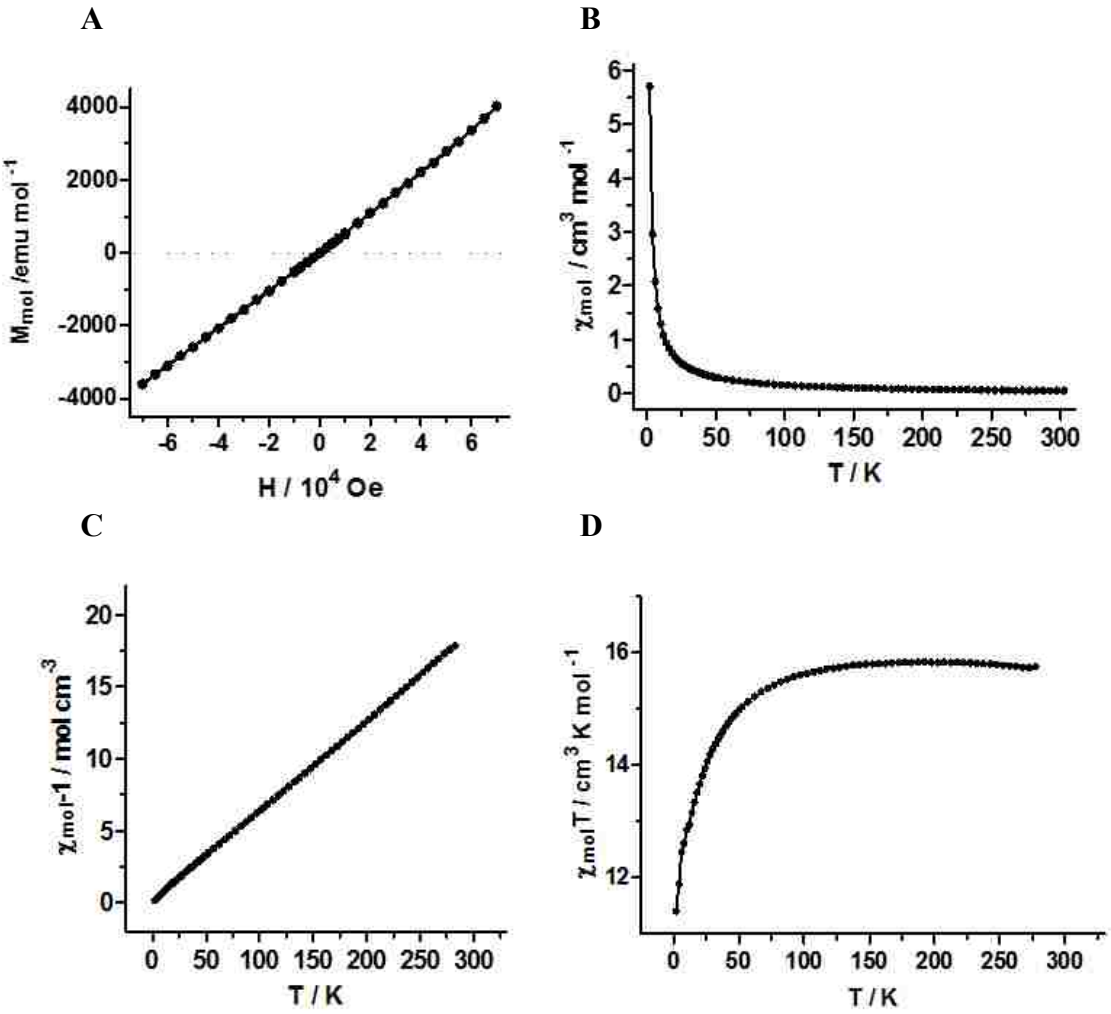

Figure 4.2. Magnetic property of L-[ValOMe]$_5$[Dy(SCN)$_8$]. Field dependence of (A) molar magnetization Mmol at 300 K. Temperature dependence of (B) static molar magnetic susceptibility χmol, (C) reciprocal molar magnetic susceptibility χmol-1, and (D) product of temperature and static molar magnetic susceptibility χ_{mol}T at a field of 1000 Oe.

4.3.3. Luminescent Properties of LMCILs

Fluorescence spectroscopy was performed to investigate the luminescence properties of these LMCILs. Dy^{3+} with its $4f^9$ electron configuration is known for its intense luminescence transitions, $^4F_{9/2} \rightarrow {}^6H_{15/2}$ and $^4F_{9/2} \rightarrow {}^6H_{13/2}$ in the blue and yellowish-green spectral region of the visible light spectrum, respectively. An excitation spectrum was

obtained for L-$[ValOMe]_5[Dy(SCN)_8]$ at λ_{em} = 480 nm along with an emission spectrum at λ_{ex} = 352 nm (Figure 4.1). All LMCILs exhibited two characteristic emission peaks at 480 nm and 574 nm corresponding to the $^4F_{9/2} \rightarrow {}^6H_{15/2}$ and and $^4F_{9/2} \rightarrow {}^6H_{13/2}$ transitions.

4.3.4. Magnetic Properties of LMCILs

In addition to its luminescence, the Dy^{3+} ion with its $4f^9$ electron configuration is also magnetically active. As a result the LMCILs exhibited paramagnetic behavior at room temperature. Their magnetic susceptibilities were measured by use of a superconducting quantum interference device (SQUID) magnetometer. The magnetization at 300 K was measured in a magnetic field ranging from -70 000 to 70 000 Oe and exhibited an expected linear dependence on the applied magnetic field according to Curie's law (Figure 4.2a). From the slopes of the fitted lines, the respective molar magnetic susceptibilities of L-$[AlaOMe]_5[Dy(SCN)_8]$, L-$[ValOMe]_5[Dy(SCN)_8]$, and L-$[LeuOMe]_5[Dy(SCN)_8]$ at 300 K were obtained as χ_{mol} = 0.043, 0.047, 0.042 $cm^3\ mol^{-1}$, which fit well to the expected value for Dy^{3+}.[6] The effective magnetic moment (μ_{eff}) for Dy^{3+} has been calculated as 10.48 μB.[6] The measured respective μ_{eff} values of the L-$[AlaOMe]_5[Dy(SCN)_8]$, L-$[ValOMe]_5[Dy(SCN)_8]$, and L-$[LeuOMe]_5[Dy(SCN)_8]$ were 10.2, 10.6, 10.4 μB, which were very close to the calculated value. The increase in χ_{mol} with decreasing temperature in the plot of magnetic susceptibility against temperature confirms that L-$[ValOMe]_5[Dy(SCN)_8]$ is paramagnetic (Figure 4.2b). The LMCILs can be manipulated by a neodymium magnet due to the large anisotropic magnetic moment of Dy^{3+}.

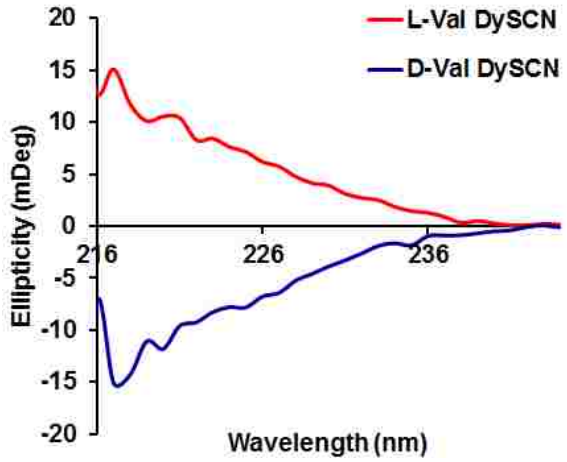

Figure 4.3. Circular dichroism spectra of L- and D-$[ValOMe]_5[Dy(SCN)_8]$ in MeOH (1mM).

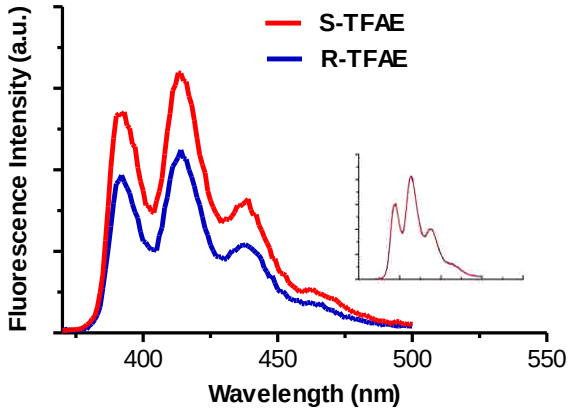

Figure 4.4. Emission of TFAE in MeOH (10 µM) with L-$[ValOMe]_5[Dy(SCN)_8]$ as chiral selector (1 mM). Insert: Emission of TFAE in MeOH (10 µM) without L-$[ValOMe]_5[Dy(SCN)_8]$.

4.3.5. Chiral Properties of LMCILs

Circular dichroism (CD) measurements were performed on both L- and D-$[ValOMe]_5[Dy(SCN)_8]$ to assess their enantiopurity (Figure 4.3). The L- and D-enatiomers displayed a positive and negative CD band respectively at 217 nm, with a maximum of 15 mDeg. Thus, optical purity was confirmed as both enantiomers displayed an opposite CD signal of equal magnitude.

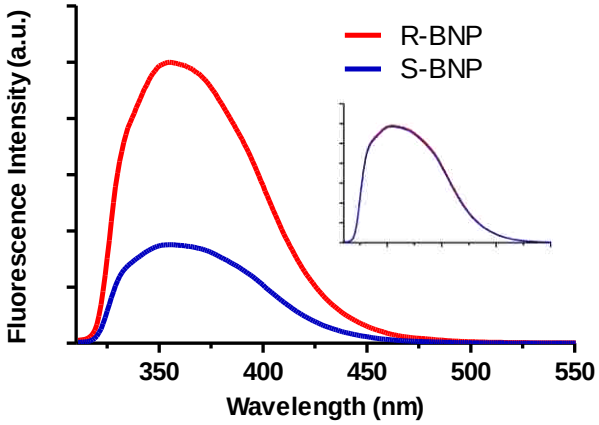

Figure 4.5. Emission of BNP in MeOH (10 µM) with L-$[ValOMe]_5[Dy(SCN)_8]$ as chiral selector (1 mM). Insert: Emission of BNP in MeOH (10 µM) without L-$[ValOMe]_5[Dy(SCN)_8]$.

4.3.6. Enantiomeric Recognition of Chiral Analytes by LMCILs through the use of Steady-State Fluorescence Spectroscopy

Enantioselectivity and chiral recognition ability of L- $[ValOMe]^5[Dy(SCN)^8]$ were subsequently investigated by use of steady state fluorescence spectroscopy, as previously reported for other chiral ILs.[7, 9, 11] Chiral recognition of intrinsically fluorescent chiral analytes was determined in methanol solutions with L-$[ValOMe]^5[Dy(SCN)^8]$ as the chiral selector (Figure 4.4). In the presence of the IL, differences in fluorescent intensities were observed for either (R)- or (S)-2,2,2-trifluoro-1-(9-anthryl)- ethanol (TFAE), thus confirming its chiral discrimination ability. The observed decrease in fluorescence intensity for R-TFAE compared to S-TFAE appears to be the result of a more favorable diastereomeric interaction for the former, resulting in quenching of the fluorophore. It should be mentioned that both R-TFAE and S-TFAE exhibited equal fluorescence intensity in the absence of the LMCIL (Figure 4.4, insert). Chiral recognition studies were also performed on (R)- and (S)-1,1'-binaphthyl-2,2'-diylhydrogen-phosphate (BNP). Similar to TFAE, enantiomers of BNP displayed drastically different fluorescence intensities, allowing for L-$[ValOMe]^5[Dy(SCN)^8]$ discrimination between the BNP

enantiomers (Figure 4.5).

4.4. Conclusions

In conclusion, novel multifunctional ionic liquids were conveniently synthesized, employing a facile two-step procedure. These trifunctional ILs represent the first examples of room temperature ionic liquids that simultaneously exhibit luminescent, magnetic, and chiral properties. Their luminescent propeties were confirmed by the distinctive luminescence signal of Dy^{3+} with its sharp emission bands. Observations from SQUID measurements revealed the paramagnetic behavior of the LMCILs, while their enantiopurity was evidenced by CD measurements. Fluorescence steady-state measurements further confirmed the chiral discrimination ability of these ILs. The LMCILs reported here may possibly find use in responsive materials where chiral properties can be manipulated through optical, photophysical and magnetic stimuli or vice versa.

4.5. References

1. Hayashi, S.; Hamaguchi, H. O., Discovery of a magnetic ionic liquid bmim FeCl4. *Chemistry Letters* **2004,** *33* (12), 1590-1591.

2. Tang, S.; Babai, A.; Mudring, A.-V., Europium-based ionic liquids as luminescent soft materials. *Angewandte Chemie-International Edition* **2008,** *47* (40), 7631-7634.

3. Branco, L. C.; Pina, F., Intrinsically photochromic ionic liquids. *Chemical Communications* **2009,** (41), 6204-6206.

4. Branco, A.; Branco, L. C.; Pina, F., Electrochromic and magnetic ionic liquids. *Chemical Communications* **2011,** *47* (8), 2300-2302.

5. Wasserscheid, P.; Bosmann, A.; Bolm, C., Synthesis and properties of ionic liquids derived from the 'chiral pool'. *Chemical Communications* **2002,** (3), 200-201.

6. Mallick, B.; Balke, B.; Felser, C.; Mudring, A.-V., Dysprosium room-temperature ionic liquids with strong luminescence and response to magnetic fields. *Angewandte Chemie-International Edition* **2008,** *47* (40), 7635-7638.

7. Bwambok, D. K.; Challa, S. K.; Lowry, M.; Warner, I. M., Amino Acid-Based Fluorescent Chiral Ionic Liquid for Enantiomeric Recognition. *Analytical Chemistry* **2010,** *82* (12), 5028-5037.

8. de Rooy, S. L.; Li, M.; Bwambok, D. K.; El-Zahab, B.; Challa, S.; Warner, I. M., Ephedrinium-Based Protic Chiral Ionic Liquids for Enantiomeric Recognition. *Chirality* **2011,** *23* (1), 54-62.

9. Li, M.; De Rooy, S. L.; Bwambok, D. K.; El-Zahab, B.; DiTusa, J. F.; Warner, I. M., Magnetic chiral ionic liquids derived from amino acids. *Chemical Communications* **2009,** (45), 6922-6924.

10. Schulz, P. S.; Müller, N.; Bösmann, A.; Wasserscheid, P., Effective Chirality Transfer in Ionic Liquids through Ion-Pairing Effects. *Angew. Chem.* **2007,** *119* (8), 1315-1317.

11. Tran, C. D.; Oliveira, D., Fluorescence determination of enantiomeric composition of pharmaceuticals via use of ionic liquid that serves as both solvent and chiral selector. *Analytical Biochemistry* **2006,** *356* (1), 51-58.

CHAPTER 5

FLUORESCENT ONE-DIMENSIONAL NANOSTRUCTURES FROM A GROUP OF UNIFORM MATERIALS BASED ON ORGANIC SALTS

5.1. Introduction

Organic nanostructures continue to receive widespread attention due to their inherent chemical tunability,[1] which makes them suitable for applications in optics, optoelectronics,[2] and electronics.[3] In addition to altering their molecular structure and crystallinity, further tunability can be achieved through changing the morphology of these materials.[4] In particular, one-dimensional (1D) organic nanostructures such as tubes, wires and belts display interesting optoelectronic properties, ideal for use as lasers,[5] waveguides,[5b, 6] organic light emitting diodes (OLEDs),[7] and organic field effect transistors (OFETs).[1c, 8]

Typical strategies for preparing organic 1D nanostructures include vapor-deposition,[9]self-assembly,[1c, 7a, 10] and template-assisted synthesis.[11] Both soft and hard templates have previously been used in the preparation of 1D organic nanomaterials.[11b, 12] Soft templates such as microemulsions have been widely reported in the fabrication of low dimensional metal and inorganic structures and only more recently in organic structures.[13] Alternatively, hard templates from porous materials have also been used for growing 1D organic nanostructures. The most commonly applied hard templates are track-etched polycarbonate filters[14] and anodic aluminum oxide (AAO) membranes. The first assembly of 1D nanomaterials in a porous membrane was reported by Martin and coworkers.[11c] Polymer nanotubes fabricated through this method have been applied in bioanalytical chemistry for sensing different types of proteins and DNA.[15] Applying similar techniques, nanowires were also reported for conductive,[16] magnetic, molecularly imprinted polymers,[17] and semiconducting polymers.[18] In addition to polymers, metals, inorganic materials,[19,20] small organic molecules[8] have also been templated in porous

membranes. However, nanostructures derived from organic salts using a hard templating approach have previously not been reported.

Recently, our group reported the preparation of nanoparticles from frozen ionic liquids and higher melting organic salts that were dubbed a *G*roup of *U*niform *M*aterials *B*ased on *O*rganic *S*alts (GUMBOS).[21] These organic salts are highly functional and tunable materials that can be designed to have different properties built into their respective cations and anions.[21a,21b,22] Nanostructures composed of GUMBOS combine the physical advantages of nanomaterials and the chemical functionality of GUMBOS in a single nanostructure. The current work describes the first report of fluorescent organic salts that were templated in porous alumina membranes to fabricate 1D nanostructures.

5.2 Materials and Methods

5.2.1. Chemicals and Materials

Rhodamine 6G chloride, sodium tetraphenylborate, and industrial grade phosphoric acid were purchased from Sigma-Aldrich (Milwaukee, WI). Porous alumina membranes with a 13 mm disc diameter, a thickness of 20 μm, and 200 nm pore sizes were purchased from SPI Supplies and Structure Probe Inc. (West Chester, PA). Organic solvents, including acetonitrile, acetone, and dichloromethane were of HPLC grade (J.T. Baker, Philipsburg, NJ). Triply deionized ultra-pure water (18.2 MΩ) was acquired using an Elga model PURELAB Ultra™ water filtration system.

5.2.2. General Instrumental Methods

^{1}H NMR (400 MHz) and ^{13}C NMR (100 MHz) spectra were acquired by use of a Bruker Avance 400 NMR spectrometer. The ^{1}H and ^{13}C chemical shifts are given in parts per million (δ) with TMS as an internal standard. All samples were dissolved in deuterated DMSO for NMR

analysis. Additional characterizations were performed with high resolution mass spectrometry (HR-MS) on an Agilent 6210 electrospray ionization time-of-flight instrument in the positive and negative ion mode. The melting point of the GUMBOS was determined using a MEL-TEMP® capillary melting point apparatus.

Electron micrographs were obtained by use of a JEOL 100CX transmission electron microscope (TEM) and SM-6610, JSM-6610LV high and low vacuum scanning electron microscope (SEM). The TEM samples were prepared by dropcasting a dilute suspension of the nanomaterials onto carbon-coated copper grids and drying under vacuum for 4 hours. The SEM samples were either dropcast or immobilized (nanoarray) onto double-sided tape and sputter-coated using a thin conductive gold layer for 2 min.

Absorbance measurements were performed using a Shimadzu UV-3101PC UV–Vis–near-IR scanning spectrometer (Shimadzu, Columbia, MD). Absorbance was collected using a 1.0 cm^2 quartz cuvette at room temperature and the blank was subtracted from each spectrum.

Fluorescence studies were performed in the steady-state mode on a Spex Fluorolog-3 spectrofluorimeter (model FL3-22TAU3; Jobin Yvon Edison, NJ) equipped with a 450 Watt Xe lamp and R928 PMT emission detector. Excitation and emission wavelengths with 3 nm bandpasses were selected as well as an integration time of 0.1 s per point. Fluorescence data was corrected by taking the quotient of the analyte signal and the reference signal. Fluorescence images were obtained using a Leica TCS SP2 scanning laser confocal system with a 63× NA 1.4 lens. Images (1024 × 1024 pixels) were acquired based on six averages.

Fluorescence Lifetime Imaging Microscopy (FLIM) was performed at Horiba Scientific, Edison, NJ with a DynaMyc - Lifetime Microscope System. A picosecond pulsed excitation source of 495 nm was used and emission was collected at 550 nm with a TBX detector. The time

correlated single photon counting (TSCPC) mode was used for data acquisition with a resolution of 50 ps/channel. The automated 3-dimensional scanning combined with automated confocal ability of the instrument generated FLIM images with micron level spatial resolution.

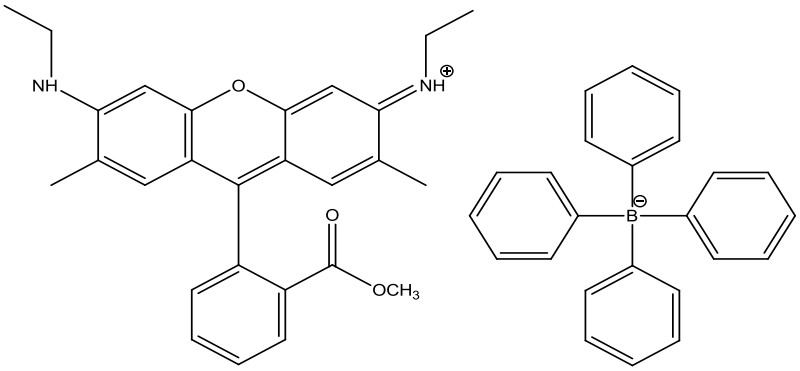

Figure 5.1. Chemical structure of [R6G][TPB].

5.2.3. Synthesis of Rhodamine 6G Tetraphenylborate ([R6G][TPB]) GUMBOS

The rhodamine 6G tetraphenylborate ([R6G][TPB]) GUMBOS was synthesized through a facile metathesis reaction between rhodamine 6G chloride and sodium tetraphenylborate in a biphasic mixture of water and dichloromethane (DCM). The molar ratio between rhodamine 6G chloride ([R6G][Cl]) and sodium tetraphenylborate ([Na][TPB]) was chosen to be 1 to 1.1 to ensure complete conversion. Following the reaction, the organic phase containing rhodamine 6G tetraphenylborate ([R6G][TPB]) GUMBOS was rinsed several times with ultrapure water (18.2 MΩ cm) to remove any sodium chloride byproduct. The [R6G][TPB] was determined to be highly water insoluble, in contrast to the precursor [R6G][Cl]. Finally, the DCM was evaporated after which the product was freeze-dried and lyophilized overnight. Dry [R6G][TPB] was obtained (Figure 5.1).

5.2.4. Preparation of One-Dimensional GUMBOS Nanostructures

Commercially obtained aluminum oxide membranes (Whatman Anodisc supported membrane filter) were wetted with a concentated solution of [R6G][TPB] in a volatile organic

solvent such as acetone. Upon evaporation of the solvent, the pores were filled with the GUMBOS. Afterwards, the membranes were placed in a container saturated with acetone vapor at 60 ºC, for the duration of one hour to ensure complete and even filling of the membrane pores by [R6G][TPB]. Excess [R6G][TPB], accumulated on top of the membrane was removed by use of 180-Grit fine sandpaper. The templated membranes were subsequently submerged into a 1.0 M phosphoric acid solution and allowed to sit overnight. Alternatively, membranes were immobilized onto a substrate with an epoxy adhesive, allowing them to dry for 12 hours prior to dissolution in the phosphoric acid solution. The resulting 1D-nanoGUMBOS were rinsed several times with ultrapure water and placed on a lyophilizer overnight to dry. Free nanowires and nanowire arrays were obtained after drying. Similarly, nanotubes and nanotube arrays were obtained through slight modification of the procedure to employ dilute solutions of [R6G][TPB] (1 μM), instead of concentrated (0.1 M) solutions. A schematic of the synthesis procedure is depicted in Figure 5.2.

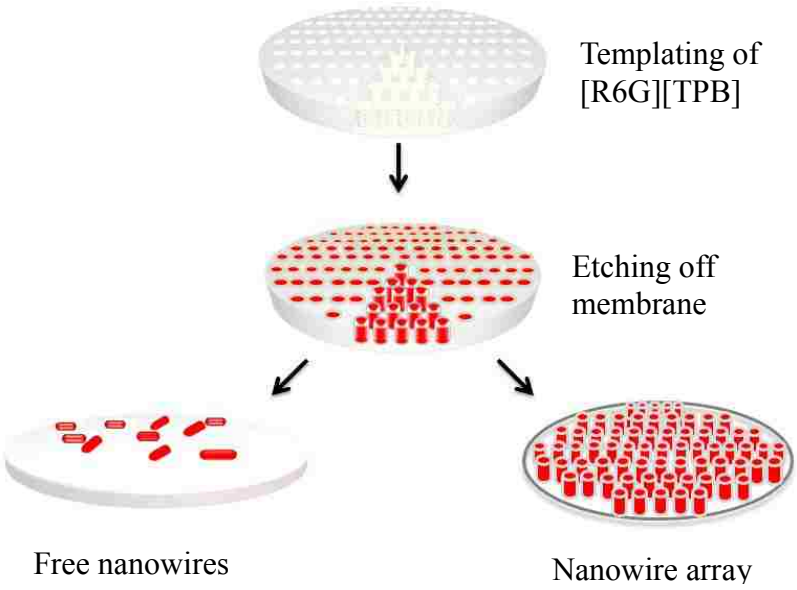

Figure 5.2. Fabrication of [R6G][TPB] nanowires and nanoarrays by AAO templating.

5.3. Results and Discussion

5.3.1. Synthesis and Characterization of [R6G][TPB] GUMBOS

Rhodamine 6G chloride (100.0 mg, 0.21 mmol) was reacted with 1.1 molar equivalent of sodium tetraphenylborate to yield rhodamine 6G tetraphenylborate (129.6 mg, yield 80.9 %), mp. 86 – 89 ºC. ^{1}H NMR (400 MHz, DMSO-d6), δ (ppm): 8.31 (d, 1H), 7.75 (m, 2H), 7.41 (d, 1H), 7.01 (d, 3H), 6.83 (d, 4H), 4.05 (s, 3H), 3.49 (q, 4H), 2.29 (s, 6H), 1.40 (t, 6H). ^{13}C NMR (100 MHz, DMSO-d6), δ (ppm): 157.4, 156.2, 133.6, 131.3, 130.8, 128.9, 125.9, 113.3, 94.0, 61.4, 40.6, 38.4, 18.1, 14.1, 13.8. IR (neat), ν (cm^{-1}): 3462, 3154, 3089, 2982, 1712, 1648, 1587, 1441, 1245, 805, 746. Anal. Calcd for $[C_{28}H_{31}N_2O_3][B(C_6H_5)_4]$, C, 81.88; H, 6.74; N, 3.67. Found: C, 80.25; H, 6.53; N, 3.89.

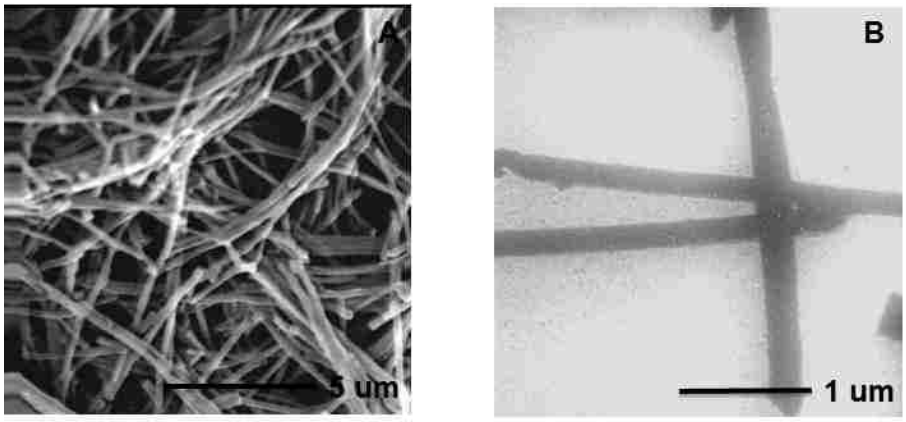

Figure 5.3. SEM micrograph (A) and TEM micrograph (B) of [R6G][TPB] nanowires.

5.3.2. Electron Microscopy Studies of One-Dimensional GUMBOS Nanostructures

The templated 1D-nanostructures exhibited wirelike features with diameters larger than the inner pores of the AAO membranes (200 nm), ranging from 260 nm to 330 nm (Figure 5.3). The nanotubes exhibited somewhat larger diameters, between 350 nm and 410 nm, with a thickness of around 60 nm (Figure 5.4). These results indicate a swelling of the nanostructures

outside the confinements of the AAO membranes similar to previously reported silica-coated organic nanorods.[23]

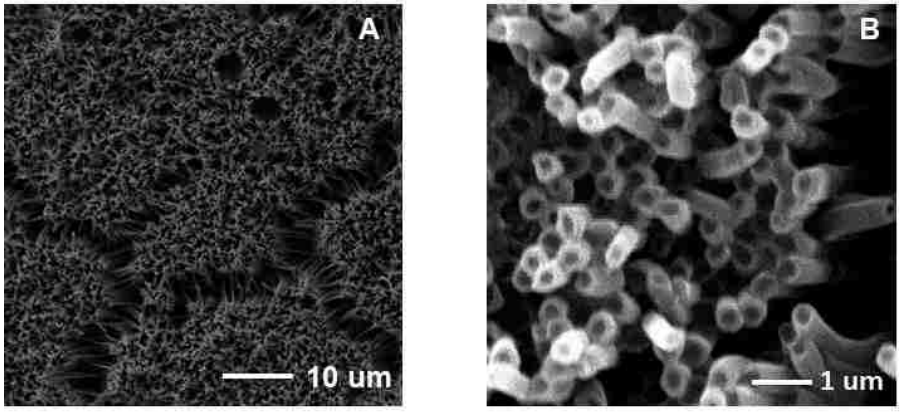

Figure 5.4. SEM micrographs of [R6G][TPB] nanotube arrays.

.

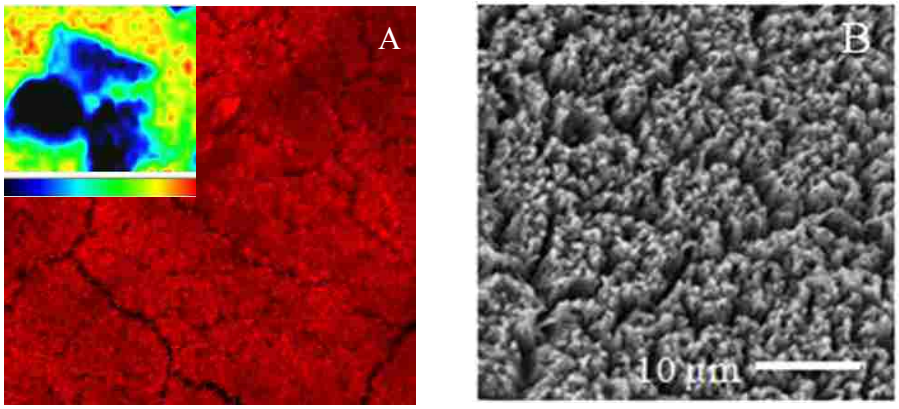

Figure 5.5. Fluorescence microscopy image (A) and SEM micrograph (B) of [R6G][TPB] nanowire arrays (inset: fluorescence lifetime imaging map; range 2.4 - 3.4 ns).

5.3.3. Spectroscopic Properties of [R6G][TPB] GUMBOS Nanostructures

The spectral properties of the nanoarrays were investigated using a Leica TCS SP2 scanning laser confocal fluorescence microscope with a 63x NA 1.4 lens with excitation at 543 nm. Emitted light was collected in the 555 to 700 nm range (Figure 5.5). The nanostructures displayed high fluorescence intensity with reference to the background as seen in Figure 5.5

Compared with the absorbance of bulk [R6G][[TPB] in ethanolic solution, the absorption spectrum of the [R6G][TPB] nanowires exhibited broader peaks and a slight shift of the absorption maximum from 525 nm to 529 nm, as seen in Figure 5.6. Similarly, fluorescence of the [R6G][TPB] nanowires showed a broader spectrum and red shift from 551 nm to 564 nm. These results are indicative of a supramolecular type of arrangement that couples the spectral transitions of individual fluorescent structures.

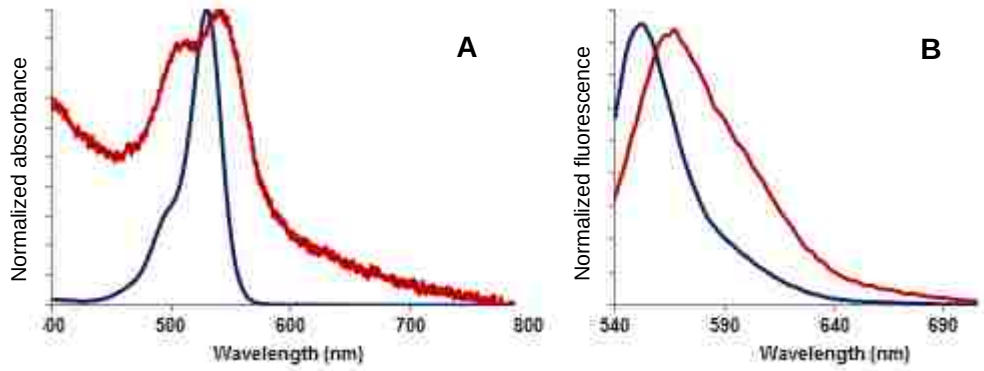

Figure 5.6. (A) UV-visible absorption spectra of [R6G][TPB] solution in ethanol (blue) and nanowires (B) Fluorescence spectra of [R6G][TPB] solution in ethanol (blue) and nanowires.

Fluorescence lifetime mapping of the nanowire arrays (inset Figure 5.5) reveals the presence of multiple lifetime components. The data were best fitted to a bi-exponential decay. The dark blue areas represent a shorter lifetime of 2.4 ns whereas the orange areas represent a longer lifetime of around 3.4 ns. Similar results were reported in the literature for solutions of rhodamine 6G in methanol, where shorter lifetimes recorded at higher concentrations of the dye were attributed to excimer formation.[24] A shift to longer wavelengths and increase in the relative intensity of the vibronic shoulder as seen in Figure 5.6 were previously reported for rhodamine 6G adsorbed onto thin solid films of laponite.[25] Likewise a broad red shifted fluorescence emission band was also recorded in addition to decreasing lifetimes. These results can be explained by the presence of multiple higher-order H-type aggregates with the possibility of

some J-type dimers.[25] Furthermore, the [R6G][TPB] nanowires displayed high photostability when irradiated at 526 nm over a period of 5000 s with emission and excitation slit widths set at 14 nm (Figure 5.7). The fluorescent 1D nanomaterials discussed here may be considered as potential materials for solid-state lasing applications.

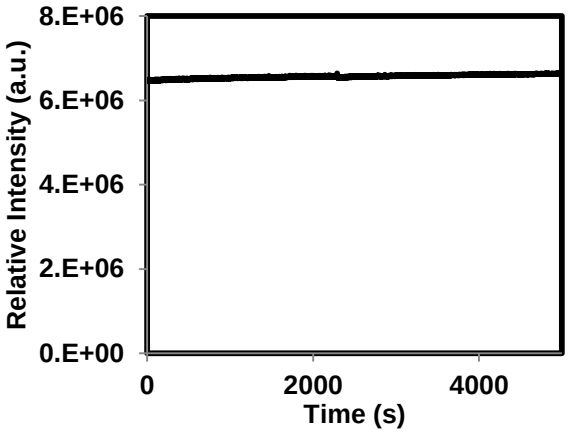

Figure 5.7. Photostability of [R6G][TPB] nanowire array excited at 526 nm for the duration of 5000 s (14 nm slit width).

5.4. Conclusion

In summary, for the first time a facile templating nanofabrication method is reported for the preparation of 1D fluorescent organic salts. Water-insoluble [R6G][TPB] was obtained through ion-association between a hydrophilic cationic dye and a hydrophobic anion. The [R6G][TPB] fluorescent nanowires exhibited intense fluorescence, as well as high photostability and diameters greater than the template pores. Further studies are underway to determine the utility of [R6G][TPB] 1D-nanostructures as waveguides for applications in optoelectronics and in chemical sensing devices. Finally, this templating method can also be utilized for preparation of 1D-nanostructures from organic salts with chiral, magnetic, electroluminescent, conductive, or combinations of these properties.

5.5. References

1. (a) An, B. K.; Gihm, S. H.; Chung, J. W.; Park, C. R.; Kwon, S. K.; Park, S. Y., Color-Tuned Highly Fluorescent Organic Nanowires/Nanofabrics: Easy Massive Fabrication and Molecular Structural Origin. *Journal of the American Chemical Society* **2009,** *131* (11), 3950-3957; (b) Tian, Z. Y.; Chen, Y.; Yang, W. S.; Yao, J. N.; Zhu, L. Y.; Shuai, Z. G., Low-dimensional aggregates from stilbazolium-like dyes. *Angewandte Chemie-International Edition* **2004,** *43* (31), 4060-4063; (c) Briseno, A. L.; Mannsfeld, S. C. B.; Reese, C.; Hancock, J. M.; Xiong, Y.; Jenekhe, S. A.; Bao, Z.; Xia, Y., Perylenediimide nanowires and their use in fabricating field-effect transistors and complementary inverters. *Nano Letters* **2007,** *7*, 2847-2853; (d) Zhao, Y. F.; Mu, X. Y.; Bao, C. X.; Fan, Y.; Zhang, J. Y.; Wang, Y., Alkyl Chain Length Dependent Morphology and Emission Properties of the Organic Micromaterials Based on Fluorinated Quinacridone Derivatives. *Langmuir* **2009,** *25* (5), 3264-3270.

2. Zhao, Y. S.; Fu, H.; Peng, A.; Ma, Y.; Liao, Q.; Yao, J., Construction and Optoelectronic Properties of Organic One-Dimensional Nanostructures. *Accounts of Chemical Research* **2009,** *43* (3), 409-418.

3. Li, R.; Hu, W.; Liu, Y.; Zhu, D., Micro- and Nanocrystals of Organic Semiconductors. *Accounts of Chemical Research* **2010,** *43* (4), 529-540.

4. Lee, J. W.; Kim, K.; Park, D. H.; Cho, M. Y.; Lee, Y. B.; Jung, J. S.; Kim, D. C.; Kim, J.; Joo, J., Light-Emitting Rubrene Nanowire Arrays: A Comparison with Rubrene Single Crystals. *Advanced Functional Materials* **2009,** *19* (5), 704-710.

5. (a) O'Carroll, D.; Lieberwirth, I.; Redmond, G., Microcavity effects and optically pumped lasing in single conjugated polymer nanowires. *Nature Nanotechnology* **2007,** *2* (3), 180-184; (b) Zhao, Y. S.; Peng, A. D.; Fu, H. B.; Ma, Y.; Yao, J. N., Nanowire waveguides and ultraviolet lasers based on small organic molecules. *Advanced Materials* **2008,** *20* (9), 1661-+.

6. (a) Takazawa, K.; Kitahama, Y.; Kimura, Y.; Kido, G., Optical waveguide self-assembled from organic dye molecules in solution. *Nano Letters* **2005,** *5* (7), 1293-1296; (b) Zhao, Y. S.; Xu, J. J.; Peng, A. D.; Fu, H. B.; Ma, Y.; Jiang, L.; Yao, J. N., Optical waveguide based on crystalline organic microtubes and microrods. *Angewandte Chemie-International Edition* **2008,** *47* (38), 7301-7305.

7. (a) Che, Y. K.; Yang, X. M.; Balakrishnan, K.; Zuo, J. M.; Zang, L., Highly Polarized and Self-Waveguided Emission from Single-Crystalline Organic Nanobelts. *Chemistry of Materials* **2009,** *21* (13), 2930-2934; (b) Zhao, Y. S.; Di, C. A.; Yang, W. S.; Yu, G.; Liu, Y. Q.; Yao, J. N., Photoluminescence and electroluminescence from tris(8-hydroxyquinoline)aluminum nanowires prepared by adsorbent-assisted physical vapor deposition. *Advanced Functional Materials* **2006,** *16* (15), 1985-1991.

8. Briseno, A. L.; Mannsfeld, S. C. B.; Jenekhe, S. A.; Bao, Z.; Xia, Y., Introducing organic nanowire transistors. *Materials Today* **2008,** *11* (4), 38-47.

9. (a) Tang, Q. X.; Li, H. X.; Liu, Y. L.; Hu, W. P., High-performance air-stable n-type transistors with an asymmetrical device configuration based on organic single-crystalline submicrometer/nanometer ribbons. *Journal of the American Chemical Society* **2006,** *128* (45), 14634-14639; (b) Zhao, Y. S.; Wu, J. S.; Huang, J. X., Vertical Organic Nanowire Arrays: Controlled Synthesis and Chemical Sensors. *Journal of the American Chemical Society* **2009,** *131* (9), 3158-+; (c) Li, R. J.; Li, H. X.; Song, Y. B.; Tang, Q. X.; Liu, Y. L.; Xu, W.; Hu, W. P.; Zhu, D. B., Micrometer- and Nanometer-Sized, Single-Crystalline Ribbons of a Cyclic Triphenylamine Dimer and Their Application in Organic Transistors. *Advanced Materials* **2009,** *21* (16), 1605-+.

10. Zang, L.; Che, Y. K.; Moore, J. S., One-Dimensional Self-Assembly of Planar pi-Conjugated Molecules: Adaptable Building Blocks for Organic Nanodevices. *Accounts of Chemical Research* **2008,** *41* (12), 1596-1608.

11. (a) Yoon, H.; Chang, M.; Jang, J., Formation of 1D poly(3,4-ethylenedioxythiophene) nanomaterials in reverse microemulsions and their application to chemical sensors. *Advanced Functional Materials* **2007,** *17* (3), 431-436; (b) Zhao, L. Y.; Yang, W. S.; Ma, Y.; Yao, J. N.; Li, Y. L.; Liu, H. B., Perylene nanotubes fabricated by the template method. *Chemical Communications* **2003,** (19), 2442-2443; (c) Martin, C. R.; Vandyke, L. S.; Cai, Z. H.; Liang, W. B., Template Synthesis of Organic Microtubules. *Journal of the American Chemical Society* **1990,** *112* (24), 8976-8977.

12. Fu, H. B.; Xiao, D. B.; Yao, J. N.; Yang, G. Q., Nanofibers of 1,3-diphenyl-2-pyrazoline induced by cetyltrimethylammonium bromide micelles. *Angewandte Chemie-International Edition* **2003,** *42* (25), 2883-2886.

13. (a) Song, J. H.; Kim, F.; Kim, D.; Yang, P. D., Crystal overgrowth on gold nanorods: Tuning the shape, facet, aspect ratio, and composition of the nanorods. *Chemistry-a European Journal* **2005,** *11* (3), 910-916; (b) Shi, H. T.; Qi, L. M.; Ma, J. M.; Cheng, H. M., Synthesis of single crystal BaWO4 nanowires in catanionic reverse micelles. *Chemical Communications* **2002,** (16), 1704-1705.

14. Martin, C. R., Membrane-based synthesis of nanomaterials. *Chemistry of Materials* **1996,** *8* (8), 1739-1746.

15. (a) Sexton, L. T.; Horne, L. P.; Sherrill, S. A.; Bishop, G. W.; Baker, L. A.; Martin, C. R., Resistive-pulse studies of proteins and protein/antibody complexes using a conical nanotube sensor. *Journal of the American Chemical Society* **2007,** *129*, 13144-13152; (b) Martin, C. R.; Siwy, Z. S., Learning nature's way: Biosensing with synthetic nanopores. *Science* **2007,** *317* (5836), 331-332.

16. Il Cho, S.; Lee, S. B., Fast electrochemistry of conductive polymer nanotubes: Synthesis, mechanism, and application. *Accounts of Chemical Research* **2008,** *41* (6), 699-707.

17. Li, Y.; Yin, X. F.; Chen, F. R.; Yang, H. H.; Zhuang, Z. X.; Wang, X. R., Synthesis of magnetic molecularly imprinted polymer nanowires using a nanoporous alumina template. *Macromolecules* **2006,** *39* (13), 4497-4499.

18. Moynihan, S.; Iacopino, D.; O'Carroll, D.; Doyle, H.; Tanner, D. A.; Redmond, G., Emission color tuning in semiconducting polymer nanotubes by energy transfer to organo-lanthanide dopants. *Advanced Materials* **2007,** *19* (18), 2474-+.

19. Zhang, F.; Mao, Y.; Park, T. J.; Wong, S. S., Green synthesis and property characterization of single-crystalline perovskite fluoride nanorods. *Advanced Functional Materials* **2008,** *18* (1), 103-112.

20. Zhou, H. J.; Wong, S. S., A facile and mild synthesis of 1-D ZnO, CuO, and alpha-Fe2O3 nanostructures and nanostructured arrays. *Acs Nano* **2008,** *2* (5), 944-958.

21. (a) Tesfai, A.; El-Zahab, B.; Kelley, A. T.; Li, M.; Garno, J. C.; Baker, G. A.; Warner, I. M., Magnetic and Nonmagnetic Nanoparticles from a Group of Uniform Materials Based on Organic Salts. *Acs Nano* **2009,** *3* (10), 3244-3250; (b) Bwambok, D. K.; El-Zahab, B.; Challa, S. K.; Li, M.; Chandler, L.; Baker, G. A.; Warner, I. M., Near-Infrared Fluorescent NanoGUMBOS for Biomedical Imaging. *Acs Nano*, ACS ASAP.

22. Li, M.; De Rooy, S. L.; Bwambok, D. K.; El-Zahab, B.; DiTusa, J. F.; Warner, I. M., Magnetic chiral ionic liquids derived from amino acids. *Chemical Communications* **2009,** (45), 6922-6924.

23. Al-Kaysi, R. O.; Dillon, R. J.; Zhu, L. Y.; Bardeen, C. J., Template assisted synthesis of silica-coated molecular crystal nanorods: From hydrophobic to hydrophilic nanorods. *Journal of Colloid and Interface Science* **2008,** *327* (1), 102-107.

24. Selanger, K. A.; Falnes, J.; Sikkeland, T., Fluorescence Lifetime Studies of Rhodamine 6G in Methanol. *Journal of Physical Chemistry* **1977,** *81* (20), 1960-1963.

25. Martinez, V. M.; Arbeloa, F. L.; Prieto, J. B.; Arbeloa, I. L., Characterization of rhodamine 6G aggregates intercalated in solid thin films of laponite clay. 2 - Fluorescence spectroscopy. *Journal of Physical Chemistry B* **2005,** *109* (15), 7443-7450.

CHAPTER 6

IONICALLY SELF-ASSEMBLED, MULTI-LUMINOPHORE ONE-DIMENSIONAL MICRO- AND NANOSCALE AGGREGATES OF THIACARBOCYANINE GUMBOS

6.1. Introduction

Nanoscale aggregates of organic materials have gained widespread attention in fields such as biomedicine and optoelectronics due to the versatility and tunability of the electronic and photophysical properties of these materials.[1] The impact of such materials in these fields and others is expected to grow with new developments such as thin organic films in energy harvesting and in solid-state laser technology.[2] In the present work we examine dye aggregation within molecular aggregates, specifically thiacarbocyanines. We refer to these aggregates as molecular micro- and nano-scale aggregates to specify that their dimensions are either several microns or smaller than 100 nm. One-dimensional nanomaterials are defined as those structures in which only one dimension is confined to the nanoscale, i.e. wires, rods, tubes.[3]

Fluorescent one-dimensional (1-D) nanomaterials have been the subject of considerable research over the past few years due to their potential use in fields such as nanoelectronics, energy harvesting, and bioimaging.[4] Designing such nanostructures has been achieved through various templated and non-templated approaches. Fabrication of nanomaterials with desired morphologies and properties through spontaneous molecular self-assembly is particularly desirable since such strategies require neither the use of additives nor templates.

Arrangement of organic dyes into extended supramolecular arrays is a well-established area and is usually recognized as the result of oriented dye aggregation, arising from various dispersive forces such as π-π, cation-π, electrostatic, ion-dipole, hydrophobic, and hydrogen bonding interactions between individual dye molecules.[5] As a result, coupled optical transitions often occur, leading to the formation of a diversity of aggregates, each with unique spectral

properties. Dye aggregates are often classified based on the type or directionality of intermolecular stacking. Head-to-tail molecular stacking is characterized by a narrow, bathochromically-shifted (red-shifted) absorption band as compared to the monomeric dye and these aggregates are referred to as J-aggregates. The study of dye aggregation has led to seminal developments in a wide range of areas including molecular imaging,[6] photodynamic therapy,[7] polarizing and non-linear optics,[8] laser technology,[9] and dye-sensitized solar cells.[10]

Cyanines, a family of versatile dyes which were initially used in the photographic industry, have received particular attention in the study of dye aggregation. Their aggregation behavior has been investigated in solution[11] as well as in thin films,[12] hybrid organoclays,[13] and electrospun fibers.[14] To date, however, there have only been a handful of reports on the synthesis and application of nanomaterials containing cyanine dyes.[15]

As described in the previous chapter, our group has recently reported on a class of polyionic nanomaterials we have come to refer to as "GUMBOS".[16] These GUMBOS are designer salts comprising bulky organic ions arranged in a disordered ionic lattice. A variety of these materials have been prepared with fluorescent, magnetic, and tumor-targeting properties.[16b, 17]

The current study provides a facile route to examples of 1D nano- and microscale morphologies derived from a series of thiacarbocyanine (TC)-based GUMBOS with distinctive and attractive photoluminescent features. Nanomaterials derived from a series of thiacyanine iodide dyes bearing different alkyl side-chain lengths have been previously reported. In one particular study by Takazawa, dye molecules were dissolved in water at elevated temperature, allowing for self-assembly into nanowires under controlled-cooling conditions.[15a] In a later study from the same author, microrings were obtained through surface-assisted self-assembly of

similar dyes.[15b] The resulting thiacyanine nanowires and microrings exhibited interesting optical waveguide properties, allowing them to function as suitable candidates for signal transduction in microelectronics devices. In another study, nanoparticles were prepared from a thiatricarbocyanine iodide dye using a reprecipitation approach in a variety of "bad" solvents to yield nanoparticles of various shapes and sizes.[18]

Unlike dye aggregates which are typically encountered in solution at concentrations in the millimolar range, the nano- and micro-sized aggregates discussed here are formed in water at low micromolar concentrations. Thus, these concentrations are significantly lower than those typically observed for formation of aggregates. The micro- and nano-scale aggregates reported herein are obtained in solution as they are formed by reprecipitation, after rapidly injecting a small amount of TC dissolved in a dissoluting solvent into a non-solvent. This study reports a straightforward anion-exchange procedure for synthesizing TC-based GUMBOS characterized by different spectral properties. The overall morphology of micro- and nano-scale structures subsequently obtained via room temperature reprecipitation[19] was dependent upon the particular TC dye chosen. Notably, the [$BETI^-$] anion was selected to impart pronounced hydrophobicity to the GUMBOS as compared to their iodide counterpart, facilitating the formation of ionically self-assembled[20] micro- and nano-scale aggregates in water at a 10^3-fold lower dye concentration (i.e, 2 μM) than reported previously. Studies employing transmission and scanning electron microscopy (TEM and SEM, respectively) imaging reveal that varying the methyne chain lengths exerts profound influence over the relative dimensions of the aggregates formed. Multi-luminophore aggregates consisting of blends of two or three different TC species were prepared and found to exhibit different types of dye aggregation (J-, H-, and random) and Förster Resonance Energy Transfer (FRET) between dyes within the aggregates. To the best of our

knowledge, this represents the first example clearly illustrating FRET based on organic nanomaterials derived wholly from structural analogs of the same parent dye. These nano and microscale blends with their unique and highly tunable spectral properties represent promising candidates for applications in areas including optoelectronics, bioimaging, energy harvesting, and biochemical sensing.

6.2. Materials and Methods

6.2.1. Chemicals and Materials

The thiacarbocyanine (TC) dyes 3,3'-diethylthiacyanine iodide ([TC0][I]), 3,3'-diethylthiacarbocyanine iodide ([TC1][I]), and 3,3'-diethylthiadicarbocyanine iodide ([TC2][I]), as well as the deuterated solvents chloroform-d_1 and dimethyl sulfoxide-d_6, were purchased from Sigma-Aldrich (Milwaukee, WI). HPLC grade organic solvents, including acetonitrile, tetrahydrofuran, ethanol, methanol and dichloromethane, were acquired from J.T. Baker (Philipsburg, NJ). Triply-deionized ultrapure water (18.2 MΩ cm) was obtained using an Elga model PURELAB ultrapure water filtration system. Lithium bis(pentafluoroethane)sulfonimide salt was a generous gift from 3M. All reagents were used without further purification.

6.2.2. General Instrumental Methods

^{1}H NMR (400 MHz) and ^{13}C NMR (100 MHz) spectra were acquired by use of a Bruker Avance 400 NMR spectrometer. The ^{1}H and ^{13}C chemical shifts are given in parts per million (δ) with TMS as an internal standard. All samples were dissolved in deuterated DMSO for NMR analysis. Additional characterizations were performed with high resolution mass spectrometry (HR-MS) on an Agilent 6210 electrospray ionization time-of-flight instrument in the positive and negative ion mode.

The melting point of the GUMBOS was determined using a MEL-TEMP® capillary melting point apparatus.

Electron microscopy images of the TC-based nanostructures were captured using a SM-6610, JSM-6610LV high- and low-vacuum scanning electron microscope (SEM) and a JEOL 100CX transmission electron microscope (TEM).

The spectral properties of these TC-based micro- and nano-sized self-assemblies were investigated by use of absorbance and fluorescence spectroscopies. Absorbance measurements were performed on a Shimadzu UV-3101PC UV-vis-NIR scanning spectrometer (Shimadzu, Columbia, MD). Fluorescence emission was collected using a Spex Fluorolog-3 spectrofluorimeter (model FL3-22TAU3); Jobin-Yvon, Edison, NJ). Both fluorescence and absorbance were acquired using a 0.4 cm^3 quartz cuvet (Starna Cells) and water as the blank.

Fluorescence images were obtained using a Leica TCS SP2 scanning laser confocal system with a 63× NA 1.4 lens. Images (1024 × 1024 pixels) were acquired based on six averages.

Fluorescence lifetime measurements were performed at Horiba Jobin Yvon, NJ using time domain mode. A picosecond pulsed excitation source of 408 nm and 495 nm were used respectively with TBX detector. Data acquisition was carried out using time-correlated single-photon counting (TSCPC) mode with a resolution of 7 ps/channel.

6.2.3. Synthesis of Thiacarbocyanine GUMBOS

The TC GUMBOS were prepared utilizing a metathesis reaction between thiacarbocyanine iodides and lithium bis(pentafluoroethane)sulfonimide at a molar ratio of 1 to 1.1. The reaction was performed in a biphasic mixture of water and dichloromethane (1:5, v/v) under stirring for 24 h. Afterwards, the organic phase which contained the TC GUMBOS was

washed several times with distilled water to remove residual LiI byproduct. Finally, the GUMBOS were isolated by solvent removal using rotary evaporation. These TC-based salts were characterized with nuclear magnetic resonance (H^1, C^{13}, and F^{19}-NMR) and high-resolution mass spectrometry (HR-MS).

6.2.4. Preparation of One-Dimensional Micro- and Nanoscale TC GUMBOS Aggregates

The TC-based micro- and nano-scale molecular aggregates were prepared using a well-known reprecipitation method at room temperature.[21] In brief, ethanolic solutions at a GUMBOS concentration of 0.1 mM were prepared and 100 uL aliquots were added to 5 mL of distilled water under sonication (BRANSON 3510RDTH model bath ultrasonicator, 335 W, 40 kHz frequency) for 5 min. The resulting solutions were left to equilibrate for 10 min. As a result 1-D micro- or nano-scale aggregates were formed from an initial dye concentration of 2 μM, with each TC dye yielding a unique morphology with its associated spectral properties as evidenced by electron microscopy and spectral analysis.

Blended nanoscale molecular aggregates containing multiple TC luminophores were similarly prepared from mixtures of ethanolic stocks consisting of the desired TC GUMBOS. By our nomenclature, [TC01][BETI] denotes GUMBOS formed from a precursor solution of [$TC0^+$] and [$TC1^+$] subjected to the reprecipitation process, [TC02][BETI] is formed from [$TC0^+$] and [$TC2^+$], and so on. The molar ratios of TC precursor solutions (0.1 mM) were varied to examine the effect of concentration on spectral properties and morphologies of blended nanostructures. Thus binary materials with molar ratios of *1:100*, *10:100*, *100:100*, *100:10*, and *100:1*, respectively were prepared, where *100* and *1*, represent concentrations of 2 μM and 0.02 μM for the initial TC dye concentration in the aggregate. Similarly molar ratios of *100:10:10*,

10:100:10, 10:10:100, and *100:100:100* for each TC GUMBOS were employed for the ternary blend [TC012][BETI].

6.3. Results and Discussion

6.3.1. Synthesis and Characterization of TC GUMBOS

Analysis of H^1- and C^{13}-NMR spectra of the GUMBOS revealed peaks similar to those of the thiacarbocyanine iodide parent compound, confirming the presence of $[TC]^+$ cations after ion-exchange. Two peaks were observed in F^{19}-NMR spectra, with chemical shifts of –78.9 Hz and –117.7 Hz, both of which are characteristic of the presence of the $[BETI^-]$ anion. Additional characterization was performed using HR-MS on an Agilent 6210 electrospray ionization time-of-flight instrument. In positive-ion mode, intense peaks with *m*/*z* of 339.10, 365.13, and 391.14 were observed, corresponding to molecular weights for the $[TC0^+]$, $[TC1^+]$, and $[TC2^+]$ cation, respectively. In negative-ion mode a peak was observed at 379.91 *m*/*z* characteristic of the $[BETI^-]$ anion.

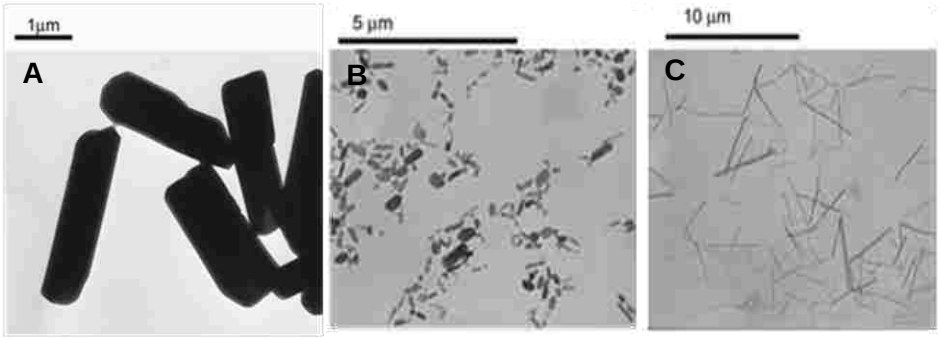

Figure 6.1. TEM micrographs of (A) [TC0][BETI], (B) [TC1][BETI], and (C) [TC2][BETI] aggregates.

6.3.2. Electron Microscopy Studies of Electron Microscopy Studies of Micro- and Nanoscale TC GUMBOS Aggregates

Electron microscopy (TEM and SEM) images of the TC micro- and nano-scale molecular aggregates obtained via reprecipitation are shown in Figures 6.1 and 6.2, respectively. Rodlike

[TC0][BETI] aggregates with diameters of 0.82 ± 0.13 μm and lengths of 2.42 ± 0.20 μm, for an aspect ratio near three were found. Close examination of the SEM images of Figure 6.2 reveals that some of these aggregates exhibit semi-tubular features. In the case of [TC1][BETI], the aspect ratios of the aggregates varied widely, exhibiting both rod and wirelike morphologies with diameters of 153 ± 74 nm and lengths of 0.53 ± 0.16 μm. Finally, well-defined [TC2][BETI] wire-shaped aggregates were obtained with diameters of 137 ± 37 nm and lengths of 3.16 ± 1.13 μm.

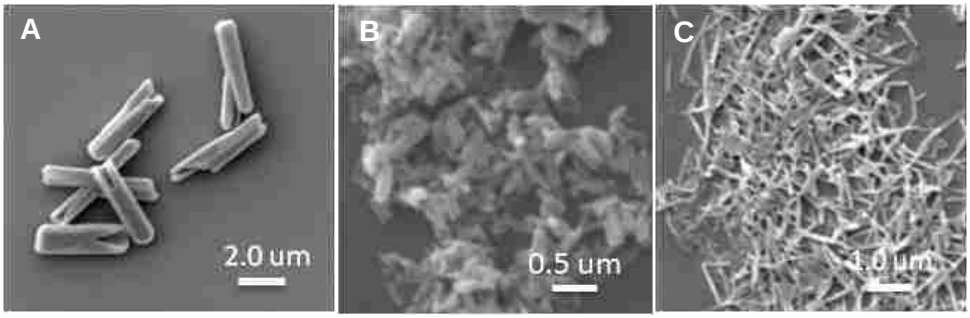

Figure 6.2. SEM micrographs of (A) [TC0][BETI], (B) [TC1][BETI], and (C) [TC2][BETI] aggregates.

TC-based GUMBOS with different anions such as [BF_4^-], [PF_6^-] and tetraphenylborate ([TPB^-]) were prepared as controls. In contrast to the [$BETI^-$]-based GUMBOS, these compounds failed to self-assemble into either defined 1-D aggregates or any specific morphology for that matter. Thus, the formation of micro and nanoscale aggregates is clearly linked to a unique and favorable association between [TC^+] cations and [$BETI^-$] counter ions. A further series of control experiments performed using the iodide precursors of the TC dyes (i.e., [TC0][I], [TC1][I], [TC2][I]) revealed that only [TC0][I] yielded 1-D nanoscale aggregates upon reprecipitation. We note that the final solution concentration of [TC0][I] used in this experiment, was three orders of magnitude lower than previous reports on the preparation of nanowires from similar dyes.[15a] The TC-based molecular aggregates reported in this work have another distinct

advantage in that they can be prepared at room temperature in only a handful of minutes employing a very simple and general reprecipitation approach.

6.3.3. Spectroscopic Properties of Micro- and Nanoscale TC GUMBOS Aggregates

The absorbance properties of the TC materials were measured at dye concentrations equivalent to 2 μM in water. Based on solution electronic absorption measurements, the maximum absorbance wavelengths for [TC0][BETI], [TC1][BETI], and [TC2][BETI] structures were 423 nm, 557 nm, and 649 nm, respectively, consistent with the increased conjugation across the series (Figure 6.4). In addition to the absorption maximum, [TC1][BETI] aggregates exhibited a red-shifted peak at 631 nm representative of J aggregation. An additional blue-shifted peak was observed at 475 nm for the [TC2][BETI] spectrum, characteristic of H aggregation. Fluorescence spectroscopic measurements were also performed for the TC nanostructures. Dispersions of [$TC0^+$]-, [$TC1^+$]-, and [$TC2^+$]- aggregates were excited at 423 nm, 541 nm, and 644 nm, respectively. Their corresponding emission maxima were recorded at 464 nm, 564 nm, and 664 nm.

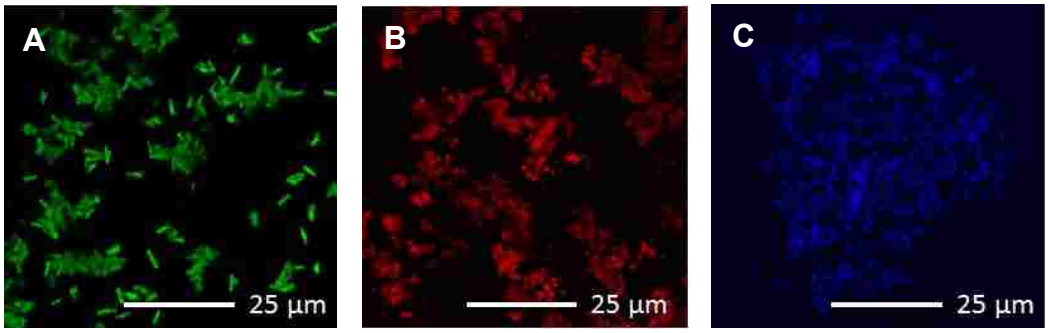

Figure 6.3. Fluorescence micrograph of (A) [TC0][BETI] aggregates (Excitation was performed with a ArKr laser at 488 nm and emission was collected between 500 and 578 nm), (B) [TC1][BETI] aggregates (Excitation was performed with a green HeNe laser at 543 nm and emission was collected between 555 and 700 nm), (C) [TC2][BETI] aggregates (Excitation was performed with a HeNe laser at 633 nm with emission collected between 650 and 750 nm). Images were pseudo-colored blue in order to distinguish them from the [TC1][BETI] aggregates.

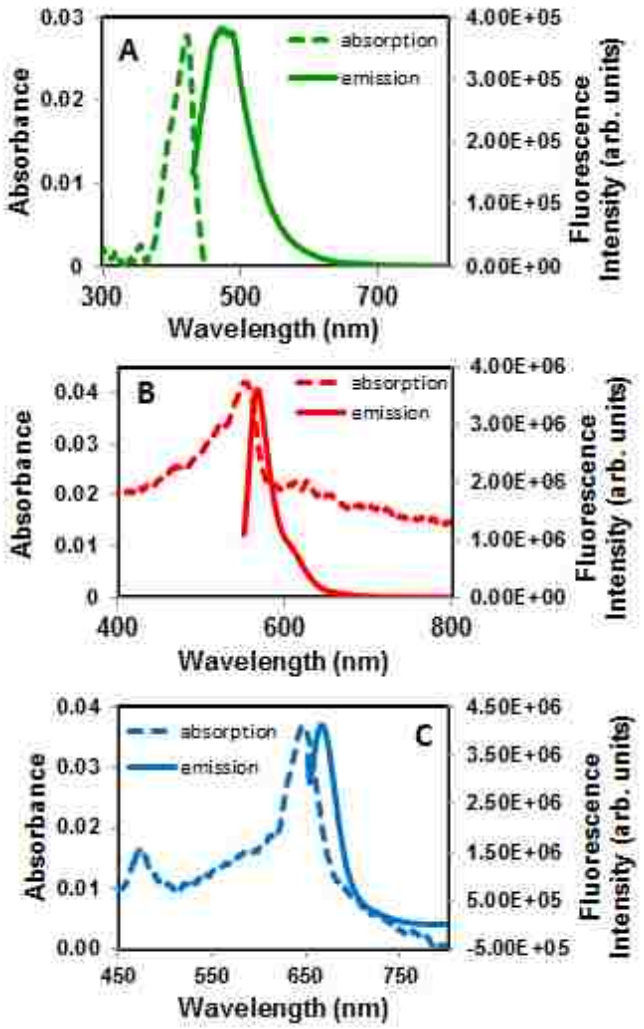

Figure 6.4. Normalized UV-Vis and fluorescence emission spectra of nanoscale aggregates of (A) [TC0][BETI] , (B) [TC1][BETI], and (C) [TC2][BETI]. Fluorescence excitation at 423 nm ($[TC0]_0$ = 2 μM), 541 nm ($[TC1]_0$ = 2 μM), and 644 nm ($[TC2]_0$ = 2 μM) respectively.

In addition to spectroscopic analysis, dispersions of TC-based micro- and nano-scale aggregates were also investigated by use of fluorescence microscopy (Figure 6.3). [TC0][BETI] microparticles excited using a 488-nm argon-ion laser line yielded strong emission in the green. Likewise, [TC1][BETI] nanowires and rods excited by a 543 nm laser displayed red luminescence. In the case of [TC2][BETI], the nanowires were excited using a 633 nm laser and imaged in the NIR (650–750 nm). A false-colored image of these nanostructures is shown in

Figure 6.3. It should be noted that these various micro and nanoscale aggregates exhibited bright, dye-specific fluorescence, suggesting possible avenues in multi-color imaging.

6.3.4. Binary and Ternary Nanoscale TC GUMBOS Aggregates

Biomimetic photosystems of cyanine triads have been previously reported.[22] Oppositely-charged polyelectrolytes that self-assembled into capsules served as templates to which negatively-charged thiacyanine dyes could adhere, allowing for FRET to occur between the exterior and interior of the capsule. In the present study, molecular aggregates from TC blends were prepared by co-precipitation of a mixture of TC GUMBOS, resulting in structures containing multiple TC dyes, making the prospect of FRET an intriguing possibility. Verification for the formation of intimately blended nanostructures was evidenced through examination of TEM images with comparison to physical mixtures of pre-formed aggregates prepared from the individual TCs. Dual- and multi-luminophore aggregates possessing different morphologies and spectral features were observed in the case where a dye mixture is subjected to reprecipitation conditions.

6.3.4.1. Electron Microscopy Studies

TEM micrographs were obtained of the blended binary and ternary nanomaterials for different molar ratios (Figure 6.5). Interestingly the morphologies of the nanostructures seemed to be highly dependent on the concentrations of TC dyes, i.e. higher ratios of [$TC0^+$] resulted in increasing lengths and diameters of the aggregates, similar to [TC0][BETI] microstructures. Likewise higher ratios of [$TC1^+$] lead to decreasing length and diameter of the structures, as was the case with [TC1][BETI] nanostructures. The corresponding lengths and diameters of the blended nanostructures at different dye ratios are depicted in Figure 6.6.

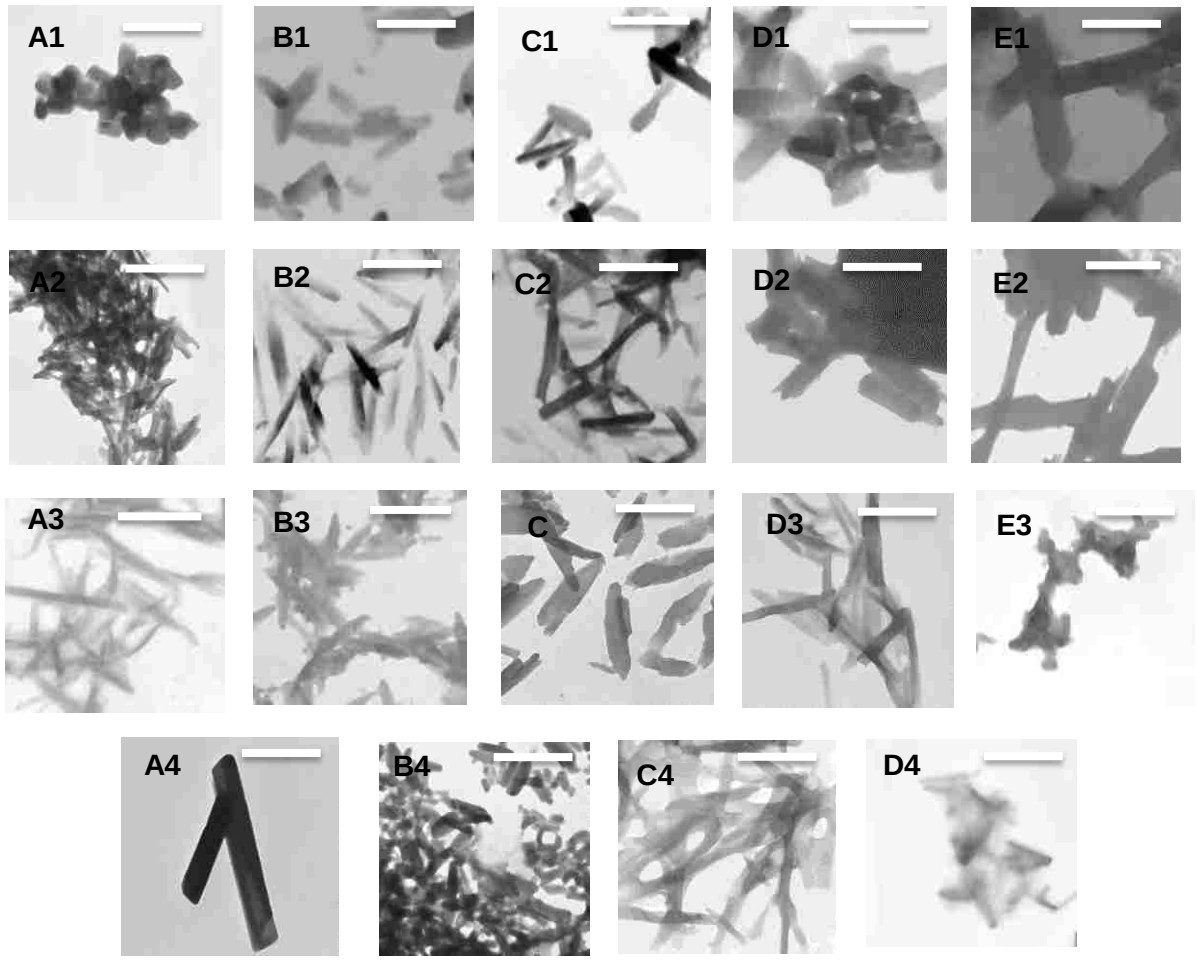

Figure 6.5. TEM micrographs of blended TC nanoscale aggregates of (A1-E1) [TC01][BETI], (A2-E2) [TC02][BETI], (A3-E3) [TC12][BETI] at molar ratios of *1:100, 10:100, 100:100, 100:10,* and *100:1* respectively and (A4-E4) [TC012][BETI] at molar ratios of *100:10:10, 10:100:10, 10:10:100,* and *100:100:100*. Scale bar represents 1μm.

6.3.4.2. Absorption Spectroscopy Studies

Absorption spectra for binary ([TC01][BETI], [TC02][BETI], [TC12][BETI]) and ternary ([TC012][BETI]) nanostructures were obtained at various molar ratios of individual fluorophores. The respective absorption spectra are provided in Figure 6.7. These data clearly indicate that the absorption features of the individual TC-based dyes are retained within the blended nanostructures with the appearance of additional peaks in some cases. For example, [TC01][BETI] exhibits two monomer peaks of the parent TC dyes at 423 nm and 557 nm

respectively. At higher molar concentrations of [$TC1^+$] (*100*) a red-shifted peak corresponding to J aggregation was also observed at 631 nm. For [TC02][BETI] the monomer peaks of [$TC0^+$] and [$TC2^+$] were observed at 423 nm and 649 nm, respectively. In addition, two blue-shifted peaks were observed for [$TC2^+$] at 475 nm and 567 nm which are indicative of H aggregation. The peak observed at 475 nm appeared to be relatively sharp, suggesting a possible twisted H aggregation. For [TC12][BETI] the monomer peaks of [$TC1^+$] and [$TC2^+$] were observed at 557 nm and 649 nm respectively. H aggregation was observed for [$TC2^+$] with a distinctive red-shifted peak at 475 nm appearing at higher molar ratios of this species (*100*). Interestingly J aggregation was also observed at certain molar ratios. A characteristic peak at 753 nm was observed for molar ratios of *100:100* and *100:10* between [$TC1^+$] and [$TC2^+$]. [TC012][BETI] exhibits a complex absorption profile containing features representative of the individual TC-based species. Similar to [TC12][BETI], J aggregation was also observed for [TC012][BETI] at a molar ratios of *100:100* and *100:10*.

6.3.4.3. Fluorescence Spectroscopy Studies

Fluorescence spectroscopy was used to study the spectral properties and examine the possibility of FRET within the binary as well as the ternary TC-based nanostructures. The emission spectra for these blended TC aggregates are shown in Figure 6.8. The most pronounced decrease in donor fluorescence was observed at higher molar ratios of donor and acceptor species. The overlap integral, $J(\lambda)$, and energy transfer efficiencies, E, for these blended TC nanostructures in water were calculated using equation 1 and 2, respectively and are found in Table 6.1.

Table 6.1. Overlap integrals ($J(\lambda)$) and energy transfer efficiencies (E) of various TC donor (D)-acceptor (A) pairs.

D-A pair	$J(\lambda)$	E
TC01	2.07×10^{-13}	30.3%
TC12	2.78×10^{-13}	49.1%
TC02	9.56×10^{-14}	30.2%
TC012	–	45.0%, 61.4%

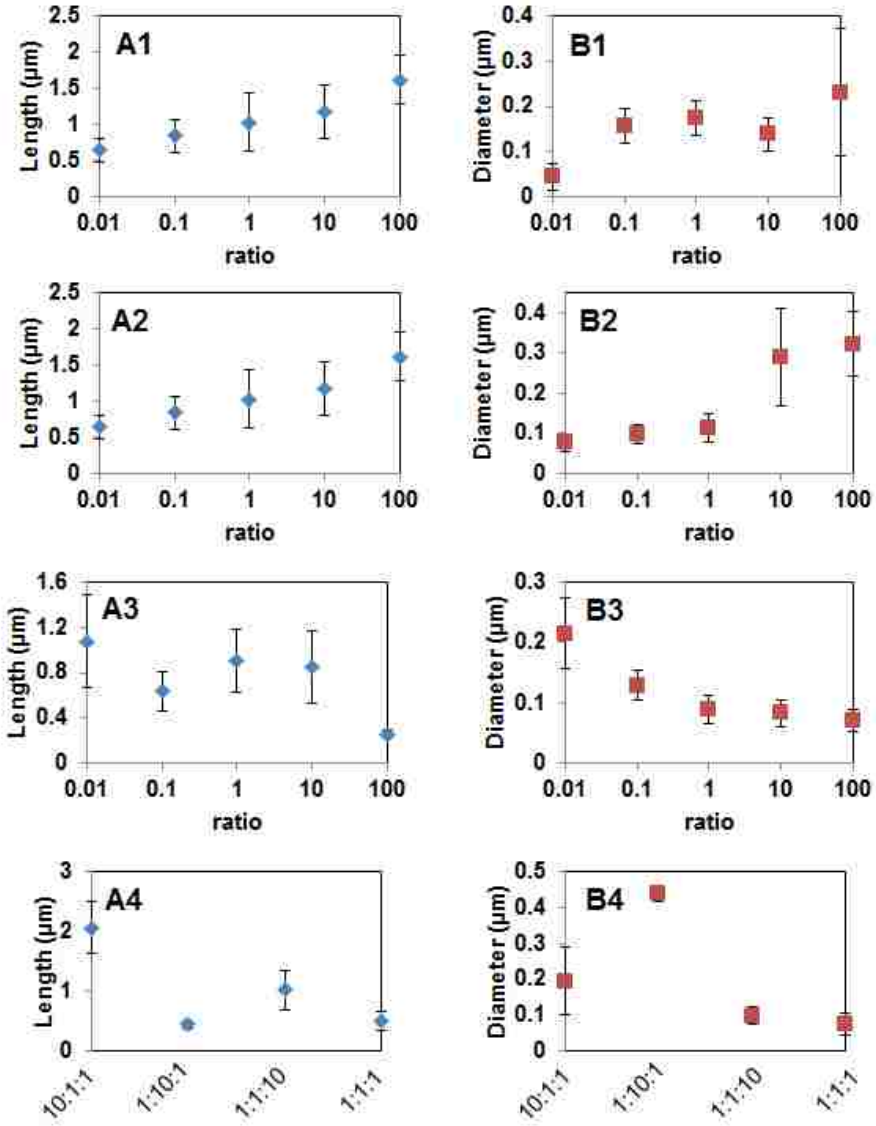

Figure 6.6. Length (A) and diameter (B) of nanoscale aggregates at different molar ratios (1) [TC01][BETI], (2) [TC02][BETI], (3) [TC12][BETI] and (4) [TC012][BETI].

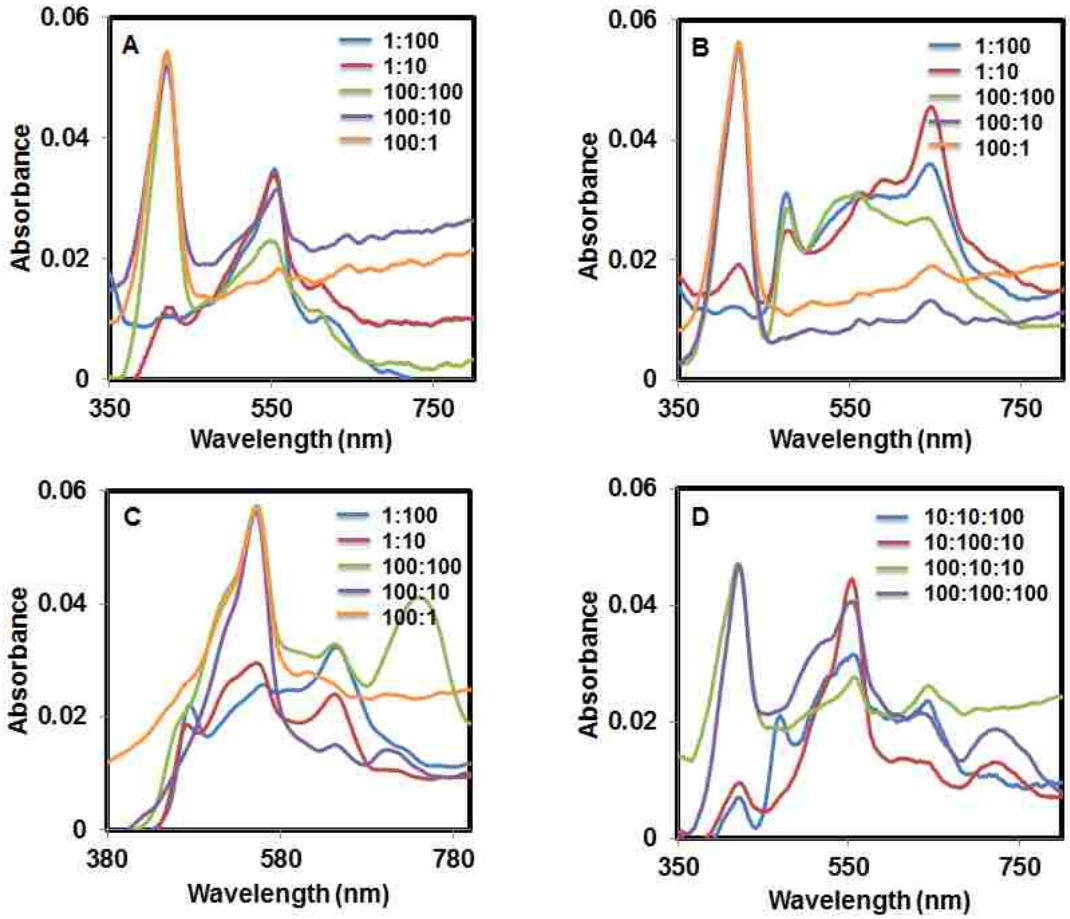

Figure 6.7. Normalized UV-Vis spectra of binary (A) [TC01][BETI], (B) [TC02][BETI], (C) [TC12][BETI], and ternary aggregates (D) [TC012][BETI] at different molar ratios.

It appears from these calculations that the $J(\lambda)$ value for [TC12][BETI] is the highest, followed by the value determined for [TC01][BETI] which is itself over twice that in [TC02][BETI]. The energy transfer efficiency for [TC12][BETI] is also the highest in the binary blends at roughly 49%. Interestingly, the fluorescence yield of the acceptor followed excitation of the donor is found to be enhanced in some cases whilst remaining unaffected in other systems. For instance, in the case of [TC01][BETI], [TC02][BETI], and [TC012][BETI], it was observed that, upon excitation of the [$TC0^{+}$] donor, the donor fluorescence decreased with respect to the pure donor concomitant with an enhanced acceptor emission relative to lone acceptor,

predictable FRET behavior. In [TC01][BETI], two peaks were observed for the acceptor at a molar ratio of *100:100* for the individual TC dyes. The peak at 583 nm is believed to be that of the monomer species, while the second at 613 nm is associated with J aggregation. As the relative concentration of the donor species [$TC0^+$] is reduced (*10:100* and *1:100*), the intensity of the acceptor monomer species [$TC1^+$] decreases significantly, while that of the J aggregate is still present upon excitation of the donor. This finding suggests that the fluorescence emission around 583 nm is the result of FRET between [$TC0^+$] and [$TC1^+$]. Alternatively, higher fluorescence intensity is recorded for the acceptor monomer species when the relative concentration of this species is reduced (*100:1* and *100:10*). It seems FRET is no longer distributed evenly between the acceptor monomer species and the J aggregate, rather it is restricted to the monomer species. As a result, an increase in fluorescence intensity at 583 nm for the monomer peak is observed.

[TC12][BETI] exhibited maximum FRET for the *100:100* molar ratio with the most significant decrease in donor intensity and increase in acceptor intensity. There appeared to be no FRET between the monomer emission of [$TC1^+$] and the absorption of the J aggregate of [$TC2^+$] due to the absence of spectral overlap between both. Lower concentration of the acceptor (*100:10*) resulted in a reduced FRET as can be seen in a decrease in energy transfer efficiency and intensity of the donor emission. Interestingly for the molar ratio of *100:1* a red-shifted emission was recorded with high fluorescence intensity at 707 nm. This emission peak appears to be the result FRET between the donor and acceptor species.

In [TC02][BETI], FRET was observed at higher relative concentrations of the donor species [$TC0^+$] (*100*). At lower concentrations of [$TC0^+$], energy transfer was not observed. In comparison to [TC01][BETI], the observed FRET appeared to be lower at all ratios. These findings are believed to be the result of a smaller overlap integral (Table 1) and the occurrence of

H aggregation in [TC2^{+}] at higher molar ratios. Therefore similar fluorescence intensity observed for [TC02][BETI] at a molar ratio of *100:10* and *100:100* can be attributed to occurrence of these non-fluorescent H aggregates.

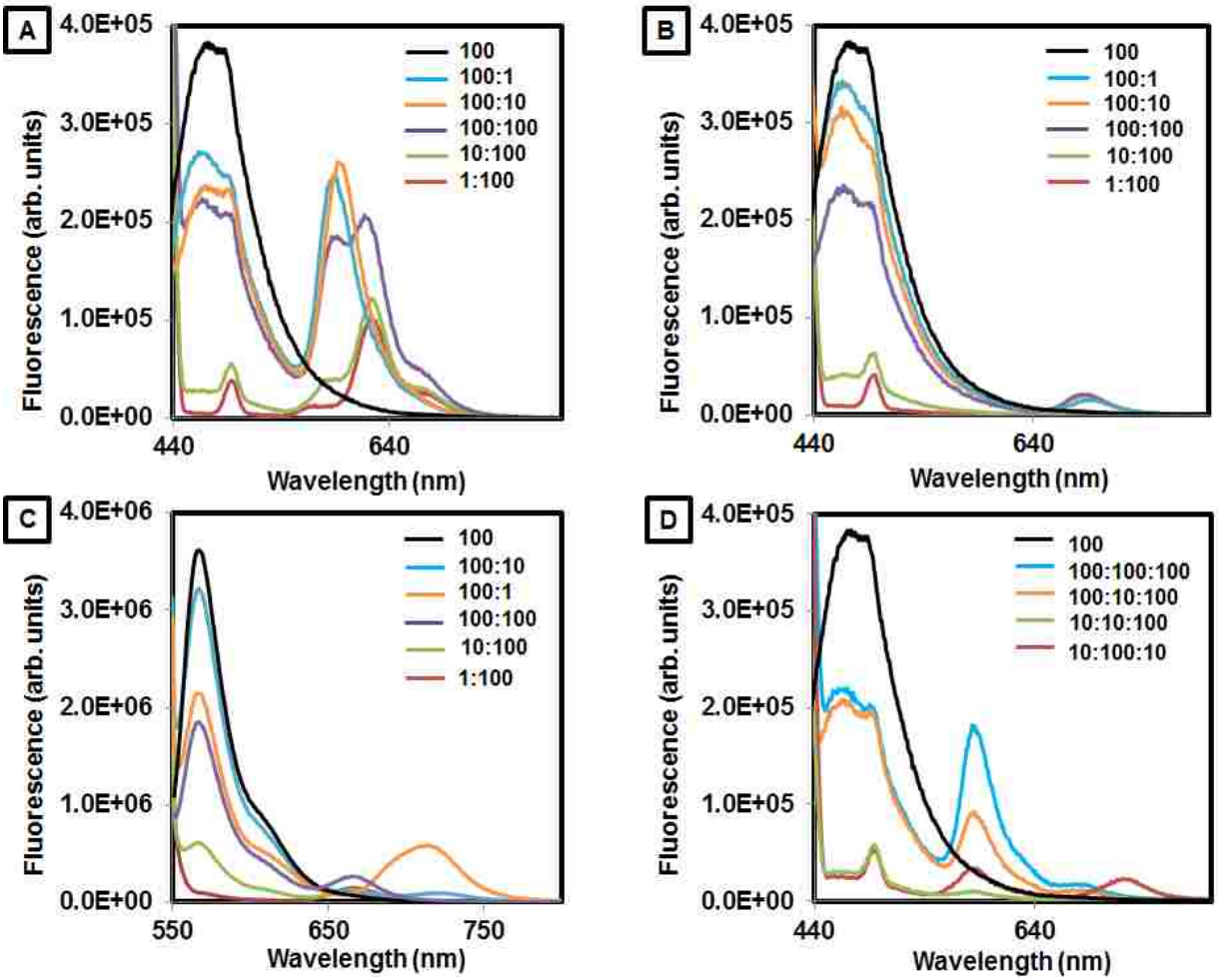

Figure 6.8. Fluorescence spectra of (A) [TC01][BETI], (B) [TC02][BETI], (C) [TC12][BETI], and (D) [TC012][BETI] binary and ternary aggregates at different molar ratios.

The ternary [TC012][BETI] system revealed significant energy transfer efficiency for higher concentrations of [TC0^{+}] at molar ratios of *100:100:100* and *100:10:10*. FRET appeared to be more apparent in the former, where a higher intensity was recorded for the [TC1^{+}] species. Similarly, energy transfer from [TC1^{+}] to [TC2^{+}] appeared to be more prominent at this molar

ratio (*100:100:100*). However, some H aggregation is believed to occur, limiting a drastic increase in acceptor fluorescence as was observed in [TC01][BETI]. When the [$TC0^+$] concentration was decreased, FRET from [$TC0^+$] to [$TC1^+$] was very low. At a molar ratio of *10:100:10*, an additional red-shifted peak was observed at 712 nm, suggesting FRET between [$TC1^+$] and [$TC2^+$], similar to [TC12][BETI] (*100:1*).

Thus it appears that FRET was found to occur within the binary and ternary blends and was favored at higher concentrations of TC species. In addition, non-fluorescent H-aggregates involving the acceptor within blended nanostructures appeared in [TC02][BETI] and [TC012][BETI], resulting in traps which open up additional non-radiative pathways of energy loss.

6.3.4.4. Fluorescence Lifetime Analysis

Binary and ternary TC-based nanostructures were further analyzed using fluorescence decay analysis. Excited-state decay data were analyzed in terms of a multi-exponential decay model and the recovered parameters are summarized in Table 6.2.

Excited-state lifetimes were determined for structures consisting of single-species ([TC0][BETI] and [TC1][BETI]) as well as multiple species ([TC01][BETI], [TC02][BETI], and [TC012][BETI]). In the case of [TC0][BETI], two discrete excited-state lifetimes were observed which we attribute to the approximately equal contributions from J-aggregates (681 ps, 47%) and monomeric species (1.55 ns, 52%). The [TC1][BETI] nanostructures exhibited a much shorter average lifetime resulting from the prevalence of J-aggregation (96 %) which exhibited an apparent lifetime of 158 ps. Comparable lifetimes have been reported for thia(carbo)cyanines in other systems.[23] The lifetimes of the binary and ternary TC-based nanostructures were all similar

to that in the [TC1][BETI] nanostructures. These results support our claim for the occurrence of FRET.

Table 6.2. Recovered intensity decay parameters for single- and multi-luminophore micro and nanoscale aggregates based on TC parent ion structures.

	Lifetime	Pre-exponential factor	Amplitude	Average lifetime	χ^2
[TC0][BETI]	τ_1 = 681 ps τ_2 = 1.55 ns τ_3 = 5.14 ns	47% (J) 52% (M) 1%	27% 68% 5%	1.19 ns	1.08
[TC1][BETI]	τ_1 = 158 ps τ_2 = 7.59 ns τ_3 = 2.37 ns	96% (J) 3% (M) 1%	80% 15% 5%	167 ps	1.03
[TC01][BETI]	τ_1 = 135 ps τ_2 = 1.07 ns τ_3 = 4.34 ns	96% 4% <1%	67% 22% 11%	191 ps	1.30
[TC02][BETI]	τ_1 = 104 ps τ_2 = 1.19 ns τ_3 = 5.3 ns	99% 1% <1%	81% 12% 7%	128 ps	1.27
[TC012][BETI]	τ_1 = 75 ps τ_2 = 1.46 ns τ_3 = 5.83 ns	99% 1% <1%	82% 10% 8%	92 ps	1.25

6.4. Conclusion

Thiacarbocyanine-based GUMBOS were successfully prepared through a facile anion-exchange reaction. The iono-hydrophobic properties of these materials facilitate a room temperature preparation of 1-D structures on the micron and nanoscale via a straightforward reprecipitation at ultradilute (i.e., micromolar) dye concentrations. The micro- and nano-scale molecular aggregates were rapidly obtained through spontaneous formation of ionic self-assemblies. Binary and ternary aggregates were similarly obtained by intimately mixing multiple TCs prior to initiating the reprecipitation. These materials exhibited tunable spectral properties as a result of efficient FRET, as well as changes in dye aggregation within the blended materials, which was most pronounced at higher molar ratios of the TCs. The highest energy transfer efficiency was

obtained from [$TC1^+$] to [$TC2^+$]. Measurement of the fluorescence lifetimes of the binary and ternary nanoscale aggregates confirmed the stationary-state results suggesting the occurrence of FRET. Further studies are being conducted to better understand and improve the FRET efficiency, aggregation-induced fluorescence changes in similar cyanine dye nanostructures, and multi-color multi-luminophore aggregates. The TC-based aggregates reported here, and especially their tunable spectral properties, offer potential applications in optoelectronics, (bio)chemical sensing, and bioimaging.

6.5. References

1. (a) Imahori, H.; Umeyama, T.; Ito, S., Large π-Aromatic Molecules as Potential Sensitizers for Highly Efficient Dye-Sensitized Solar Cells. *Accounts of Chemical Research* **2009,** *42* (11), 1809-1818; (b) Fernanda, R., Photophysical properties of porphyrins in biological membranes. *Journal of Photochemistry and Photobiology B: Biology* **1995,** *29* (2–3), 109-118.

2. (a) Sayama, K.; Tsukagoshi, S.; Mori, T.; Hara, K.; Ohga, Y.; Shinpou, A.; Abe, Y.; Suga, S.; Arakawa, H., Efficient sensitization of nanocrystalline TiO2 films with cyanine and merocyanine organic dyes. *Solar Energy Materials and Solar Cells* **2003,** *80* (1), 47-71; (b) Costela, A.; Garcia-Moreno, I.; Sastre, R., Polymeric solid-state dye lasers: Recent developments. *Physical Chemistry Chemical Physics* **2003,** *5* (21), 4745-4763.

3. Zang, L.; Che, Y.; Moore, J. S., One-Dimensional Self-Assembly of Planar pi-Conjugated Molecules: Adaptable Building Blocks for Organic Nanodevices. *Accounts of Chemical Research* **2008,** *41* (12), 1596-1608.

4. Zhao, Y. S.; Fu, H. B.; Peng, A. D.; Ma, Y.; Liao, Q.; Yao, J. N., Construction and Optoelectronic Properties of Organic One-Dimensional Nanostructures. *Accounts of Chemical Research* **2010,** *43* (3), 409-418.

5. Fabian, J.; Nakazumi, H.; Matsuoka, M., Near-Infrared Absorbing Dyes. *Chemical Reviews* **1992,** *92* (6), 1197-1226.

6. Advincula, R. C.; Fells, E.; Park, M. K., Molecularly ordered low molecular weight azobenzene dyes and polycation alternate multilayer films: Aggregation, layer order, and photoalignment. *Chemistry of Materials* **2001,** *13* (9), 2870-2878.

7. Kim, S.; Ohulchanskyy, T. Y.; Pudavar, H. E.; Pandey, R. K.; Prasad, P. N., Organically modified silica nanoparticles co-encapsulating photosensitizing drug and aggregation-enhanced two-photon absorbing fluorescent dye aggregates for two-photon photodynamic therapy. *Journal of the American Chemical Society* **2007,** *129* (9), 2669-2675.

8. (a) Wurthner, F.; Yao, S.; Debaerdemaeker, T.; Wortmann, R., Dimerization of merocyanine dyes. Structural and energetic characterization of dipolar dye aggregates and implications for nonlinear optical materials. *Journal of the American Chemical Society* **2002,** *124* (32), 9431-9447; (b) Williams, D. J., Organic Polymeric and Non-Polymeric Materials with Large Optical Nonlinearities. *Angew. Chem. Int. Edit.* **1984,** *23* (9), 690-703.

9. (a) Maeda, M., *Lasers Dyes*. Academic Press: Tokyo, 1984; (b) Rahn, M. D.; King, T. A., Comparison of laser performance of dye molecules in sol-gel, polycom, ormosil, and poly(methyl methacrylate) host media. *Applied Optics* **1995,** *34* (36), 8260-8271.

10. Robertson, N., Optimizing dyes for dye-sensitized solar cells. *Angew. Chem. Int. Edit.* **2006,** *45* (15), 2338-2345.

11. Khairutdinov, R. F.; Serpone, N., Photophysics of cyanine dyes: Subnanosecond relaxation dynamics in monomers, dimers, and H- and J-aggregates in solution. *Journal of Physical Chemistry B* **1997,** *101* (14), 2602-2610.

12. Ariga, K.; Lvov, Y.; Kunitake, T., Assembling alternate dye-polyion molecular films by electrostatic layer-by-layer adsorption. *Journal of the American Chemical Society* **1997,** *119* (9), 2224-2231.

13. Eren, E.; Afsin, B., Investigation of a basic dye adsorption from aqueous solution onto raw and pre-treated bentonite surfaces. *Dyes Pigments* **2008,** *76* (1), 220-225.

14. Demir, M. M.; Ozen, B.; Ozcelik, S., Formation of Pseudoisocyanine J-Aggregates in Poly(vinyl alcohol) Fibers by Electrospinning. *Journal of Physical Chemistry B* **2009,** *113* (34), 11568-11573.

15. (a) Takazawa, K.; Kitahama, Y.; Kimura, Y.; Kido, G., Optical waveguide self-assembled from organic dye molecules in solution. *Nano Letters* **2005,** *5* (7), 1293-1296; (b) Takazawa, K., Micrometer-sized rings self-assembled from thiacyanine dye molecules and their waveguiding properties. *Chemistry of Materials* **2007,** *19* (22), 5293-5301.

16. (a) Tesfai, A.; El-Zahab, B.; Bwambok, D. K.; Baker, G. A.; Fakayode, S. O.; Lowry, M.; Warner, I. M., Controllable formation of ionic liquid micro- and nanoparticles via a melt-emulsion-quench approach. *Nano Letters* **2008,** *8* (3), 897-901; (b) Tesfai, A.; El-Zahab, B.; Kelley, A. T.; Li, M.; Garno, J. C.; Baker, G. A.; Warner, I. M., Magnetic and Nonmagnetic Nanoparticles from a Group of Uniform Materials Based on Organic Salts. *Acs Nano* **2009,** *3* (10), 3244-3250; (c) Bwambok, D. K.; El-Zahab, B.; Challa, S. K.; Li, M.; Chandler, L.; Baker, G. A.; Warner, I. M., Near-Infrared Fluorescent NanoGUMBOS for Biomedical Imaging. *Acs Nano* **2009,** *3* (12), 3854-3860; (d) Das, S.; Bwambok, D.; Ei-Zahab, B.; Monk, J.; de Rooy, S. L.; Challa, S.; Li, M.; Hung, F. R.; Baker, G. A.; Warner, I. M., Nontemplated Approach to Tuning the Spectral Properties of Cyanine-Based Fluorescent NanoGUMBOS. *Langmuir* **2010,** *26* (15), 12867-12876.

17. Li, M.; De Rooy, S. L.; Bwambok, D. K.; El-Zahab, B.; DiTusa, J. F.; Warner, I. M., Magnetic chiral ionic liquids derived from amino acids. *Chemical Communications* **2009,** (45), 6922-6924.

18. Jia, Z. Q.; Ma, Y.; Yang, W. S.; Yao, J. N., Effects of bad solvents on thiatricarbocyanine particles formation. *Colloid Surface A* **2006,** *272* (3), 164-169.

19. (a) Kasai, H.; Nalwa, H. S.; Oikawa, H.; Okada, S.; Matsuda, H.; Minami, N.; Kakuta, A.; Ono, K.; Mukoh, A.; Nakanishi, H., A Novel Preparation Method of Organic Microcrystals. *Jpn J. Appl. Phys. 2* **1992,** *31* (8A), L1132-L1134; (b) Welton, T., Room-temperature ionic liquids. Solvents for synthesis and catalysis. *Chemical Reviews* **1999,** *99* (8), 2071-2083; (c) Kasai, H.; Yoshikawa, Y.; Seko, T.; Okada, S.; Oikawa, H.; Mastuda, H.; Watanabe, A.; Ito, O.; Toyotama, H.; Nakanishi, H., Optical properties of perylene microcrystals. *Mol. Cryst. Liq. Crys. A* **1997,** *294*, 173-176.

20. Faul, C. F. J.; Antonietti, M., Ionic self-assembly: Facile synthesis of supramolecular materials. *Advanced Materials* **2003,** *15* (9), 673-683.

21. Kasai, H.; Nalwa, H. S.; Oikawa, H.; Okada, S.; Matsuda, H.; Minami, N.; Kakuta, A.; Ono, K.; Mukoh, A.; Nakanishi, H., A Novel Preparation Method of Organic Microcrystals. *Japanese Journal of Applied Physics Part 2-Letters* **1992,** *31* (8A), L1132-L1134.

22. Dai, Z. F.; Dahne, L.; Donath, E.; Mohwald, H., Mimicking photosynthetic two-step energy transfer in cyanine triads assembled into capsules. *Langmuir* **2002,** *18* (12), 4553-4555.

23. Kabatc, J.; Paczkowski, J., The photophysical and photochemical properties of the oxacarbocyanine and thiacarbocyanine dyes. *Dyes Pigments* **2004,** *61* (1), 1-16.

CHAPTER 7

CONCLUSIONS AND FUTURE DIRECTIONS

The work presented in this dissertation discusses two classes of ionic materials, namely room temperature ionic liquids (RTILs) and a *Group of Uniform Materials Based on Organic Salts* (GUMBOS). Both categories are essentially low melting salts that essentially differ in their melting properties; RTILs are characterized by melting points below 25 ºC and GUMBOS by melting points between 25 ºC and 250 ºC. The different RTILs discussed in this work are all chiral in addition to other properties that they have. The GUMBOS, derived from fluorescent dyes were used to prepare micro and nanoscale materials, employing template and templateless methods. They exhibit tunable photophysical properties which were thoroughly investigated.

The first chapter provides a brief overview of previous studies and foundations of the field, including ionic liquids, chirality, GUMBOS, fluorescence, and nanomaterials. In chapter 2 the synthesis and characterization of a series of protic chiral ionic liquids (PCILs) is described. The PCILs differed in their degree of amine alkylation and were prepared via facile Brønsted acid-base neutralization between various ephedrines and imide acids. Their chiral recognition capabilities as measured by ^{19}F-NMR and fluorescence spectroscopy were dependent on their chemical structure.

In chapter 3, various bifunctional magnetic, chiral ionic liquids (MCILs) were reported. The MCILs were synthesized through the reaction between an amino acid ester hydrochloride (Lewis acid) and iron(III)chloride (Lewis base). In addition to their thermal stability, these MCILs exhibited strong magnetic susceptibility and good chiral recognition capability for a variety of chiral analytes.

Similarly, in chapter 4, a series of multifunctional luminescent, magnetic, chiral ionic liquids (LMCILs) are discussed. The LMCILs were prepared in two steps and consist of cations derived from amino acid esters and dysprosium thiocyanate anions. Like the MCILs (chapter 3), these LMCILs exhibited good thermal stability, strong magnetic susceptibility, and good chiral recognition capability. These ILs were further characterized by a strong luminescence. In addition to their chiral sensing capabilities, the various bi and multifunctional CILs discussed in chapter 2-4 may also find use in enantioselective catalysis. Moreover further studies on tuning chiral selectivity through magnetic as well as magnetic and luminescent stimuli (for MCILs and LMCILs respectively) would be of interest in chiral sensing and catalysis.

In chapter 5, fluorescent GUMBOS were prepared by ion-pairing of the rhodamine 6G dye cation with the hydrophobic tetraphenylborate anion. An anodic alumina template was used to grow one-dimensional (1D) nanostructures (wires, tubes, and arrays). These fluorescent GUMBOS nanostructures were characterized by strong photostability.

A series of structurally similar thiacarbocyanine (TC) GUMBOS are reported in chapter 6. By employing a reprecipitation approach, 1D micro and nanostructures were produced through self-assembly of the GUMBOS. These aggregated structures exhibited unique morphologies and spectro-chemical properties. Blended nanomaterials, consisting of multiple TCs were similarly prepared, yielding FRET as well as controlled aggregation, thereby allowing for further tunability of the spectral properties of these structures. Studies are currently underway to investigate the use of 1D fluorescent nanoscale GUMBOS as probes for vapors, biomolecules and other analytes. In some cases the ionic conductive properties exhibited by selected dye based nanoscale GUMBOS are altered in the presence of certain vapors. To this end, there remains a need to further synthesize novel chemoresponsive GUMBOS, with tunable fluorescent, ionic and

electronic properties. Moreover the development of nanofabrication methods that allow for controllable organization of 1D nanoscale GUMBOS is highly desirable. Such developments allow for future photonic and optoelectronic devices, including sensors, waveguides, and OLEDs.

APPENDIX

LETTER OF PERMISSION

Sergio De Rooy <sderoo1@tigers.lsu.edu>

Permission

2 messages

Sergio De Rooy <sderoo1@tigers.lsu.edu> **Thu, Feb 9, 2012 at 3:26 PM**
To: contracts-copyright@rsc.org

Dear Sir/Madam,

I am currently writing my doctoral dissertation and I hereby request permission to reproduce text, data and figures in my dissertation from the publications listed below:

Magnetic chiral ionic liquids derived from amino acids
Min Li, Sergio L. De Rooy, David K. Beambok, Bilal El-Zahab, John F. DiTusa and Isiah M. Warner
Chem. Commun., 2009, 6922-6924
DOI: 10.1039/B917683

Fluorescent one-dimensional nanostructures from a group of uniform materials based on organic salts
Sergio L. de Rooy, Bilal El-Zahab, Min Li, Susmita Das, Ellen Broering, Lin Chandler and Isiah M. Warner
Chem. Commun., 2011, **47**, 8916-8918
DOI: 10.1039/C1CC12478A

Sincerely,
Sergio L. de Rooy
Ph.D. Candidate
232 Choppin Hall,
LSU, Chemistry Department,
Baton Rouge, LA 70803
Fax 225-578-3971
Telephone: 225-578-3919

CONTRACTS-COPYRIGHT (shared) <Contracts-Copyright@rsc.org> **Fri, Feb 10, 2012 at 7:25 AM**

To: Sergio De Rooy <sderoo1@tigers.lsu.edu>

Dear Sergio

The Royal Society of Chemistry hereby grants permission for the use of the material specified below in the work described and in all subsequent editions of the work for distribution throughout the world, in all media including electronic and microfilm. You may use the material in conjunction with computer-based electronic and information retrieval systems, grant permissions for photocopying, reproductions and reprints; translate the material and to publish the translation, and authorize document delivery and abstracting and indexing services. The Royal Society of Chemistry is a signatory to the STM Guidelines on Permissions (available on request).

Please note that if the material specified below or any part of it appears with credit or acknowledgement to a third party then you must also secure permission from that third party before reproducing that material.

Please ensure that the published article carries a credit to The Royal Society of Chemistry in the following format:

[Original citation] – Reproduced by permission of The Royal Society of Chemistry

and that any electronic version of the work includes a hyperlink to the article on the Royal Society of Chemistry website. The recommended form for the hyperlink is http://dx.doi.org/10.1039/*DOI suffix*, for example in the link http://dx.doi.org/10.1039/b110420a the DOI suffix is "b110420a". To find the relevant DOI suffix for the RSC paper in question, go to the Journals section of the website and locate your paper in the list of papers for the volume and issue of your specific journal. You will find the DOI suffix quoted there.

Regards

Gill Cockhead

Publishing Contracts & Copyright Executive

Gill Cockhead (Mrs), Publishing Contracts & Copyright Executive

Royal Society of Chemistry, Thomas Graham House

Science Park, Milton Road, Cambridge CB4 0WF, UK

Tel +44 (0) 1223 432134, Fax +44 (0) 1223 423623

http://www.rsc.org

From: Sergio De Rooy [mailto:sderoo1@tigers.lsu.edu]
Sent: 09 February 2012 21:27
To: CONTRACTS-COPYRIGHT (shared)
Subject: Permission

[Quoted text hidden]

Copyright Clearance Center RightsLink®

Home | Account Info | Help

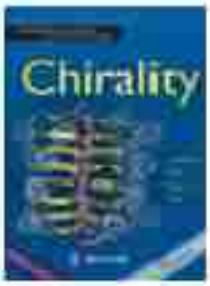

Title:	Ephedrinium-based protic chiral ionic liquids for enantiomeric recognition
Author:	Sergio L. De Rooy,Min Li,David K. Bwambok,Bilal El-Zahab,Santhosh Challa,Isiah M. Warner
Publication:	Chirality
Publisher:	John Wiley and Sons
Date:	Jan 1, 2011

Logged in as:
Isiah Warner
Account #:
3000182984

LOGOUT

Order Completed

Thank you very much for your order.

This is a License Agreement between Isiah M Warner ("You") and John Wiley and Sons ("John Wiley and Sons"). The license consists of your order details, the terms and conditions provided by John Wiley and Sons, and the payment terms and conditions.

Get the printable license.

License Number	2844330438431
License date	Feb 08, 2012
Licensed content publisher	John Wiley and Sons
Licensed content publication	Chirality
Licensed content title	Ephedrinium-based protic chiral ionic liquids for enantiomeric recognition
Licensed content author	Sergio L. De Rooy,Min Li,David K. Bwambok,Bilal El-Zahab,Santhosh Challa,Isiah M. Warner
Licensed content date	Jan 1, 2011
Start page	54
End page	62
Type of use	Dissertation/Thesis
Requestor type	Author of this Wiley article
Format	Electronic
Portion	Full article
Will you be translating?	No
Order reference number	
Total	0.00 USD

ORDER MORE... | CLOSE WINDOW

Copyright Clearance Center RightsLink®

Home | Account Info | Help

ACS Publications High quality. High impact.

Title: Ionically Self-Assembled, Multi-Luminophore One-Dimensional Micro- and Nanoscale Aggregates of Thiacarbocyanine GUMBOS

Author: Sergio L. de Rooy et al.

Publication: The Journal of Physical Chemistry C

Publisher: American Chemical Society

Date: Apr 1, 2012

Logged in as:
Isiah Warner
Account #:
3000182984

LOGOUT

PERMISSION/LICENSE IS GRANTED FOR YOUR ORDER AT NO CHARGE

This type of permission/license, instead of the standard Terms & Conditions, is sent to you because no fee is being charged for your order. Please note the following:

- Permission is granted for your request in both print and electronic formats.
- If figures and/or tables were requested, they may be adapted or used in part.
- Please print this page for your records and send a copy of it to your publisher/graduate school.
- Appropriate credit for the requested material should be given as follows: "Reprinted (adapted) with permission from (COMPLETE REFERENCE CITATION). Copyright (YEAR) American Chemical Society." Insert appropriate information in place of the capitalized words.
- One-time permission is granted only for the use specified in your request. No additional uses are granted (such as derivative works or other editions). For any other uses, please submit a new request.

BACK CLOSE WINDOW

VITA

Sergio Leon de Rooy was born in Paramaribo, Suriname, to Andre Friedrich de Rooy and Herwati Mieke Soemodihardjo. He attended Christiaan David elementary school, I. P. J Berkenveld High School, and Mr. Dr. J. C. de Miranda Lyceum (High School). Thereafter, he received his Bachelor of Education in chemistry (May 2001) from the Advanced Teacher Training Institute in Suriname. After having worked as a teacher for several years, Sergio obtained a scholarship from the government of Indonesia to pursue graduate studies in chemistry. He was awarded a Master of Science Degree from the Gadjah Mada University under the guidance of Professor Endang Tri Wahyuni (March 2007). In the spring of 2008, he continued his graduate studies under the diligent tutelage of Professor Isiah M. Warner. Sergio has received several honors, most notably the American Chemical Society Division of Analytical Chemistry nine month fellowship funded by Eli Lilly and Company, and the James G. Traynham Distinguished Graduate Student Award. He is a member of *the American Chemical Society (ACS)* and *the National Organization for the Professional Advancement of Black Chemists and Chemical Engineers (NOBCChE)*. Sergio will graduate with the degree of Doctor of Philosophy in chemistry from Louisiana State University in May 2012. His publications, patents, conference presentations as well as awards and honors during his graduate career are listed below.

PUBLICATIONS

1. **De Rooy, S. L.**; Das, S.; Li, M.; El-Zahab, B.; Jordan, A.; Warner, I. M. "Ionically Self-Assembled, Multi-Luminophore One-Dimensional Thiacarbocyanine Micro and Nanoscale GUMBOS", *J. Phys. Chem.C.*, **2012**, *116*, 8251-8260.

2. **De Rooy, S. L.**; El-Zahab, B.; Li, M.; Das, S.; Warner, I. M.. "Fluorescent One-Dimensional Nanomaterials from a Group of Uniform Materials Based on Organic Salts", *Chem.Commun.*, **2011**, *47*, 8916-8918.

3. **De Rooy, S. L.**; Li, M.; Bwambok D.K.; El-Zahab B.; Challa S.; Isiah M. Warner. "Ephedrinium-Based Protic Chiral Ionic Liquids for Enantiomeric Recognition". *Chirality.* 2011, 23, 54-62.

4. Das, S.; **De Rooy, S. L.**; Jordan, A.; El-Zahab, B.; Warner, I. M. "Tunable Size and Spectral Properties of Fluorescent NanoGUMBOS in Modified Deoxycholate Hydrogels", Langmuir, 2012, 28, 757-765.

5. Li, M.; Visser, G.G.; Lu, C.; **De Rooy, S. L.**; El-Zahab, B.; Fernand, V. E., Rongying, J.; Aggarwal, S.; Warner, I.M. "Lipophilic Phosphonium-Lanthanide Compounds with Magnetic, Luminescent, and Tumor Targeting Properties", J. Inorg. Biochem., 2011, 107, 40-46 .

6. Deng, N.; Li, M.; Zhao L.; Lu, C.; **De Rooy**, **S. L.**; Warner, I.M. "Highly Efficient Extraction of Phenolic Compounds by Magnetic Room Temperature Ionic Liquids for Environmental Remediation", *J. Hazard. Mater.,* **2011**, *3*,1350-1357.

7. Das, S.; Bwambok, D.; El-Zahab, B.; Monk, J.; **De Rooy, S. L.**; Challa, S.; Li, M.; Hung, F.; Baker, G.; Warner, I.; "A Nontemplated Approach for Tuning the Spectral Properties of Cyanine-Based Fluorescent NanoGUMBOS". *Langmuir*, **2010**, *26*, 12867-12876.

8. Li, M.; **De Rooy, S. L.**; Bwambok, D.K.; El-Zahab, B.; Ditusa, J.F.; Warner, I.M. "Magnetic Chiral Ionic Liquids Derived from Amino Acids". *Chem. Commun.,* **2009**, *45*, 6922-6924.

9. Li, M.; Gardella J.; Bwambok D.K.; El-Zahab B.; **De Rooy, S.**; Cole, M.; Lowry M.; Warner, I.M. Combinatorial Approach to Enantiomeric Discrimination: Synthesis and ^{19}F NMR Screening of a Chiral Ionic Liquid-Modified Silane Library. *J. Comb. Chem*., **2009**, *11*, 1105-1114.

10. Li, M.; **De Rooy, S. L.**; Lu, C; Warner, I. M. "Multifunctional Ionic Liquids with Magnetic, Chiral, and Fluorescent Properties", submitted to *Chem. Commun.*

PATENTS

Warner Isiah M; Tesfai Aaron; Bwambok David; Baker Gary A; Fakayode Sayo O; Lowry Mark; Tolocka Michael P; **de Rooy, Sergio**, "Frozen ionic liquid microparticles and nanoparticles, and methods for their synthesis and use" World Intellectual Property Office (WIPO). Patent Collaboration Treaty (PCT) Patent 2009/082618

PROFESSIONAL PRESENTATIONS

1. **De Rooy, S. L.**; Lodes, R.; Das, S.; Warner, I. M. 'Task Specific Ionic Liquids for Applications in Photonics and Optoelectronics", presented at Pittcon Conference & Expo 2012, Orlando, March 11-15, 2012.

2. **De Rooy, S. L.**; Lodes, R.; Das, S.; Negelescu, I; Monk J.; Hung, F. R.; Warner, I. M. 'Cyclodextrin-Based Ionogels", presented at the 2011 Materials Research Society (MRS) Fall Meeting and Exhibit, Boston, Nov. 28 – Dec. 1, 2011.

3. **De Rooy**, **S. L.;** El-Zahab, B; Li, M.; Das, S.; and Warner I. M. **"**Template Assisted Fluorescent Nanotubes and Nanowires from a Group of Uniform Materials Based on Organic Salts", presented at the 38th Annual NOBCChE Conference, Houston, April 18-22, 2011.

4. Warner, I. M. Das, S.; Li, M.; El-Zahab, B.; **De Rooy, S. L.;** Regmi, B. "NanoGUMBOS: A Novel Group of Designer Nanomaterials", presented at the 38th Annual NOBCChE Conference, Houston, April 18-22, 2011.

5. **De Rooy**, **S. L.;** Das, S.; Li, M.; El-Zahab, B.; and Warner I. M. **"**Ionic Self-assembly of Low-dimensional Nanostructures from Thiacarbocyanine-Based GUMBOS", presented at Pittcon Conference & Expo 2011, Atlanta, March 13-18, 2011.

6. **De Rooy, S. L.;** El-Zahab, B.; Li, M.; Das. S.; and Warner, I. M. "Fluorescent One-Dimensional NanoGUMBOS", presented at the 66th Southwest and 62nd Southeastern Regional Meeting of the American Chemical Society, New Orleans, Nov. 30-Dec. 4, 2010.

7. Jordan, A.; Das, S.; **De Rooy, S. L.;** Li, M.; El-Zahab, B.; Warner, I. M. "Tunable morphology and spectral properties of pseudoisocyanine-based nanoGUMBOS", presented at the 66th Southwest and 62nd Southeastern Regional Meeting of the American Chemical Society, New Orleans, Nov. 30-Dec. 4, 2010.

8. Das, S.; **De Rooy, S. L.;** Jordan, A.; Sylvain, M.; El-Zahab, B.; Warner, I. M. "Tunable Size and Spectral Properties of Fluorescent NanoGUMBOS in Modified Hydrogels", presented at the 66th Southwest and 62nd Southeastern Regional Meeting of the American Chemical Society, New Orleans, Nov. 30- Dec. 4, 2010.

9. **De Rooy**, **S. L.;** Das, S.; Jordan, A.; Li, M.; El-Zahab, B. and Warner I. M. "Spectroscopic Properties of One-Dimensional Nano and Microstructures from Thiacarbocyanine Frozen Ionic Liquids", presented at the 218th Meeting of the Electrochemical Society, Las Vegas, Oct. 10-15, 2010.

10. Deng, N.; Li, M.; **De Rooy, S. L.;** El-Zahab, B.; Warner, I. M. "Extraction of Phenols from Aqueous Solution by Magnetic Ionic Liquids for Environmental Remediation", presented at the 218th Meeting of the Electrochemical Society, Las Vegas, Oct. 10-15, 2010.

11. El-Zahab, B.; Tesfai, A.; Bwambok, D.; **De Rooy, S. L.;** Li, M.; Das, S.; Warner, I. M. "Synthesis of Applications of Frozen Ionic Liquid Nanomaterials", presented at the 218th Meeting of the Electrochemical Society, Las Vegas, Oct. 10-15, 2010.

12. El-Zahab, B.; **De Rooy, S. L.**; Jordan, A.; Das, S.; Li, M.; Warner, I. M.. "Preparation of 0-D, 1-D, and 2-D Nano-GUMBOS", presented at the Third US-China Workshop on Nanostructured Materials for Global Energy and Environmental Challenge, Beijing, China September 20-22, 2010.

13. Warner, I. M.; El-Zahab, B.; Li, M.; Das, S.; **De Rooy, S. L.**; Hung, F.; Baker, G. "Application of Nano-GUMBOS", presented at the Third US-China Workshop on Nanostructured Materials for Global Energy and Environmental Challenge, Beijing, China September 20-22, 2010.

14. Weber, A. E.; **De Rooy, S. L.;** El-Zahab, B.; Li, M.; Warner, I. M. "Nanostructured Plastic Ionic Crystals for Electrical Storage", presented at Summer Undergraduate Research Forum, Baton Rouge, Louisiana, July 29, 2010.

15. Lodes R. M.; **De Rooy, S. L.;** Li, M.; El-Zahab, B.; Warner, I. M. "Ionic Liquid Inverse Opals for Applications in Optoelectronics", presented at Summer Undergraduate Research Forum, Baton Rouge, Louisiana, July 29, 2010.

16. Warner, I. M.; El-Zahab, B.; Li, M.; Bwambok, D. K.; De Rooy, S. L.; Das, S.; Challa, S.; Tesfai, A.; Wright, A. R. "Production of Tunable Nanoparticles Using a Group of Uniform Materials Based on Organic Salts (GUMBOS)", presented at Pittcon Orlando, Florida, February 28-March 5, 2010.

17. Li, M.; **De Rooy, S. L.;** Bwambok, D. K.; El-Zahab, B.; DiTusa, J. F.; Warner, I. M. "Magnetic Chiral Ionic Liquids Derived from Amino Acids", presented at Pittcon Orlando, Florida, February 28-March 5, 2010.

18. Broering, E.; **De Rooy, S. L.;** El-Zahab, B.; Warner, I. M. "Nano-structured Coatings as Biomimetic Non-wetting Surfaces", presented at Summer Undergraduate Research Forum, Baton Rouge, Louisiana, July 30, 2009.

19. **De Rooy, S. L.**; Li, M.; Bwambok, D. K.; El-Zahab, B.; Challa, S.; Warner, I. M.. "Novel Protic Chiral Ionic Liquids Based on Ephedrine Derivatives" presented at Chirality 2009, 21st International Symposium on Chirality, Breckenridge, Colorado, July 12-15, 2009.

20. **De Rooy, S. L.;** Ismail, J.; Wahyuni E. T. "Extraction and Characterization of Poly-3-hydroxybutyrate (PHB) from Cupriavidus Necator", presented at the 2nd Biannual Meeting on Bioprocess Engineering, Yogyakarta, Indonesia, Nov. 20-24, 2006.

AWARDS AND HONORS

2011 – 2012	American Chemical Society Division of Analytical Chemistry nine month fellowship funded by Eli Lilly and Company
2008 – 2012	Graduate School Enhancement, LSU
2011	James G. Traynham Distinguished Graduate Student Award, LSU
2012	Graduate School Travel Award (PITTCON), LSU
2011	NOBCChE Advancing Science Graduate Student Travel Award
2011	Graduate School Travel Award (MRS-Fall), LSU
2011	Graduate School Travel Award (PITTCON), LSU
2009	Graduate School Travel Award (Chirality), LSU
2008	Best Student Speaker Analytical Chemistry Seminar, LSU
2004 – 2007	Developing Countries Partnership Scholarship of Indonesia

PROFESSIONAL AFFILIATIONS

2010 – Present	American Chemical Society (ACS)
2010 – Present	National Organization for the Professional Advancement of Black Chemists and Chemical Engineers (NOBCChE)